Emergency Evacuation Planning Problem under Uncertainty in Events

Presented to

the Faculty of the Department of Industrial Engineering

University of Houston

In Partial Fulfillment

of the Requirements for the Degree

Doctor of Philosophy

in Industrial Engineering

Chair of Committee: Gino J. Lim

Committee Member: Taewoo Lee

Committee Member: Ying Lin

Committee Member: Cumaraswamy Vipulanandan

Committee Member: Christoph Eick

by

Ayda Darvishan

December 2020

Dedication

To my dear family, for all their support and love from thousands of miles away

To my friends, whose love empowers me to achieve impossible

Acknowledgments

I would like to express my sincere gratitude towards Dr. Gino Lim for his continuous support of my research, for his patience, motivation, immense knowledge, and significant technical insights. He challenged me to continuously improve myself and to expand my knowledge. It was a great honor to work under his supervision. Many thanks to the dissertation committee members, Dr. Taewoo Lee, Dr. Ying Lin, Dr. Cumaraswamy Vipulanandan, and Dr. Christoph Eick for providing valuable comments that improved the quality of my work.

Abstract

Large-scale emergency evacuations in the wake of hazardous events, such as hurricanes, tsunamis, volcanic disruptions, nuclear meltdowns, etc., are an important part of disaster management as they directly associate with protecting human lives. Due to the unpredictable nature of disasters, an evacuation plan can be heavily affected by the uncertainty of events. The resulting deviations can contribute to road congestions, prolonged evacuation process, unstable traffic behaviors, and lead to chaos, injuries, and loss of life. Two approaches can be taken to handle these uncertainties. First could be to develop an evacuation route plan and schedule prior to the arrival of the adversarial event by considering the risk of exposure to the disaster impact (pro-active planning), and second would be to monitor the progress of the evacuation, detect deviations, and make adjustments if needed (recovery strategy). Our proposed research focuses on developing pro-active plans and recovery strategies to handle associated uncertainties that are either due to the occurrence of probable incidents or randomness in data. Using the theory of dynamic network flow optimization, the following studies are conducted:

First, emergency evacuation management under possible road disruptions in the transportation network is studied. During an evacuation, roads can be cut off due to road flooding, blocked because of wild-fire propagation, accidents or collapse of highway structures, etc. A comprehensive approach for rerouting the disturbed flow is introduced which can address disruptions on multiple roads occurring at different times. Two innovative algorithms for parameter calculation are introduced to reduce mathematical complexity and computational burden. Using these algorithms, a MIP formulation for rerouting the disturbed flow is proposed. Computational results show the validity of our

approach.

Second, the effect of uncertain road closures on traffic dynamics in a system-optimal setting is investigated to provide a proactive evacuation plan while considering a recovery strategy (rerouting) to compensate for the negative effects of the disruption. The previously mentioned algorithms for parameter calculation are extended to be implemented for disruption scenarios, and a *MIP* two-stage stochastic program is introduced to solve the problem. The first stage of the two-stage program aims to find the proactive evacuation plan while the second stage finds the best recovery strategy in the face of each scenario of disruption. Comparisons are made between the plans yielded from existing deterministic models with the plans provided by our proposed approach which demonstrates the superiority of our developed stochastic program.

Third, an evacuation planning problem under uncertainty of the number of would-be evacuees (demand) is investigated. It is assumed that based on the available historical data, accurate predictions on demand are not possible and the probability distribution function of demand cannot be estimated. Accordingly, a data-driven robust optimization approach is developed to solve the evacuation planning problem by directly incorporating data samples in the mathematical formulation of the problem. To build the uncertainty sets, an unsupervised machine learning approach (support vector clustering) is used which employs a piecewise linear kernel function to effectively capture the distributional geometry of massive demand data. Furthermore, to provide tighter uncertainty sets, an uncertainty set based on the intersection of the previous uncertainty set (SVC-based uncertainty set) and a conventional robust optimization uncertainty set (e.g., Box uncertainty set) is introduced. Mixed-integer programming (MIP) data-driven formulations for each of the introduced uncertainty sets are developed and numerical experiments are conducted. Results show that by using a regularization parameter it is possible to adjust the level of robustness and conservatism in the optimization models.

Fourth, a framework to provide proactive evacuation plans under the risk of unexpected capacity disruptions in the evacuation network is proposed. It is assumed that due to the uniqueness of disastrous events, enough information on the uncertain road disruptions is not available, the uncertainty distributions are not perfectly known, and only partial information on the probability distributions is accessible. The problem is formulated as a distributionally robust data-driven model to ensure that constraints affected by uncertainties are satisfied under any probability distribution consistent with the constructed uncertainty set. Auxiliary variables are introduced to reformulate the problem and build a MIP optimization framework. A heuristic algorithm is introduced to even more reduce the complexity of the problem and decrease its computational time. Numerical experiments indicate that by using the heuristic approach the computational time is significantly reduced. Moreover, compared to the existing deterministic models, the proposed distributionally robust data-driven program can reduce the percentage of disturbed evacuees and negative consequences of road disruptions.

Table of Contents

List of Tables

List of Figures

Chapter 1

Introduction

1.1 Background

Danger and risk are inevitable parts of life. Risk is defined as a process or an event that is potentially capable of causing loss. One of Nature's mandates is posing risk to people's health, lives, and properties. The incidents that are likely to occur have a huge impact on the environment, economic and social processes, and can lead to major casualties or financial loss are called disasters. Disasters are events with low probability and high impact. Every year numerous disastrous events happen all around the world affecting millions of people (see Figure 1.1). They can be categorized in various forms. Examples include biological attacks such as locust attacks, Geophysical (Geological) incidents like earthquakes, volcano, tsunamis, or weather-related events such as storms, hurricanes, droughts, and tornados. The most commonly encountered natural disasters include floods, hurricanes, volcanic eruptions, and earthquakes (Hooke, 2000; Newkirk, 2001). However, disasters do not only arise from nature. Various technological failures and intentional malevolence such as nuclear meltdowns, hazardous-material spills, and terrorist attacks resulting from human deeds can also cause damages to communities.

Despite the scientific and technological advances, it is not possible to fully dominate these events and their negative effects. They are still some of the greatest problems in societies. Table 1.1 indicates the number of losses and fatalities due to the top 10 natural disasters from 1980 to 2015. The significance of the destruction and damage caused by hazardous events is to such an extent that in recent years many international emergency management centers have increased their efforts to make preparation for and carry out all emergency functions necessary to mitigate, prepare for, respond to, and recover from hazardous events.

Vulnerability to disasters is dependent on many factors, including the level of the associated risk, as well as the economic and social growth of the community. Most of the casualties are correlate to less-developed or developing countries. Major economic losses can occur due to disasters. However, a direct threat to human life is considered the most serious and most devastating . In developing countries, due to the growing population, the number of people living in high-risk areas is increasing. In underdeveloped countries, such as Ethiopia and Bangladesh, because of settlements in endangered areas, human casualties are more than economic losses. Meanwhile, after a disaster, developed countries, such as the United States of America and Japan, mostly suffer from financial losses (Smith, 2003).

When assessing the vulnerability of communities to the risks posed by nature, aside from the magnitude and impact of hazardous events, we also need to take into account the hazardous events' frequency of occurrence. Due to climate changes, disastrous events are becoming more frequent. Table 1.2 lists the most recent major disasters (2018 disasters) defined by the Federal Emergency Management Agency (FEMA) in the United States.

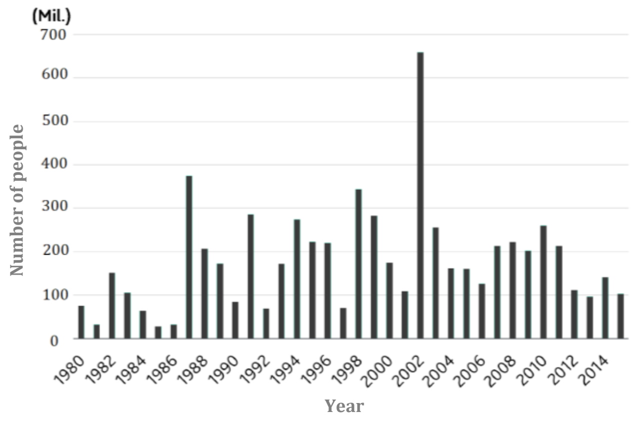

Figure 1.1: People affected by disasters each year (Source: EM-DAT)

One of the most important factors in reducing or mitigating the amount of damage and the number of human casualties is the existence or absence of a proper emergency management system. All states in the United States are required by the US federal government to have a comprehensive emergency management plan. The Comprehensive Emergency Management Model (National Governors' Association, 1978) has four main areas: disaster mitigation, disaster preparedness, disaster response, and disaster recovery. Mitigation, which usually is the first phase of emergency management, refers to the act of reducing damaging consequences and losses due to a disaster. Preparedness includes developing capabilities and plans in order to effectively respond to a disaster. The response can begin before the strike of the disaster or when it begins and comprises actions that take place as a reaction to the event. Often early responses are related to the saving human lives. Recovery actions focus on reconstruction and restoring critical community functions.

Federal and state governments, as well as local authorities (e.g. mayor, city council, county law enforcement, county judge, and county president), are responsible for disaster management. From the early 1980s, the Integrated Emergency Management System

(*IEMS*) has been used by emergency managers to integrate partnerships and coordinate emergency management efforts between government, key community partners, non-governmental organizations (*NGOs*), and the private sector. The system aims in both vertical and horizontal integration. This means that emergency plans at the local level must be provided with respect to related activities of the government. Also, local government plans should be integrated and consistent with the community's vision. Information on primarily responsible agencies and their roles can be found in *USDOT* & *USDHS* (2006).

Table 1.1: Top 10 natural disasters ordered by losses, 1980-2015 (Source: Munich Re, NatCatSERVICE, 2016)

Year	Event	Affected Area	Overall Losses in Mil. US$	Overall Losses as % of GDP	Fatalities
2011	Earthquake, Tsunami	Japan: Aomori, Chiba, Fukushima, Ibaraki, Iwate, Miyagi, Tochigi, Tokyo, Yamagata	210,000	3.6	15,880
2005	Hurricane Katrina, Storm surge	United States: LA, MS, AL, FL	125,000	1.0	1,720
1995	Earthquake	Japan: Hyogo, Kobe, Osaka, Kyoto	100,000	1.9	6,430
2008	Earthquake	China: Sichuan, Mianyang, Beichuan, Wenchuan, Shifang, Chengdu, Guangyuan, Ngawa,Ya'an	85,000	1.9	84,000
2012	Hurricane Sandy, Storm surge	Bahamas, Cuba, Dominician Republic, Haiti, Jamaica, Puerto Rico, United States, Canada	68,500	N/A	210
1994	Earthquake	United States: Northridge, Los Angeles, San Fernando Valley, Ventura	44,000	0.6	61
2011	Floods, Landslides	Thailand: Phichit, Nakhon Sawan, Phra Nakhon Si Ayuttaya, Phthumthani, Nonthaburi, Bangkok	43,000	11.6	813
2008	Hurricane Ike	United States, Cuba, Haiti, Dominican Republic, Turks and Caicos Islands, Bahamas	38,000	N/A	170
2010	Earthquake, Tsunami	Chile: Concepcion, Metropolitana, Rancagua, Talca, Temuco, Valparaiso	30,000	13.8	520
2004	Earthquake	Japan: Honshu, Niigata, Ojiya, Tokyo, Nagaoka, Yamakoshi	28,000	0.6	46

Every year, billions of dollars are spent by states and municipalities for providing and managing emergency response and recovery actions. On the other hand, with the increase in land use, population growth, urbanization, development of countries, as well as climate change, losses from hazardous events has increased. The frequency and intensity of disasters as well as their complexity have an increasing trend. Hence, providing more efficient emergency management decisions and plans have become of great importance. With the advancement of knowledge and technology, we can use scientific innovations in order to effectively and efficiently manage and mitigate disasters.

Table 1.2: US Major disasters in 2018 listed by FEMA

Major Disaster	**Incident Date**
American Samoa Tropical Storm Gita	February 07, 2018
Kentucky Severe Storms, Flooding, Landslides, And Mudslides	February 09, 2018
Ohio Severe Storms, Landslides, And Mudslides	February 14, 2018
West Virginia Severe Storms, Flooding, Landslides, And Mudslides	February 14, 2018
Indiana Severe Storms And Flooding	February 14, 2018
Maine Severe Storm And Flooding	March 02, 2018
New Hampshire Severe Storm And Flooding	March 02, 2018
Maine Severe Storm And Flooding	March 02, 2018
Massachusetts Severe Winter Storm And Flooding	March 02, 2018
New Jersey Severe Winter Storm And Snowstorm	March 06, 2018
New Jersey Severe Winter Storm And Snowstorm	March 06, 2018
New Hampshire Severe Winter Storm And Snowstorm	March 13, 2018
Alabama Severe Storms And Tornadoes	March 19, 2018
Oklahoma Wildfires	April 11, 2018
Hawaii Severe Storms, Flooding, Landslides, And Mudslides	April 13, 2018
Nebraska Severe Winter Storm and Straight-line Winds	April 13, 2018
North Carolina Tornado And Severe Storms	April 15, 2018
Hawaii Kilauea Volcanic Eruption And Earthquakes	May 03, 2018
Maryland Severe Storms And Flooding	May 15, 2018

One of the most important responses to a major disaster is evacuating citizens, as it directly associates with protecting lives. Evacuation is defined as the mass physical movements of people from endangered areas in order to get to safe shelters prior to the onset of, or during, an emergency. It includes decisions on route planning, time and schedule of evacuees' departure, resource allocation, etc. Due to variations in the population of states, geography characteristics, and transportation systems, evacuation plans provided at the state and local levels are different from each other. However, the federal government requires the states to provide evacuation plans using guidelines from the following documents: Robert T. Stafford Disaster Relief and Emergency Assistance Act (*FEMA*, 2014), and *FEMA* Comprehensive Planning Guide 101 (*FEMA*, 2010).

According to a 2005 report by the Nuclear Regulatory Commission (U.S. Nuclear Regulatory Commission, 2005), about every three weeks, the need for the evacuation of 1,000 or more Americans arises. In another report, *FEMA* (2008) declared that, annually, approximately 45 to 75 major evacuations take place in the United States. Also, a recent study by Sandia National Laboratories illustrates that between the years of 1990 to 2003, there have been 230 evacuations involving the movement of more than 1,000 people from their homes or places of work (Jones et al., 2008). The frequency and type of hazard related to these evacuations are depicted in Figure 1.2. Also, evacuation population sizes have been depicted in Figure 1.3.

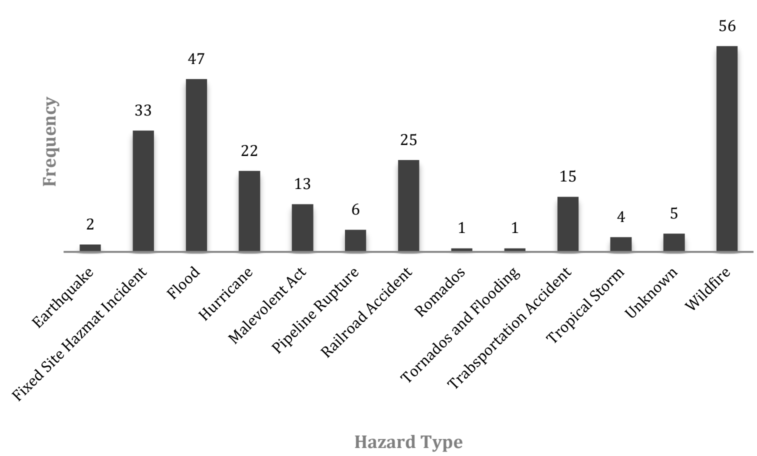

Figure 1.2: Evacuation frequency for different hazard type (Source: Jones et al., 2008)

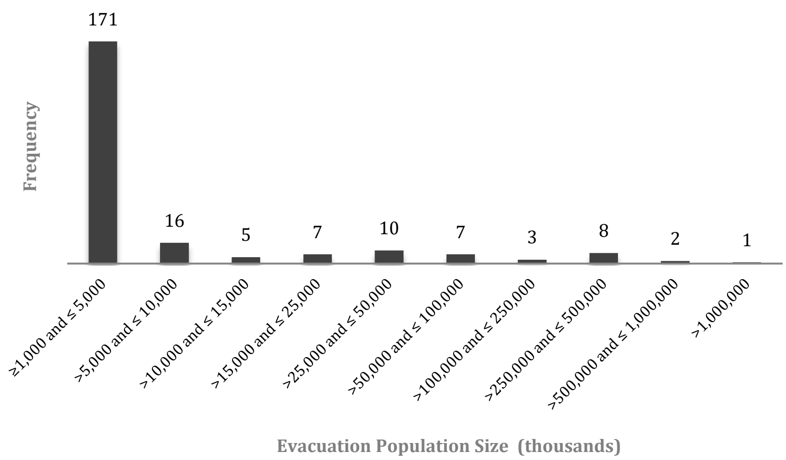

Figure 1.3: Evacuation frequency based on evacuating population size (Source: Jones et al., 2008)

Many researchers have devoted themselves to introducing frameworks that provide efficient evacuation plans. Both simulation and optimization techniques have been used, aiming to analyze and make decisions on route planning and schedule, as well as make predictions on the minimum amount of time required to complete the evacuation process. In our work, we use the theory of dynamic flow optimization in order to represent the highly complex dynamics of route planning in an evacuation network. The main purpose of our research is to provide recovery strategies as well as proactive strategies in the face of unexpected events.

1.2 Evacuation Planning Methodologies

1.2.1 Microscopic and Macroscopic Models

Generally, traffic flow models can be categorized as microscopic or macroscopic models. In microscopic modeling, individual behaviors of vehicles are taken into consideration in the traffic flow model while macroscopic models focus on the movement of a stream of vehicles. Microscopic models use a system of differential equations to represent stream motion, calculate the vehicle position and velocity, and gain an equivalent state. The intelligent driver model (*IDM*) and the Gipps model are examples of microscopic models (Gipps, 1981; Treiber et al., 2000). On the other hand, macroscopic models mostly use Lighthill and Whitham's (1955) equations, as well as Richards's hydrodynamic theory (Richards, 1956) to simulate traffic flow. In fact, compared to microscopic models, they simplify the model by representing traffic patterns as a continuous flow in which hydrodynamic and fluid flow formulations can be applied. Each vehicle is seen as a continuous fluid with a given density and, accordingly, a relationship between speed and density is developed. In Richards's hydrodynamic theory, an increase in density leads to a decrease in the velocity of cars. Using this technique, the model can demonstrate flow changes due to shock waves through the stream of vehicles.

Microscopic models are mostly used in traffic simulation models when simulating individual behaviors are concerned. However, the macroscopic concept is used in both simulation and optimization models. In the following sections, descriptions of the traffic flow simulation platform and optimization techniques are presented.

1.2.2 Simulation Approaches

One of the earliest traffic flow pattern simulators is *NETVAC*, a macroscopic simulation model (Sheffi et al., 1981, 1982). Later it was used for emergency evacuations to simulate flow patterns and estimate clearance times in hazardous situations caused by nuclear power plant accidents. Queue formation, path assignment, the intersection as well as lane controls were included as the evacuation planning options for customizing plan strategies. Interactive DYNamic Evacuation (*IDYNEV*) has been developed by KLD Associates for *FEMA*, providing evacuation route plans for five nuclear power stations using *IDYNEV* as described in *FEMA* (1984). *IDYNEV* has three modules. (i) Traffic assignment module which analyzes traffic routes using static user-equilibrium principle, (ii) Capacity module which analyzes the capacity of the roads, and (iii) Traffic simulation module in which user selected paths of the Traffic assignment module simulates dynamic traffic movements to check road congestions and make decisions on alternate roads if the former are overflowed. One microscopic simulation model, known as *CEMPS* (Configurable Emergency Management and Planning System) and developed by Pidd et al. (1996), Pidd et al. (1997), and de Silva and Eglese (2000) acts as a *DSS* which utilizes the geographic information system (*GIS*). The *GIS* platform is used to manage geographical and infrastructural data and results in visualization as the evacuation plan is developed by the simulation model.

MASSVAC (*MASS* eVACuation) is a macroscopic simulation platform which is able to mimic flow propagation using analytical traffic flow relationships (Hobeika and Jamei, 1985; Hobeika et al., 1994). In this model, the S-shape curve is used to present the demand load for evacuation in endangered areas. *MASSVAC* has been used as the main core module of another evacuation software named *TEDSS* (Transportation Evacuation Decision Support System. *TEVACS* (Transportation EVACuation System) is a decision support system including a macroscopic simulation model (similar to *NETVAC*) for evacuations using public transportation (Han, 1990). This *DSS* considers mixed flows, allowing evacuation to be put into place using different transportation options, such as buses, automobiles, motorcycles and bicycles, etc. *OREMS* (Oak Ridge Evacuation Modeling System) developed in Oak Ridge National Laboratory (*ORNL*) is a microcomputer-based system for comprehensive evacuation planning studies related to natural or man-made catastrophes. It can be used to estimate clearance times, analyzing different traffic management and control strategies and evacuation routes (Rathi and Solanki, 1993).

There are several other traffic flow simulators related to evacuation planning concepts or general traffic simulations. However, most of them focus only on strategy and scenario analysis rather than developing plans (Southworth and Chin, 1987; Church and Sexton, 2002; Chen and Zhan, 2008; Murray-Tuite and Mahmassani, 2004; Theodoulou and Wolshon, 2004; Kwon and Pitt 2005; Yuan et al., 2006, etc).

Using simulation software, one can accurately imitate the behavior of an actual traffic flow and road congestion. However, in order to model the environment, these models require calibration, data collection, and data entrance for the software. Computational time and effort required by microscopic simulation models may lead to an inability to develop traffic flow plans in a limited amount of time. Especially in case of hazardous events in which limited historical information challenges mentioned efforts, and a quick decision on evacuation planning is needed. Macroscopic evacuation simulation models perform better than microscopic simulators when addressing large evacuation networks as they skip the effect of evacuee's behavior and simplify flow movements. However, in general, simulation-based models are better for assessing and analyzing plans rather than developing plans directly. They have a trial-and-error approach for choosing and evaluating strategies. Hence, external efforts need to be done to provide plans on an aggregate level, and then the provided plans can be accurately analyzed by simulation techniques. Optimization models can provide such capability for directly developing plans.

1.2.3 Optimization Approaches

While simulation-based models act as a "what if" procedure to assess a predefined route plan, optimization-based techniques enable us to have a "what to do" methodology and directly develop plans that are optimal. Problems that have been addressed by optimization techniques can be categorized into two categories. (i) Upper optimization level and (ii) Lower optimization level.

In the upper-level network, design problems are taken into consideration and traffic assignment rules are defined. One of the main problems in evacuation network designs is the concept of contraflow operation and intersection. Contra-flow operations correspond to reversing one or more lanes of a highway to be able to travel in the opposite direction. This way capacity of the road in one direction can be increased at the time of evacuation (Urbina, 2002). This approach was first introduced by *FEMA* in the 1980s and originally was considered as an option during nuclear missile attacks.

In the lower optimization level traffic, dynamics and congestion are addressed using dynamic Traffic assignment (*DTA*) models for evacuation purposes. Generally, DTA has evolved from the work of Merchant and Nemhauser (1978a, 1978b). DTA refers to a broad range of problems, with different variables and settings, trying to represent traffic systems. The first mathematical *DTA* formulation (Merchant and Nemhauser 1978a, 1978b) was a deterministic, fixed demand, single-commodity which has been provided for a single-destination network considering system-optimal (*SO*) concept. The model which is also referred to as the Merchant-Nemhauser (*M-N*) model presents travel cost as a function of road volume and, to represent traffic propagation, uses a road exit function. This leads to non-convex non-linear mathematical formulation. The optimum solution of the program is achieved through solving a piecewise linear version of the model (Peeta, and Ziliaskopoulos, 2001). Carey (1987) reformulated the *M-N* problem into a convex non-linear program by changing the exit function by bounding the road outflow. Since then, many models have extended this work, aiming to handle multiple destinations and commodities in a SO setting. The earliest attempt to model a user-equilibrium (*UE*) *DTA* was made by Johnson (1991a, 1991b). The main idea of the model is that instead of instantaneous travel times, it considers experienced travel times to reach an equilibrium. The resulting model is a non-linear mixed-integer program. The first attempt to extend the M-N model to a stochastic model has been made by Birge and Ho (1993). They provide a non-convex non-linear multi-stage stochastic program that considers a finite number of scenarios representing origin-destination desires.

Ziliaskopoulos (2000) proposed a linear program reformulation for the cell transmission model (*CTM*) that was first introduced by Daganzo (1994). The wide concept for studying the macroscopic behavior of traffic is a hydrodynamic theory in which differential equations need to be solved to predict traffic evolution. Daganzo's model (*CTM*) is a discrete approximation of the hydrodynamic model. *CTM* decomposes the link of a network into small, homogeneous segments called cells and calculates flow at the links connecting the cells. The length of a cell equals the distance traveled by free-flow traffic in the corresponding link in a unit of time. The primary advantage of *CTM* is its ability to simulate spillback propagation of congestion. However, the main drawback of the original *CTM* is in its non-linear flow-density relationships. This motivated Ziliaskopoulos (2000) to provide a linear version of *CTM* to optimize routing and traffic controls.

The most commonly used optimization models in the literature of evacuation planning use the LP *CTM* model (literature review of this concept will be provided in Chapter 2). In our work, we use and extend the path-based model (*PBM*) introduced by Lim et al. (2012). Arc-based models such as *CTM* rely on the representation of flow on each arc (or segments of an arc) of the network, increasing the number of variables and constraints of the model and making the problem complex. Rungta et al. (2012) justified the use of *PBM* using an evacuation network in which the *PBM* found an optimal solution in only a few seconds, while the arc-based model could not find a feasible solution after three hours of computation. As mentioned, *CTM* breaks the arc of the network into several sections called cells, and traffic flow is provided for each yielded cell. Variables are defined to represent flow passing through each cell, which makes the problem even more complex. Moreover, as per the *FEMA* report prepared by DOT and DHS (2006), effective implementation and ease of managing routes loaded by evacuation traffic is the most important aspect of an evacuation plan.

In *PBM*, first, a set of paths are prepared to enumerate all possible paths between each *O-D* pair. Path enumeration is possible through obtaining a solution pool of the shortest paths problem or applying a successive shortest-path algorithm. Next, among the available paths, paths that are not considered proper are omitted. Selected paths are then fed into a mathematical optimization model that defines flow and schedule on the paths. Eliminating excess paths reduces the complexity of the model and makes it scalable for large network evacuation networks. Also, *PBM* enables us to address specific desirable functions such as limiting the number of used paths in the plan to avoid using specific paths (e.g. long paths).

1.3 Motivation

Traffic planning in the event of an evacuation can be a very complex problem as it involves dynamics of flow and road congestions, evacuee's behavior as well as unforeseen events. Unless properly planned and implemented, evacuation planning can become a failure in saving lives and precious time. An example is the failure of evacuation efforts prior to and after the strike of Hurricane Katrina. Hurricane Katrina, which struck the Gulf Coast in August 2005, is reported as the third-worst hurricane in U.S. history. The disaster resulted in 1,800 deaths and $81 billion in property damage (The United States Congress, 2006). The major cause of fatalities in the city of New Orleans has been reported by various investigations to be failures due to the evacuation process (Xie, 2008). Just a few weeks later in 2005, Hurricane Rita, the fourth-most intense Atlantic hurricane, produced a significant storm surge, causing about 119 fatalities (113 of those in Texas) and $9.4 billion (Carpender et al., 2006) in damage from eastern Texas to Alabama. In an evacuation effort that has been recognized as the largest emergency evacuation in U.S. history, 2.5 million people left the Houston region. The evacuation was a disaster itself. While local emergency management officials were successful in preparing a plan and setting up evacuation routes, a huge traffic jam was created in the roadway system making it gridlock as a result of an enormous number of vehicles. During the process, many cars ran out of gas and many people left their vehicles behind, altogether, which led to a 100-mile traffic jam. Dozens lost their life from heatstroke, car accidents, and fires. Of 113 people that were killed in Texas, 107 deaths were reported to be due to evacuation and only 6 fatalities were directly because of the storm (wind, water, surge).

Experience from these two major disasters makes it clear that when evacuations are not effectively planned and implemented, the failure experience decreases people's tendency to go through evacuation processes in future events. This can explain why during the hurricane Harvey, which hit the city of Houston, Houston leaders decided not to order mandatory evacuations. Despite the fact that Hurricane Harvey was in the category 4 storm level hitting southeast Texas, Houston Mayor, Sylvester Turner, said at a press conference that although the situation is bad, they would prefer not to call for mandatory evacuation, believing it could worsen the situation. Hurricane Harvey eventually resulted in 107 deaths and $125 billion in damage.

One of the main reasons for evacuation failures is the inherent uncertainty involved in disaster natures. Disastrous events are rare events that do not happen frequently. The nature of each type of event is different, and because of different geographical characteristics and topological differences in regions, they result in different consequences. Hence, limited historical data about them is available which makes one-point predictions hard to make and inevitably unreliable. Lessons learned from previous hazardous event planning and response show that unexpected occurrences or changes in our predictions may result in significant differences in road congestion and evacuation duration. For instance, for the case of hurricane Rita, Harris County emergency evacuation models had predicted 800,000 to 1.2 million people as the estimated number of people who would need to be evacuated, while the actual number of evacuees raised to 1,800,000 from the Greater Houston area, leading to dramatic traffic congestion and delay (Lindell and Prater 2007).

The inability of solutions to deal with deviations in settings can lead to poor results. Inefficient plans which ignore the possibility of interrupting incidents may add to the traffic congestion and spread chaos and panic over the course of the evacuation process. This has motivated us to provide evacuation plans that take into account the occurrence of unplanned events and variation in settings such as network disruptions and/or uncertainty in parameters. There are various sources of uncertainties during evacuations. These can arise from the demand side, for instance, changes in the number of evacuees, their driving behavior, etc. It can also arise from the supply side, such as changes in road capacities, road blockage, limited network connectivity, etc. The intensity and timing of the hazardous event are examples corresponding to uncertainties in disaster characteristics. In our work, we thrive to provide managers with both response plans (recovery strategies) for after realization of unexpected/unplanned events as well as proactive plans which provide resilience under uncertainty of incidents. In the following sub-section, we clearly define the type of settings' variations addressed in our work and our contributions.

1.4 Contributions

Contributions of our work are as follows:

1.4.1 Real-time Reroute Planning under Network Disruption

Many incidents arise during an evacuation process, disturbing the initial plan, and delaying the evacuation process. Examples include car accidents, bridge collapses, roads flooding or any other type of incident during the evacuation that disrupts the evacuation network. Disturbances in road capacity can either be due to infrastructure failures (e.g. road flooding) or due to incidents that arise from traffic flow (e.g. vehicle accidents). If the severity of the incident is not tremendous, it would cause a slight change in the road capacity (capacity degradation). But in severe cases, it would lead to full failure of the capacity (capacity disruption). While the former has been the most common mode of capacity change studies, the latter has seldom come into account in the literature of evacuation planning.

Addressing disruptions in evacuation route planning can follow two approaches. The first approach is to provide an initial plan based on deterministic assumptions. Evacuation paths, flow rates, and schedules are all defined and implemented before, or during a disaster. The progress of evacuation is monitored and if an incident disturbs the evacuation process the need arises to make proper adjustments to the initial plan and provide a quick recovery strategy. The rerouting method is the most often used strategy in response to road closures. It aims to provide alternate paths and schedules in order to use the residual capacity of these paths to get disturbed evacuees to safe shelters. The process of rerouting planning and decisions on the assignment of stocked flow to alternate paths should be quick so that field officers receive the new information as soon as it is available and implement it in a short amount of time to avoid further congestions in the roads.

The second approach for dealing with incidents is to develop proactive plans considering the possibility of road disruptions. This type of plan tries to estimate possible road blockage, their probability of occurrence, and consequent damages that disruptions can have on the network flow. Analyzing these probabilistic consequences, this approach tries to propose a reliable initial plan which can perform well under most of the unexpected probabilistic incidents. The yielded route plan is to be provided before the arrival of an imminent disaster.

In our work described in Chapter 3, we follow the first approach and provide a rerouting plan in response to road incidents in the evacuation network. To the best of our knowledge, there has been only one research addressing road disruptions in evacuation networks. Lim et al. (2016) provide a methodology for real-time rerouting of the disturbed flow using the residual capacity of the evacuation network. The plan is provided to be used as a reaction to the occurrence of a road disruption, meaning that a rerouting mechanism that is introduced can be used after the realization of the road disruption. However, in their work, they have considered that disruption happens only on one road (arc) of the evacuation network. Here, we aim to provide a rerouting plan considering the possibility of disruption on multiple arcs of the network which adds to the complexity of the problem. Further, we assume that disruptions on arcs happen at different times. For better-reflecting traffic dynamics and road congestions, we present a dynamic network flow which, compared to the rerouting mechanism of Lim et al. (2016), is better able to present the traffic dynamics as well as the impact of disruption times on the flow dynamics.

We introduce two preprocessing algorithms to calculate specific parameters associated with road disruptions and the topology of the evacuation network. The use of these parameters enables us to transform the original optimization model into a linear model to reduce the computational burden. Numerical experiments are made to show the performance of the proposed model. Furthermore, the effects of specific features such as disruption time, disturbance location, and the plan updating time on the evacuation process are investigated.

1.4.2 Evacuation Planning under Uncertainty of Network Disruption

As described in the previous sub-section, there are two approaches that can be taken towards network disruptions. The first is to react to the occurrence of the incident (rerouting strategy) and the second is to provide a resilient proactive plan which is less vulnerable to possible network disturbances. The contribution of our work described in Chapter 4 is to propose a proactive plan considering the possible negative effects of disturbances on road congestion and flow.

Referring to literature related to our work, Shahparvari et al. (2017) defined a vehicle routing problem for no-notice evacuations in a bushfire situation. In the same context, disruptions in both route and shelter were addressed by Shahparvari et al. (2016). Both approaches used the chance-constraint method to solve a bi-level optimization model that maximizes the number of rescued evacuees and minimizes resource utilization. However, all of these studies assumed that an incident results in the failure of an entire path (an avenue extending from the origin to the destination point). In more realistic situations, only some sections of a route are affected by incidents; in other words, the entire path is not deemed a complete failure. Moreover, Shahparvari et al. (2017 and 2016) assumed that if a route is disturbed, all the evacuees assigned to it will be lost. The authors did not consider the flow reassignment of the affected evacuees to new pathways (recovery). These underlying assumptions, again, do not mimic real-life situations. In reality, when a road in a route becomes impassable, two distinct courses of action are highly likely: real-time rescheduling would be implemented via the unraveling of alternate routes or evacuees directly involved in the process will naturally begin exploring random routes on their own accord. Thus, to summarize, in these approaches the impact of the recovery after a disruption has been ignored. Another shortcoming of the aforementioned approaches comes from the fact that the scale of time regarding incidents is not considered. The time at which a disturbance may occur on a road is crucial. At a specific time, a disturbance may have a more destructive effect than the same disturbance occurring at a different time. The sensitivity of disruption times is not captured by these approaches.

In our work, we try to provide an improved framework that, unlike previous studies, simultaneously:

(i) Uses a dynamic traffic flow optimization approach and allows for a variation in flow rates over a timespan to capture traffic dynamics,

(ii) Considers disruptions on roads (roads defined to be a section of a path) instead of the entirety of a path within the evacuation network,

(iii) Considers simultaneous disruptions on multiple roads,

(iv) Provides a proactive plan using a two-stage stochastic model.

Two-stage programs have two distinctive components: a structural component that is fixed and free of any noise in its input data, and a control component that is subjected to noisy input data. The mathematical scheme for the program is as follows:

$$\min_{x\in X} \quad \sigma(x, y_1, y_2, \dots, y_s) \tag{1.1}$$

$$\text{s.t:} \quad Ax = b, \tag{1.2}$$

$$B_S x + C_s y_s = e_S, \qquad \forall s \in \text{S}, \tag{1.3}$$

$$x, y_s \geq 0, \qquad \forall s \in \text{S}. \tag{1.4}$$

The upper level of the model only consists of structural components, such as certain parameters and design variables. However, the lower level consists of both structural and control components because of the inherent uncertainty of the problem. All possible uncertain outcomes of the problem are displayed in scenario set S. For instance, for our problem, disruption events on multiple arcs are shown by set S, and each $s \in S$ shows a specific selection of arcs that are considered to be disrupted. The corresponding probability of this disruption is shown by P_s and we have $\sum_{s \in S} P_s$. Variable x shows design variables that are not directly influenced by uncertain set S. Consequently, constraint (1.2) belongs to the first stage since it only includes design and is free of noise variables and parameters. Variable y_s shows recourse variables that are actions that take place in response to the occurrence of an uncertain scenario s. Constraint (1.3) is the recourse constraint and belongs to the second stage since it comprises of recourse variables and uncertain parameters (such as B_S, C_S, etc). The first term of the objective function is a unique decision for the integrated objective function of $\xi = c^T x + d^T y$ which under scenario s with probability P_s is equal to $\xi_s = c^T x + d_s^T y_s$. The overall objective function is considered as $\sigma(.) = \sum_{s \epsilon \mathrm{S}} P_s \xi_s$ as it calculates the expected value of the objective function ξ_s under each scenario $s \in$ S.

In our work, our design variables show an initial reliable proactive plan which is being defined by consequences of road disruption scenarios as well as recourse variables of the model. Our recourse variables illustrate reroute planning which takes place in response to road disruptions under a disruption scenario. In developing the mathematical model, two innovative algorithms are applied for calculating parameters that are influenced by disruption scenarios. Using these preprocessing algorithms, we succeed in proposing a *MIP* program and reducing the complexity of our model to a great extent. The goal of the program is to provide an initial plan which minimizes the expected number of disturbed evacuees that, under different scenarios, cannot be rerouted through alternate paths and get to safe shelters by the end of the planning horizon. Moreover, we introduce two robustness measures to be used to assess the solution optimality as well as solution feasibility under the considered disruption scenarios. A controller is used to adjust the level of these measures and make a trade-off between them.

1.4.3 A Data-Driven Robust Optimization to Handle Demand Uncertainty

As explained in the previous section, one of the challenges to develop a successful evacuation plan is an accurate prediction of demand. Here, demand means the number of people that need to be evacuated through the transportation system. This number depends on the actual number of residents as well as their willingness to be evacuated. Demand estimations for large-scale evacuations often fail to project the actual demand. Also, different demographic information and unpredictability in residents' behavior play an important role in this regard.

Numerous evacuation studies have provided expected value problems considering estimations for the amount of demand. However, since they fail to capture the stochastic nature of the problem, they can lead to inferior or downright inaccurate decisions. What happened during Hurricane Rita is an example of how discarding the unpredictable nature of demand can lead to catastrophic outcomes. This has urged some researchers to study stochastic evacuation problems. This approach, along with robust optimization, is most widely used to deal with parameters' uncertainties. In robust optimization, it is assumed that variations in the uncertain parameter happen in a predefined range, and the goal is to provide a solution that is feasible for all possible occurrences in the range. In stochastic programs, the uncertain parameter is regarded as a random variable to which the theory of probability can be applied. The most commonly used techniques in stochastic programming are chance-constraint programming and two-stage or multi-stage stochastic programming. In this context, the preference is to use chance-constraint programming since, considering the probability distribution of the uncertain parameter, it provides more accurate results. However, using chance-constraint programming is more challenging as it can only be applied in very special cases.

In the era of big data, massive amounts of data are collected by industries motivating a shift toward data-centered decision-making processes directly from the abundant information. Accordingly, data-driven robust optimization attempts to use the intrinsic structure behind data to handle variations in data. Recently, more and more machine learning techniques have been employed for efficient pattern recognition for data sets. This has led a number of researchers to study the integration of machine learning into the optimization-based frameworks.

The contribution of our work is to use support vector clustering (SVC) as an unsupervised machine learning technique to derive an appropriate convex uncertainty set for the number of people who will be evacuating from endangered locations. We develop a data-driven evacuation planning optimization framework by constructing an "SVC-based" uncertainty set to find the robust evacuation route plans and flow schedules. Furthermore, we study the intersection of the "SVC-based" uncertainty set and a conventional robust optimization uncertainty set, e.g., box uncertainty set, and introduce the "Box+SVC-based" uncertainty set. Then, we develop a data-driven robust model associated with the "Box+SVC-based" uncertainty set in order to study the effect of reducing superfluous coverage of demand data points on the induced evacuation plan.

1.4.4 A Distributionally Robust Chance-Constraint to Handle Uncertain Network Disruptions with Unknown Probability Distributions

Huge delays and long congestion may occur if officials fail to provide effective evacuation plans that perform well under the occurrence of unexpected events and uncertainty of a disastrous situation. The capacity span of the roads can be severely reduced due to the rise in water level and flooding, wild-fire propagation, sinkholes, collapse of highway structures, debris fallen on road surfaces, etc. Effective decisions for the evacuation process considering the possibility and extent of these uncertain incidents can help to provide a complete evacuation with reduced risk of chaos, resource waste, injuries and fatalities, and prolonged delays.

In our work, we consider an evacuation planning problem subject to the risk of multiple road capacity failures. The purpose is to take into account the probable capacity disruptions during the allocation of routes and schedules in order to provide a pro-active evacuation plan that is less negatively affected after the actual realization of each probable disruption. The problem is formulated based on the dynamic network flow optimization to better project variations of evacuees' flow throughout the evacuation process. Moreover, a path-based approach introduced by Lim et al. (2012) which decomposes path generation from traffic flow assignment is applied to reduce the computational burden and make the model scalable for large networks. The road capacities are considered as uncertain parameters and, due to the uniqueness of hazardous events, it is assumed that there is not sufficient data to properly estimate the probability distribution function of the uncertain parameters and only partial information is obtainable. A distributionally robust data-driven optimization framework is introduced and is used to handle a lack of full knowledge on probability distributions. Using the mean and covariance (i.e., the first and the second moments) of the uncertain parameters, a convex uncertainty set for the unknown distributions is constructed. The constraints subject to uncertainties are satisfied under the uncertainty set that includes all types of probability distributions consistent with the assumed available partial information (e.g. the first two moments).

For an uncertain constraint of the form $F\big(x.\tilde{\xi}\big) \leq 0$ where $\tilde{\xi}$ is a random vector demonstrating uncertain parameters, and F is a function describing a performance measure in a particular system, the counterpart chance-constraint with confidence probability $(1-\epsilon)$ will be

$$\mathbb{P}\big(\mathrm{F}\big(\mathrm{x}.\tilde{\xi}\big) \leq 0\big) \geq 1-\epsilon. \tag{1.5}$$

Here, $\mathbb{P}$ is a probability measure associated with a random vector $\tilde{\xi}$ and $(1-\epsilon)$ is the confidence level of which we would like the chance constraint to reach $(\epsilon \in [0,1))$. Meaning that the probability that the uncertain constraint $F\big(x.\tilde{\xi}\big) \leq 0$ holds should be greater than the confidence level $(1-\epsilon)$.

Chance-constraint (1.5) inherently is computationally intractable for many cases. In some special cases, if the cumulative distribution function (CDF) of $\tilde{\xi}$ is known, it is possible to drive a deterministic reformulation of the probabilistic constraint by using the inverse distribution function of the uncertain parameter. However, in most cases even if the probability distribution function is known, researchers must come up with appropriate approximations of chance constraints in order to be able to solve the corresponding program.

Meanwhile, information that we have on the probability distribution function of the random vector $\tilde{\xi}$ plays a crucial role in how we can manage the chance-constraint. In all cases discussed above, it has been assumed that full information on the probability distribution function is available. However, for the case of mass evacuations, due to insufficient data, it can be very difficult to accurately identify this function.

In our work, we consider road disruption uncertainty as well as the ambiguity of disruption distribution. Meaning that we assume only partial information (Moments) of the probability distribution function of disruption is available. We define a set $\mathcal{P}$ that shows all possible probability distributions consistent with the known properties of $\mathbb{P}$ (the same moments). Then, in the distributionally robust chance-constrained modeling concept the probabilistic constraint should be satisfied for all $\mathbb{P} \in \mathcal{P}$ as

$$\mathbb{P}\left(F\left(x.\tilde{\xi}\right) \leq 0\right) \geq 1-\epsilon, \quad \forall \mathbb{P} \in \mathcal{P}. \tag{1.6}$$

As the formulation of the produced distributionally robust chance-constrained program for the evacuation problem is computationally intractable, we introduce auxiliary variables to decompose the constraint under uncertainty and reformulate the problem into a MIP formulation. Next, we use Chebyshev inequality to derive a tractable approximation for the distributionally robust chance-constrained program. Moreover, we introduce a heuristic solution methodology to reduce the complexity of the model and speed up the solution time.

1.5 Outcomes

Journal Publications

- Darvishan, A., Lim, G., Fan, L. (2020). Dynamic Network Flow Optimization for Real-time Evacuation Reroute Planning under Multiple Road Disruptions, *Reliability Engineering and System Safety*, (minor revision).

- Darvishan, A., Lim, G. (2020). A Two-Stage Stochastic Model for Evacuation Planning: Adjusting the Plan Robustness under Possible Road Disruption, *Transportation Research Parts C: Emerging Technologies*, (under review).

- Darvishan, A., Lim, G. (2020). A Data-Driven Robust Optimization Approach for Evacuation Planning under Demand Uncertainty, *Socio-Economic Planning Sciences*, (under review).

- Darvishan, A., Lim, G. (2020). A Distributionally Robust Data-Driven Model for Evacuation Planning under Uncertain Network Disruption, (draft completed).

1.6 Organization

This thesis is organized as follows. Chapter 2 provides a comprehensive literature review for the related research on deterministic evacuation programs, uncertain evacuation programs as well as most relevant researches to our work. In Chapter 3 we present a novel optimization framework for real-time reroute planning of disturbed flow under network disruption. Two different formulations are introduced for the problem. We conduct numerical experiments to measure the performance of the two models as well as sensitivity analyses on the evacuation process. Chapter 4 is devoted to describing how our two-stage stochastic model is aimed at providing proactive plans in face of probable evacuation road disruptions. Two innovative algorithms used in the model are presented for calculating input parameters which, without them, developing a linear mathematical formulation is impossible. The performance of our stochastic solution is compared with solutions derived from deterministic models using different sample sets. In Chapter 5, we introduce two different uncertainty sets for the evacuation planning problem under uncertainty of demand. The "SVC-based" uncertainty set is built using Support Vector Clustering, and the "Box+SVC-based" uncertainty set is built by intersecting the "SVC-based" uncertainty set with a conventional uncertainty set used in robust optimization. Two MIP data-driven robust optimization models corresponding to the uncertainty sets are developed and their performances under different test samples are studies. Chapter 6 develops a distributionally robust chance-constrained model to account for uncertainty in road distributions in the evacuation planning model. A distributionally robust model is proposed assuming that only partial information on the probability distribution function of road disruption times is available (the first two moments are known). The plan feasibilities of these robust models are compared with the feasibility of plans derived from chance-constraint programs under different demand scenarios. Finally, in Chapter 7 future research direction that can be pursued is discussed.

Chapter 2

Literature Review

Interest in evacuation planning problems has been started by the nuclear power plant accident occurring at Three Mile Island, Pennsylvania in March 1979. In the following years government agencies such as *FEMA*, Nuclear Regulatory Commission (NRC) and the U.S. Army Corps of Engineers have sponsored a number of evacuation planning research projects. Initial research on this concept has been published by Chalmet et al. (1982) in which a network model has been proposed for emergency building evacuations. Over the years research on this problem has evolved to provide realistic evacuation plans. A comprehensive survey on evacuation planning can be found in Hamacher and Tjandra (2002), Wolshon et al. (2005), Yusoff et al. (2008), Abdelgawad et al. (2009), Renne et al. (2011), Murray-Tuite and Wolshon (2013), and Bayram et al. (2016). A brief review of simulation and OR techniques has already been provided in the previous chapter. In this chapter, we mainly focus on the literature of works that are most relevant to our work.

2.1 Deterministic Approaches

The vast body of the literature has focused on deterministic evacuation plans. Yamada (1996) proposed two models based on network flow optimization techniques aiming to minimize the total distance traveled by evacuees. Contra-flow strategy in which lanes of roads are reversed to increase the capacity of a road has been investigated by researches such as Cova and Johnson (2003), Kim and Shekhar (2005), Kalafatas and

Peeta (2009), Xie et al. (2010), Karoonsoontawong and Lin (2011), Bretschneider and Kimms (2011), Wang et al. (2013) and Zhao et al. (2016). The related model presented by Cova and Johnson (2003) and Bretschneider and Kimms (2011) uses the network flow concept and Kalafatas and Peeta (2009), Xie et al. (2010), Karoonsoontawong and Lin (2011) and Zhao et al. (2016) developed their model based on *CTM DTA* models. A *CTM*-based system optimal (*SO*) model considering contra-flow has been developed by Tüydeş (2005) in which applies evacuation zone planning.

Using a static model Han et al. (2006) investigated route planning and shelter assignment problem. Decisions on simultaneous shelter assignment, route planning and departure times (schedule) have been studied by Chiu et al. (2007). Kimms and Maassen (2011a, 2012a, 2012b) applied *CTM* model on a large evacuation plan. In their work Kimms and Maassen (2011b) apply an optimization-based simulation method to provide route plan and schedule plan for a neighborhood in the city of Duisburg, Germany.

Dynamic network flow optimization technique has been used by various researchers as it can better project traffic dynamics (Hamacher and Tjandra, 2001; Lu et al., 2005; Kim and Shekhar, 2005; Kim et al., 2007; Lim et al., 2009; Bretschneider and Kimms 2011, 2012; Hamacher et al., 2013; Lim et al., 2012; Bretschneider, 2013; and Pillac et al., 2015, 2016). Lu et al. (2005) used time-expanded networks to minimizes network clearance time assuming the roads were capacitated. As the solution approach, a heuristic algorithm was proposed to define route assignment and flow schedule. Kim et al. (2007) improve this heuristic method to decrease the computational time of the algorithm. Kim and Shekhar (2005) used a greedy algorithm considering a time-expanded network in which decisions on contra-flow can be made to increase network capacity. A heuristic binary search algorithm has been provided by Lim et al. (2009) in which based on maximum dynamic network flow problem defines route and schedule for short notice evacuations. Hamacher et al. (2013) used dynamic network flows and locational analysis methods to provide evacuation plans. They considered both the supply and demand side of the evacuation, trying to find routes to be used by emergency units on the roads to get into a disaster zone and guide evacuees to get away from the endangered zones.

Various researchers have developed heuristic models or approaches in order to handle large-scale evacuations. Aiming to minimize evacuees left behind during an assumed planning horizon, Lim et al. (2012) presented a new path-based model to find optimum evacuation paths, flows, and schedules. A Dijkstra’s algorithm was used for decisions on paths a greedy algorithm is utilized to find the maximum flow to be assigned to each path and schedule of dispatching the flow in assumed time intervals. Bretschneider and Kimms (2012) presented a two-stage heuristic mathematical model using a dynamic network flow optimization concept to capture traffic dynamics and provide evacuation plans for urban areas. Pillac et al. (2015) used a column-generation approach to jointly optimize resource mobilization and evacuation planning for large-scale evacuations. A conflict-based path-generation approach was developed by Pillac et al. (2016) decomposing the problem into a master problem and a subproblem. While the master problem defines flow assignment to the evacuation plan, the subproblem generates evacuation routes lazily for evacuated areas.

Bi-level (BL) models have been proposed by Xie and Turnquist (2009), Abdelgawad and Abdulhai (2009), Xie et al. (2010), Ng et al. (2010), and Karoonsoontawong and Lin (2011). The upper bound of the program addresses decisions on shelters considering system optimal approach and having the defined shelters, the lower level tries to dispatch evacuees on routes using *UE* concept. Another bi-level program has been proposed by Liu and Luo (2012). In the upper level, optimal set of intersections and control strategies are defined for uninterrupted flow while the lower level considers traffic assignment based on SUE principle.

During evacuations, congestion can be reduced either by supply or demand management actions. Demand-based strategies (such as staging) have been used by several researches in order to reduce or eliminate flow congestion. Bish and Sherali (2013) examined the effectiveness of aggregate-level and staged evacuation process as a demand-based strategy in an evacuation network. The *CTM* based model was used to compare the effects of free-flow strategies with strategies under congestion in relation to tractability, normative optimality, and robustness of the solution. Bish et al. (2014) developed a CTM-based model that applies household-level (disaggregate) demand strategies for different flow types. Considering a fixed planning horizon, Tüydeş and Ziliaskopoulos (2014) provided a *CTM*-based *SO DTA* program applying demand strategies known as staggered evacuation or staging to obtain optimal zone evacuation scheduling. Hsu and Peeta (2014) proposed a framework to define risk-based evacuation subzones for stage-based evacuations. So and Daganzo (2010) proposed a simple control strategy decentralized evacuation management which is adaptive and based on real-time traffic information instead of demand estimations. Aiming to improve evacuation operations in both spatial and temporal dimensions, He and Peeta (2014) and He et al. (2015) considered the problem of dynamic allocation of movable response resources on large-scale transportation evacuation networks.

2.2 Uncertainty in Evacuation

One of the major problems associated with the development of accurate route plans and schedules is the uncertainty inherent to a hazardous situation, human behavior, and hence the evacuation process. Deterministic assumptions on parameters can lead to poor results due to the inability of solutions to deal with related deviations. As found in (Lindell and Prater 2007), there was a large difference between the estimated number of evacuees (686,000) and the actual number of evacuees (1,800,000) from the Greater Houston area during Hurricane Rita, which led to dramatic traffic congestion, and fatalities not caused by the hurricane itself (O'Driscoll et al., 2005). It is also highly probable that in a hazardous situation evacuation network loses whole or part of its capacity (e.g. due to flood or debris which has been made by collapsed buildings or landslides). In 1985, the Mexico City earthquake resulted in the loss of nearly 70% of the central transportation network (Ardekani and Hobeika, 1988). If variation in these parameters is ignored, the resulting plan can be inefficient in face of hazards, chaos and panic can be spread over the course of the evacuation process, and further injuries and fatalities may occur. However, very limited researches have addressed uncertainties in their studies.

Research focusing on uncertainty of parameters such as demand and capacity in evacuation modeling has mostly been addressed via chance-constrained programming and robust optimization. Waller and Ziliaskopoulos (2006) first used a chance-constrained program for the traffic assignment problem under a uniform distribution for traffic demand. A two-stage stochastic program was proposed Ukkusuri and Waller (2008) for evacuation planning under uncertainty of demand. Their result showed that if the uncertainty is neglected, the quality of the solutions degrades significantly. Wang et al.

(2016) used a scenario-based stochastic program to deal with uncertain capacities and travel times. Three criteria are considered for evaluating traffic routing plans and crisp linear equivalents of the strategies are used in the solution methodology. Yao et al. (2009) applied a robust optimization technique to address demand uncertainty. Chung et al. (2011) used box uncertainty sets to provide a linear tractable robust model for a system optimal dynamic traffic assignment model ($SO\ DTA$) under demand uncertainty. Goergik, et al. (2016) considered solution ranking as well as objective ranking robustness for the problem of evacuation planning. In their approach, the degree of robustness of a solution is defined by using solution ranking procedures which include both quantitative and qualitative aspects. Tarhini and Bish (2016) used a cell transmission model (CTM) for a dynamic traffic assignment (DTA) problem considering the system optimal (SO) approach instead of the commonly deployed user-equilibrium based concept. This makes the model be relevant to regional evacuation planning problems.

Yazici and Kaan (2007) proposed a chance constraint program to address uncertainties in road capacities when the distribution of the capacity of the links is known. Lim et al. (2015) used a chance-constrained model to analyze the reliability of an evacuation plan considering the uncertain capacity of road links where the uncertain capacity is modeled using a Weibull distribution. Lv et al. (2013) applied a joint-probabilistic constrained (JPC) technique for the case of a nuclear emergency evacuation. In the proposed model, uncertainties expressed as joint probability and interval values are addressed by incorporating interval-parameter programming and joint-chance constrained techniques. In all of the above studies, a priori knowledge of the underlying distribution is required.

2.3 Most Relevant Studies

As explained in the introduction, our studies can be summarized in four major categories:

- Providing an effective rerouting plan as a recovery strategy in response to an unforeseen real-time event of road disruptions. Since rerouting happens after the realization of the disruptions we assume deterministic settings.
- Developing a two-stage stochastic program in order to provide pro-active plans which mitigate negative consequences of probabilistic road disruptions.
- Developing a data-driven robust optimization framework based on uncertainty sets built using SVC and intersection of SVC and Box uncertainty to handle uncertain evacuation demand.
- Presenting distributionally robust chance-constrained programs which act as pro-active plans under uncertainty of road distribution times.

In the following subsections, the most relevant researches to our work will be presented.

2.3.1 Real-Time Evacuation Reroute Planning

In chapter 3, we propose two MIP mathematical formulations for the problem of rerouting the disturbed flow after the occurrence of road closures in evacuation networks. Few studies have reported investigations on the real-time rerouting of vehicles in the transportation network. Akgün et al. (2007) proposed a heuristic approach to find a new path for vehicles exposed to the effects of weather systems. A modified Dijkstra algorithm and heuristic dynamic programming has been applied by Kok et al. (2012) to select new routes to reduce traffic congestion. Several traffic rerouting strategies were suggested by (Pan, J., Popa, I. S., Zeitouni, K., & Borcea, C., 2013) to prepare traffic guidance for vehicles in order to avoid congestions observed on roads and reduce travel time. Desai and Lim (2013) used a stochastic dynamic programming (SDP) approach to obtain optimal real-time modifying policies for hazmat vehicles. Dynamic rerouting vehicles used in agricultural operations were investigated by Seyyedhasani and Dvorak (2018).

Related to the evacuation planning context, Lim et al. (2016) provided a preprocessing algorithm that utilizes a path-based network flow optimization approach to reassign paths for evacuees affected by an incident, assuming the availability of real-time traffic information. However, there are two limitations to their work. First, their model is limited to a single road incident. Second, evacuation vehicles are assumed to join the evacuation routes at a constant flow rate. Both assumptions are less realistic because multiple road disruptions can occur at any time, and the vehicle flow rate joining major evacuation routes can vary over the evacuation planning horizon. Therefore, the purpose of this paper is to provide an approach to relax both of the assumptions within the context of a dynamic network flow optimization, in which a variable vehicle flow rate is assigned to each time interval of the planning horizon, and disruptions can occur on multiple roads of the network. The number of evacuees leaving the intermediate nodes into new pathways in the network can vary in each time interval, which results in a more realistic representation of evacuation flow dynamics and congestion.

2.3.2 Two-stage Proactive Plan under Uncertain Disruptions

In chapter 4 we address emergency evacuation management and provide proactive reliable evacuation plans considering possible road disruptions. Generally, disruption at roads can be of two types: Complete and partial disruptions. Depending on the severity of the incidents, different approaches can be considered. If the disturbance in the capacity of the network infrastructure is not intense (road capacity degradation), the capacity can be considered as an uncertain parameter that deviates slightly from what it has been expected. This uncertainty had been addressed in the literature by either considering capacity as an uncertain parameter that follows a probability distribution (Stochastic Programming) or by defining a specific set for the parameter and derive a plan that can be feasible for the worst-case scenario of its realization (Robust Optimization) in which review of them has been provided in the last sub-section. On the other hand, if the level of infrastructure degradation is intense, it will be regarded as a failure or disruption in the infrastructure (road disruption). In this case, since the link is completely blocked, residents need to be re-routed in order to reach the safe areas. This assignment to alternative routes should be with respect to the residual capacity of other roads.

There are few studies that have presented route scheduling for short-notice evacuations under uncertainty of road disruptions in a bushfire situation in Australia (Shahparvaria et al., 2016; Shahparvaria et al., 2017). However, in these studies for obtaining their reliable plan it has been considered that after disruption in a specific route, all of the evacuees that according to the proactive plan had been assigned to the path will be lost. However, this robust plan cannot be accurate since the underlying assumptions do not mimic the real case situation. In reality, when a road in a route is blocked either real-time rescheduling would be prepared and implemented in order to get people to safe destinations via alternate routes, or people would arbitrarily change their routes and inefficiently add to the congestion of other routes. Thus, the impact of the rerouting had been ignored in the proposed reliable plans. Rerouting the disturbed flow on one way reduces number of lost evacuees and on the other way adds to the congestion of other roads and increases total clearance time. For instance, while one route might have a higher number of assigned evacuees, after disruption rerouting its flow may be easier resulting in fewer injuries or evacuees loss. This happens when based on the topology of the network, the connectivity level of the disturbed link is high. Moreover, we also need to take into account the time at which disturbance may occur for each link. For example, at a specific time disturbance may have a more destructive effect since its connected alternative paths are highly congested (flow-based importance). A methodology that uses the residual network in order to manage real-time evacuation reroute after the case of road closure in the evacuation network is proposed by Lim et al. (2016). The goal of the research effort is to minimize further delays that may happen due to the rerouting. However, the plan only works as a recovery strategy after the realization of disruption and fails to consider the probability of different disruption scenarios and providing pro-active plans. The innovation of our work to previous related works is filing the gaps illustrated in Table 2.1.

Table 2.1 summarizes the features of our proposed model in comparison to others in the literature. These features include consideration of the incident uncertainty, type of disturbed infrastructure (a road or an entire path from origin to a destination point), existence of a pro-active agenda or a recovery strategy, and usage of a variable or steady flow rates.

Table 2.1: Comparison between Respective Research Efforts with Current Study

Research effort	Uncertainty	Infrastructure	Pro-active Plan	Recovery	Flow Rate
Lim et al. (2016)		Road		✓	steady
Shahparvari et al. (2017)	✓	Path	✓		-
Shahparvari et al. (2016)	✓	Path	✓		-
The Proposed Study	✓	Road	✓	✓	Variable

2.3.3 Data-Driven Robust Optimization Based on SVC

In chapter 5, we address emergency evacuation management under uncertainty of demand and introduce data-driven robust optimization frameworks for the problem based on machine learning techniques. Robust optimization has extensively been studied in the literature on evacuation planning. A robust linear programming model under uncertainties of surface transportation networks has been introduced by Ben-Tal et al. (2009) to mitigate the loss of life or property. A linear Cell Transmission Model (CTM) based on an affinely Adjustable Robust Counterpart (AARC) is introduced by Yao et al. (2010) considering box and polyhedral uncertainty sets. Kulshrestha et al. (2011) used a robust approach to find optimal locations of public shelters and their required capacities under the uncertainty of the number of evacuees. The linear tractable robust model based on box uncertainty sets is used by Chung et al. (2011) to address demand variations in a system optimal dynamic traffic assignment model (SO DTA). Bolia (2020) studied public transit-based emergency evacuation and used a robust optimization approach to cope with external environmental uncertainties, specifically evacuation demand uncertainty, by providing robust solutions. Wang and Paul (2020) proposed a single-stage, adaptive robust model to find the optimal evacuation time and make a trade-off between increasing evacuation costs and reduced uncertainty given the time-variant characteristics of hurricanes. Hypothesis testing has been employed by various researchers to identify the worst-case realization of parameters in the uncertainty sets. Linear regression and the t-test have been employed by Goldfarb and Iyengar (2003) to construct and calibrate an uncertainty set using the moment information of the distribution. Pearson's $\chi 2$-test has been used in Klabjan et al. (2013) to introduce a data-driven distributionally robust dynamic program. A comprehensive investigation on the connection of hypothesis testing and data-driven uncertainty set construction has been presented in Bertsimas et al. (2018).

A number of researchers attempted to integrated machine learning methods for pattern recognition into optimization-based frameworks to handle the uncertainties in the input data. Ning and You (2017) employed a Dirichlet process mixture model and used a variational inference algorithm to capture the distribution of data. The machine learning technique was used to build an uncertainty set to be used in a four-level adaptive robust optimization framework. Shang et al. (2017) investigated the idea of using kernel density estimation (KDE) and support vector machines (SVM) to derive an uncertainty set from available data. They showed that using such an unsupervised learning approach enables to systematically derive an appropriate uncertainty set that is more realistic to actual events. Ning and You (2018) proposed a novel multi-objective, adaptive robust optimization for process network planning and the batch process scheduling problem that incorporates the minimax regret criterion into the multi-stage optimization framework. Shang and You (2019) used support vector clustering (SVC) to learn a polytypic high-density region of data to propose a data-driven uncertainty set to be used in a stochastic model predictive control (SMPC).

To overcome the shortcomings of existing approaches in evacuation planning, we propose a data-driven robust optimization framework directly built upon demand data structure using an unsupervised machine learning approach. We introduce two ways to define the demand uncertainty set depending on the emphasis in evacuation planning. The first approach is to define an uncertainty set to cover evacuation demand data using support vector clustering (SVC), which is suitable when a systematic approach is desired. The second approach is a new uncertainty set by intersecting the "SVC-based" uncertainty set and box uncertainty set. This can be particularly useful when it is desired to reduce the cost of robustness (evacuation efforts) when the level of conservatism is high.

2.3.4 Unknown Distribution of Uncertain Road Disruptions Times

In chapter 6, a distributionally robust approximation for an evacuation planning chance-constraints problem will be presented under unknown distributions of the road disruption times. General chance-constrained models are computationally intractable. Significant research efforts have focused on coming up with a safe and tractable approximation of chance constraints (Geletu et al. 2013). Bernstein approximation for the chance-constrained program has been developed by Nemirovski and Shapiro (2007). They showed that the yielded model is convex and tractable (can be efficiently solved). Few researchers (Calafiore and Campi, 2005; Erdogan and Iyengar, 2006; Luedtke and Ahmed, 2008) have proposed to substitute the chance-constraint with a point-wise constraint which is feasible under a finite number of scenarios drawn randomly from the distribution $\mathbb{P}$. The proposed approach yields a convex problem, however, the sampling method might be computationally intensive for the case of large problem sizes. Zymler et al. (2013) developed tractable semi-definite programming base approximations for both individual and joint chance constraints for the case that second-order information is available. This approximation can only be achieved when the decision vector is a convex closed set. Calafiore and Ghaoui (2006) showed that when the confidence level is more than 0.95, an individual chance constraint can be converted a to second-order cone constraint if the random parameter has a radial distribution.

Ng and Waller (2010) and Ng et al. (2011) considered unknown distributions and used Markov's inequality to derive a bound on travel time reliability. However, if more information is available on the probability distribution function of the uncertain parameter this bound might not be tight enough and can be over-conservative. Ben-Tal et al. (2011) extended a robust optimization approach for multi-period transportation problems and apply an affinely adjustable robust counterpart (*AARC*) approach to consider "wait and see" decisions for dynamic traffic assignments. They applied the robust optimization framework to an emergency logistics planning problem and show that the *AARC* solution provides excellent results when compared to the solutions from deterministic linear programming and stochastic programming based on Monte Carlo sampling. Lv et al. (2015) coupled chance-constrained programming with an interval chance-constrained integer program (*EICI*) in order to cope with interval uncertainties that cannot be addressed by any specific distribution functions. Chung et al. (2012) used moment information to formulate a distributionally robust chance-constrained model which allows them to derive a deterministic approximation of their model. Ng and Lin (2015) proposed an approximation of the chance-constrained cell transmission model (*CTM*) for the case that only the first and second moments of demand and capacity are known. Although the probability inequalities that they used for demand constraint is similar to the work of Ng and Waller (2010), by using Cantelli's inequality, they provide sharper equalities for approximating capacity constraints.

In our work, we investigate emergency evacuation planning problem considering uncertain road capacity disruptions in the network. Unlike previous studies, we introduce an improved framework that: (i) Provides a pro-active plan which is less interrupted by the occurrence of probable road disruptions; (ii) Better projects traffic dynamics by employing dynamic traffic network flow optimization approach which allows for variation in flow rates over the planning horizon; (iii) Provides more realistic results considering disruptions on roads (roads defined to be a section of a path) instead of an entire path in the evacuation network; (iv) Assumes simultaneous disruptions on multiple roads in the evacuation network; (v) Makes no assumptions on the type of uncertainty distributions, considers that the probability distribution functions of road disruption times are not fully known and only partial information (the first two moments) are accessible; (vi) Provides a distributionally robust optimization model which ensures that the constraints subject to parameter randomness are satisfied under actual distributions consistent with the ambiguity set built upon the distributions' moment information. To the best of our knowledge, there is no study in the literature of evacuation planning that has incorporated all of these features.

Chapter 3

Real-time Evacuation Reroute Planning under Road Disruptions

3.1 Introduction

The motivation of this chapter is to provide emergency managers with a real-time rerouting scheme to be used in the case of network disruptions. Effective evacuation process includes two phases: The first phase is to develop route planning and schedule for the flow before the arrival of a hazard. The second phase aims to monitor the progress of hazards as well as the initial evacuation plan, detect deviations from the plan, and make adjustments to the initial plan if necessary.

During the course of an evacuation, many unforeseen events can happen. Roads may become impassable due to road flooded, sinkholes in the roads, railway barriers at railroad crossings, debris fallen on road surfaces, accidents or collapse of highway structures caused by high winds, or subways submerged with stormwater, etc. These Real-Time Events (RTE) can disrupt the initial evacuation plan and change the flow congestion as well as the time required for evacuees to clear the network. Since they can heavily affect the safety of people being evacuated, a quick and effective decision on rerouting disturbed flow through alternative paths is of great importance.

While there have been some studies on reroute planning in Vehicle Routing Problem (VRP) or related to dynamic traffic assignment (DTA), yet to the best of our knowledge there has been only one work addressing the evacuation process. Lim et al. (2016) provided a preprocessing algorithm that utilizes a path-based network flow optimization approach to reassign paths for evacuees affected by an incident, assuming the availability of real-time traffic information. However, there are two limitations to their work. First, their model is limited to a single road incident. Second, evacuation vehicles are assumed to join the evacuation routes at a constant flow rate. Both assumptions are less realistic because multiple road disruptions can occur at any time, and the vehicle flow rate joining major evacuation routes can vary over the evacuation planning horizon. Therefore, the purpose of this paper is to provide an approach to relax both of the assumptions within the context of a dynamic network flow optimization, in which a variable vehicle flow rate is assigned to each time interval of the planning horizon, and disruptions can occur on multiple roads of the network. The number of evacuees leaving the intermediate nodes into new pathways in the network can vary in each time interval, which results in a more realistic representation of evacuation flow dynamics and congestion.

3.2 Problem Statement

Traffic flow and congestion on the evacuation network are represented through a dynamic network flow problem. A dynamic network is composed of multiple static networks in which each static network depicts the status of the network at a specific time (Ford Jr and Fulkerson, 2015). Let us consider a directed network $\mathcal{G} = (\mathcal{N}, \mathcal{A})$ consisting of a set of nodes $\mathcal{N}$ and a set of arcs $\mathcal{A}$ (see Figure 3.1). The nodes are categorized as origin nodes ($\mathcal{N}_o$), intermediate nodes, and destination nodes ($\mathcal{N}_d$). The planning horizon is divided into discrete time intervals represented by set $\mathbb{T} = \{0, 1, \ldots, \mathrm{T}\}$. A traffic assignment on this network relies upon a representation of traffic as a series of vehicle flows at each time interval as per the topology of the network. The transit time of arc $a \in \mathcal{A}$ is shown by τ_a, and the time it takes to reach arc $a \in \mathcal{A}$ from the origin of path $p \in \wp$ is denoted by θ_{pa}.

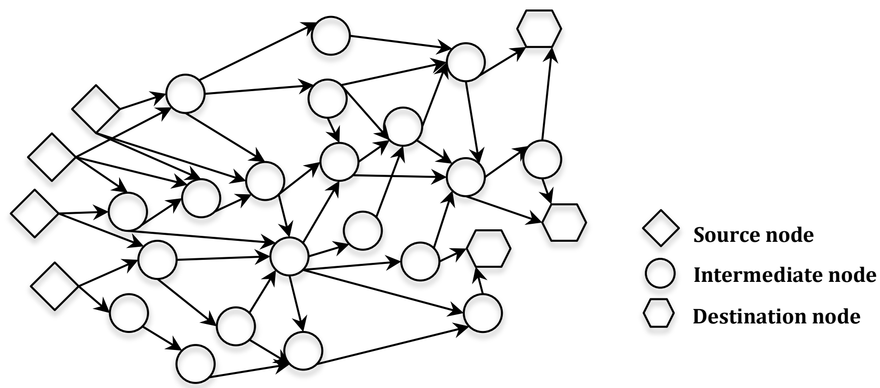

Figure 3.1: A directed graph representing an evacuation network

A path-based approach is followed to reduce the computational complexity of our evacuation rerouting problem. Consequently, all possible paths between each origin-destination (O-D) of the evacuation network are generated and enumerated *a priori* which are defined as in set $\wp$. Parameter DT_a is used to denote the disruption time on each arc $a \in \mathcal{A}$. The aim of the rerouting path-based model ($RPBM$) is to optimally utilize the residual capacity of the road networks to reassign the disturbed evacuees to new paths such that the overall evacuation reroute completion time is minimized.

The $RPBM$ assigns the disturbed flow to both unaffected paths as well as partially damaged paths or called *affected paths*. An affected path is a path involving one or more disrupted arcs. Although a path can be interrupted, the residual capacity of its intact arcs can still be used to reroute the flow and push it forward through the evacuation network. When the reassigned flow reaches a damaged arc of an affected path, it will gather and wait behind the associated node and can be sequentially rerouted to a path at another time (see Figure 3.2).

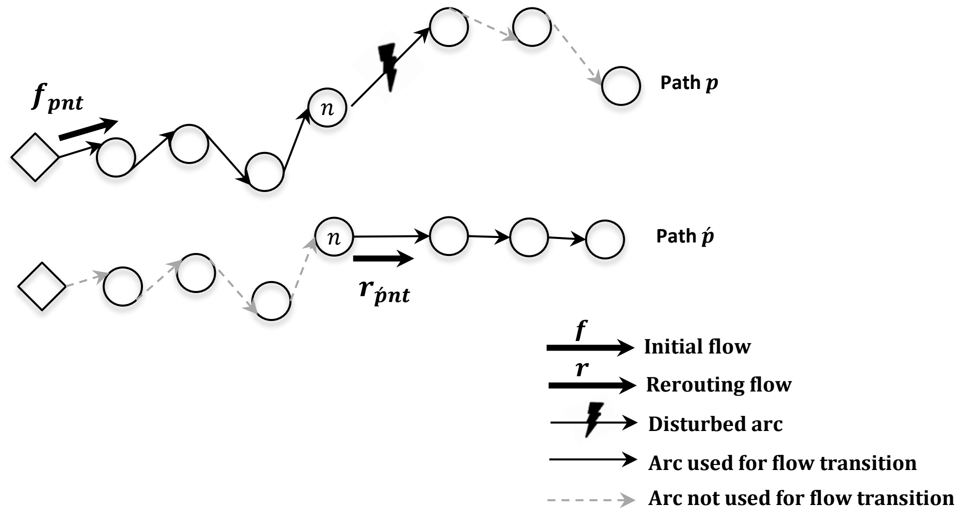

Figure 3.2: Rerouting flow in RPBM

3.2.1 Rerouting Path-Based Model (RPBM) Formulation:

For developing the mathematical formulation, the following notation is used:

Sets:

$\mathcal{N}$	Set of all nodes
$\mathbb{T}$	Set of all time slots
$\wp$	Set of all paths

Decision Variables:

r_{pnt}	Disturbed flow of node $n \in \mathcal{N}$ that is rerouted and assigned to alternate route p at time $t \in \mathbb{T}$
hc_{nt}	Accumulative disrupted flow on node $n \in \mathcal{N}$ at time $t \in \mathbb{T}$

Parameters:

f_{pt}	Flow that starts on path $p \in \wp$ at time $t \in \mathbb{T}$ (pre-disruption plan)

H_{pnt}	Disturbed flow on node $n \in \mathcal{N}$ of path $p \in \wp$ at time $t \in \mathbb{T}$
θ_{pa}	Transit time from the origin of path $p \in \wp$ to arc $a \in \mathcal{A}$
C_a	Capacity of arc $a \in \mathcal{A}$
D_n	Demand of source node $n \in \mathcal{N}$
ℓ_n	Capacity of destination node $n \in \mathcal{N}$
τ_a	Transit time on arc $a \in \mathcal{A}$
L_{pn}	Takes value 1 if node $n \in \mathcal{N}$ is the source node of path $p \in \wp$, and otherwise 0
K_{pn}	Takes value 1 if node $n \in \mathcal{N}$ is the destination node of path $p \in \wp$, and otherwise 0
$\acute{\theta}_{pn}$	Transit time from the origin of path $p \in \wp$ to node $n \in \mathcal{N}$
δ_{pa}	Takes value 1 if arc $a \in \mathcal{A}$ belongs to path $p \in \wp$, and otherwise 0
γ_{na}	Takes value 1 if node $n \in \mathcal{N}$ is the upstream (origin) node of arc $a \in \mathcal{A}$, and otherwise 0
φ_{pmn}	Takes value 1 if node $n \in \mathcal{N}$ is not behind node $m \in \mathcal{N}$ on path $p \in \wp$, and otherwise 0
W_{pnt}	Takes value 1 if the flow on path $p \in \wp$ starting at time $t \in \mathbb{T}$ reaches the merging arc from node $n \in \mathcal{N}$ before the disruption time of the arc
V_{pnt}	Takes value 1 if the flow on path $p \in \wp$ starting at time $t \in \mathbb{T}$ is disturbed and stuck behind node $n \in \mathcal{N}$, and otherwise 0
η_{ptmn}	Takes value 1 if the flow on path $p \in \wp$ starting at time $t \in \mathbb{T}$ is not affected through node $m \in \mathcal{N}$ and also is not disturbed between node $m \in \mathcal{N}$ and node $n \in \mathcal{N}$ (m is behind n), and otherwise 0
∂_{pn}	Takes value 1 if there is no disturbed arcs on path $p \in \wp$ after node $n \in \mathcal{N}$, and otherwise 0

Mathematical properties of the PBM model do not allow the direct representation of flow departing from intermediate nodes. Variables denoting the flow are always related to the evacuees leaving the source node of a path rather than the intermediate node. However, a method is needed for rerouting the flow in order to reflect the flow departing from an intermediate node (see Figure 3.3). To resolve the issue in the optimization model formulation, the rerouting variable r_{pnt} is introduced to denote the amount of flow departing from the origin of path $p \in \wp$ at time $t \in \mathbb{T}$. Nevertheless, in our constraints, we ignore the values of r_{pnt} associated with preceding nodes (or arcs) to node $n \in \mathcal{N}$. In this case, the preceding arcs are considered dummy arcs. This is done by introducing three sets of parameters W_{pnt}, V_{pnt}, and η_{ptmn} which reflect the effect of disruptions on the evacuation flow with respect to the arc incident times, the sequence of arcs in the set of paths as well as the topology of the network. Using these parameters a mathematical model with a linear structure can be developed. Note that a flow departing at time $t \in \mathbb{T}$ takes θ_{pn} time units to reach node $n \in \mathcal{N}$. Hence, based on the disturbed flow information $r_{pn(t-\theta_{pn})}$, we can address the flow reassignment from node $n \in \mathcal{N}$ onto route $p \in \wp$ during time interval $t - \theta_{pn} + \theta_{pn} = t$.

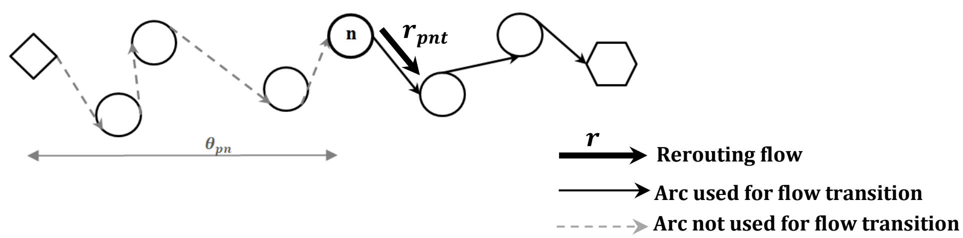

Figure 3.3: Representation of rerouting variable r_{pnt}

We now describe the proposed dynamic network flow optimization model formulation. When an arc disruption occurs, disturbed evacuees are assumed to be accumulated on the tail of the affected arc (i.e., a node behind the affected road in the evacuation network) for the purpose of rerouting them to alternative paths. The objective function of $RPBM$ aims to minimize the total number of disturbed evacuees remaining in the evacuation network by the end of the planning horizon T.

$$\text{Min} \quad \sum_{n \in \mathcal{N}} hc_{nT}$$

Constraints are explained as follows. The planning horizon set $\mathbb{T} = \{0, 1, \dots, T\}$ covers both the pre-disruption schedule (f_{pt}) as well as the post-disruption schedule ($\mathcal{R}_{pnt}$). The time periods at which the previous plan is updated are shown by set $\mathbb{T}_{updated} = \{t_{updating}, \dots, T\}$. At time $t = 0$, there are no disturbed evacuees in the system. Hence, the total amount of associated flow on all nodes is set to zero as

$$hc_{n(t=0)} = 0, \qquad \forall\, n \in \mathcal{N}. \tag{3.1}$$

The process of a plan revision can only take place during the updating time interval ($\mathbb{T}_{updated}$). The flow-route assignments before $t_{updating}$ are equal to zero as in the following constraint

$$r_{pn(t-\hat{\theta}_{pn})} = 0, \qquad \forall p \in \wp, \forall a \in \mathcal{A}, n \in \mathcal{N}, t \in \mathbb{T}/\mathbb{T}_{updated}. \tag{3.2}$$

When calculating the amount of disturbed flow on node $n \in \mathcal{N}$ at time $t \in \mathbb{T}$, we take into account both the amount of the disturbed flow from the original plan (denoted by H_{pnt}) and the amount of the rerouted flow from nodes ($m \in \mathcal{N}$) that were disturbed while passing through the alternative pathway ($W_{pnt} \sum_{m \in \mathcal{N}} \eta_{ptmn} r_{pmt}$). This is stated in

$$hc_{pn(t+\hat{\theta}_{pn})} = H_{pn(t+\hat{\theta}_{pn})} + W_{pnt} \sum_{m \in \mathcal{N}} \eta_{ptmn} r_{pmt}, \qquad \forall p \in \wp, n \in \mathcal{N}, t \in \mathbb{T}. \tag{3.3}$$

Parameter H_{pnt} used in Constraint (3.3) can be calculated as follows

$$H_{pn(t+\hat{\theta}_{pn})} = \mathrm{V}_{pnt} f_{pt}, \qquad \forall p \in \wp, n \in \mathcal{N}, t \in \mathbb{T}.$$

When flow f_{pt} is blocked on node $n \in \mathcal{N}$ (denoted by $V_{pnt} = 1$), and since the flow has started from the origin of the path at time $t \in \mathbb{T}$, the time at which it reaches and accumulates on node $n \in \mathcal{N}$ is $t + \acute{\theta}_{pn}$. Note that $\acute{\theta}_{pn}$ is the transit time from the origin of path $p \in \wp$ to node $n \in \mathcal{N}$. Accordingly, $H_{pn(t+\acute{\theta}_{pn})}$ represents the number of evacuees accumulated on $n \in \mathcal{N}$ at time $\left(t + \acute{\theta}_{pn}\right)$.

The total number of remaining interrupted evacuees at time $(t+1)$ equals its previous amount at time $t \in \mathbb{T}$, plus the newly interrupted evacuees ($\sum_{p\in\wp} hc_{pn(t+1)}$), minus the amount of rerouted evacuees at time t, as expressed as

$$h_{cn(t+1)} = hc_{\mathrm{nt}} + \sum_{p\in\wp} hc_{pn(t+1)} - \sum_{a\in\mathcal{A}} \sum_{p\in\wp} \mathfrak{I}_{pna} \left(1 - W_{pn(t-\theta_{pa})}\right) r_{pn(t-\theta_{pa})}, \qquad \forall\, n \in \mathcal{N}, t \in \mathbb{T}. \qquad (3.4)$$

Parameter $\mathfrak{I}_{pna}$ in Constraint (3.4) reflects the topology of the network and can be calculated as

$$\mathfrak{I}_{pna} = \delta_{pa}\gamma_{na}, \qquad \forall p \in \wp, a \in \mathcal{A}, n \in \mathcal{N}.$$

Considering constraints (3.2), (3.3), and (3.4), before the updating time, $hc_{n(t+1)}$ only equals the previous amount of the remaining flow plus the newly interrupted flow (i.e. $hc_{n(t+1)} = hc_{nt} + \sum_{p\in\wp} hc_{pn(t+1)}$). However, when the rerouting of the disturbed flow begins, the assigned disturbed flow $r_{pn(t-\theta_{pa})}$ at time $t \in \mathbb{T}$ to alternate paths is no longer stalled behind node $n \in \mathcal{N}$ and is subtracted from the remaining disturbed flow of the next time interval $hc_{n(t+1)}$.

$$\sum_{p\in\wp} \sum_{n\in\mathcal{N}} \sum_{m\in\mathcal{N}} \eta_{p(t-\theta_{pa})mn} \delta_{pa}\gamma_{na} \left[\left(1 - V_{pn(t-\theta_{pa})}\right) L_{pm} f_{p(t-\theta_{pa})} + \left(1 - W_{pn(t-\theta_{pa})}\right) \emptyset_{pmn} r_{pm(t-\theta_{pa})}\right] \leq C_a, \qquad \forall a \in \mathcal{A},\ t \in \mathbb{T}. \qquad (3.5)$$

Constraint (3.5) ensures that the total flow from different paths reaching a shared arc does not exceed the capacity of the arc (C_a). This flow includes (i) the pre-disruption flow schedule f_{pt}, and (ii) the post-disruption flow schedule r_{pnt}. Let us consider flow $f_{p(t-\theta_{pa})}$ departing from the origin of the path at time $t-\theta_{pa}$. Two cases can occur regarding the share of this flow in the capacity usage of arc $a \in \mathcal{A}$ (see Figure 3.4).

Case 1: Flow is disturbed before reaching arc $a \in \mathcal{A}$

Case 1 occurs when there is at least one disruption on the preceding arcs before reaching arc $a \in \mathcal{A}$ and when the disruption time of an associated arc is less than the time required for the flow to reach and pass through the arc. Hence, if there is at least one arc $\bar{a} \in \mathcal{A}$ in which the following condition holds true

$$\left(t-\theta_{p\bar{a}}\right)+\theta_{p\bar{a}}+\tau_{\bar{a}}>DT_{\bar{a}}, \quad \exists \bar{a} \in \mathcal{A} \text{ preceding to } a \in \mathcal{A} \text{ on } p \in \wp,$$

then, parameter $\eta_{p(t-\theta_{pa})mn}$ equals zero and $f_{p(t-\theta_{pa})}$ is not considered in the capacity Constraint (3.5). Note that $m \in \mathcal{N}$ represents the origin node of the path if $L_{pm}=1$. Also, $n \in \mathcal{N}$ represents the head of arc $a \in \mathcal{A}$ if $\gamma_{na}=1$. Note that the details of calculating the amount of parameter $\eta_{p(t-\theta_{pa})mn}$ using an algorithm is explained later in the chapter.

Case 2: Flow can pass through arc $a \in \mathcal{A}$

When the flow is not disturbed on preceding arcs to arc $a \in \mathcal{A}$ and reaches and passes through arc $a \in \mathcal{A}$, it occupies the capacity of arc $a \in \mathcal{A}$ until it completely passes through the arc. This occurs when the following condition holds

$$\begin{aligned} &\left(t-\theta_{p\bar{a}}\right)+\theta_{p\bar{a}}+\tau_{\bar{a}} \leq DT_{\bar{a}}, \\ \& \quad &V_{pn(t-\theta_{pa})}=0, \end{aligned} \qquad \forall \bar{a} \in \mathcal{A} \text{ preceding to } a \in \mathcal{A} \text{ on } p \in \wp.$$

When the value of $(t - \theta_{p\bar{a}}) + \theta_{p\bar{a}} + \tau_{\bar{a}}$ is less than the disruption time $(DT_{\bar{a}})$ of a preceding arc $\bar{a} \in \mathcal{A}$, the flow can reach arc $a \in \mathcal{A}$, i.e., $\eta_{p(t-\theta_{pa})mn} = 1$. At this point, if the flow is not disturbed on arc $a \in \mathcal{A}$ (i.e. $V_{pn(t-\theta_{pa})} = 0$), it can flow through the arc, and the arc capacity is reduced accordingly. Note that Algorithm 2 is used to calculate the amount of parameter $\eta_{p(t-\theta_{pa})mn}$ to be used in the optimization model.

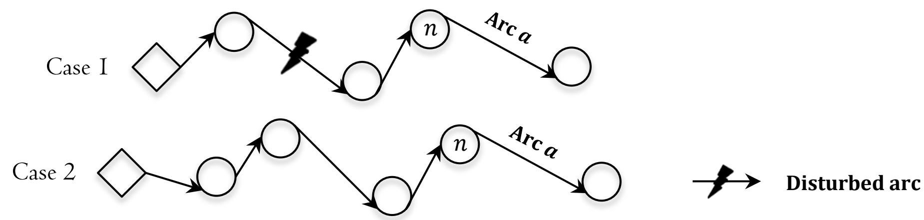

Figure 3.4: Case 1 and Case 2 presentation for flow $f_{p(t-\theta_{pa})}$

Now, let us consider situations that may arise regarding the post-disruption flow $r_{pm(t-\theta_{pa})}$(see Figure 3.5). Note that this flow is placed on path $p \in \wp$ through node $m \in \mathcal{N}$.

Case 1: Reassigned flow has been added to the path from a preceding node to arc $a \in \mathcal{A}$

When node $m \in \mathcal{N}$ comes after arc $a \in \mathcal{A}$ on path $p \in \wp$, parameter $\emptyset_{pmn}$ equals zero and $r_{pm(t-\theta_{pa})}$ is excluded in the capacity constraint.

Case 2: Rerouted flow is interrupted before reaching arc $a \in \mathcal{A}$

If node $m \in \mathcal{N}$ is directionally placed before arc $a \in \mathcal{A}$ on path $p \in \wp$ (i.e. $\emptyset_{pmn} = 1$), but the rerouted flow is disrupted before arriving at the arc ($\eta_{p(t-\theta_{pa})mn} = 0$), then $r_{pm(t-\theta_{pa})}$ is disregarded in the constraint.

Case 3: Rerouted flow can travel through arc $a \in \mathcal{A}$

If node $m \in \mathcal{N}$ is directionally placed before arc $a \in \mathcal{A}$ on path $p \in \wp$ (i.e. $\emptyset_{pmn} = 1$), and the reassigned flow can reach the arc without any interruptions ($\eta_{p(t-\theta_{pa})mn} = 1$), then $\mathcal{R}_{pm(t-\theta_{pa})}$ is included in the arc capacity constraint.

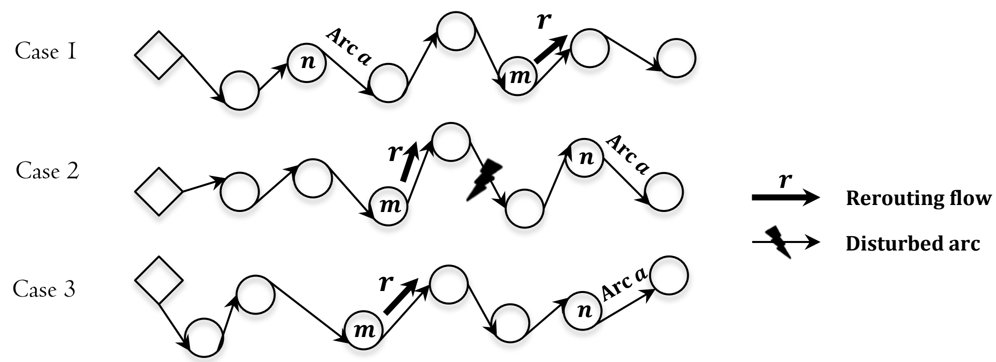

Figure 3.5: Case 1, Case 2, and Case 3 presentation for rerouted flow $r_{pm(t-\theta_{pa})}$

Constraint (3.6) ensures that all evacuees, including those who followed the pre-disruption plan and those that have been rerouted, are restricted by the capacity of the destination node (ℓ_n) when entering the shelter area.

$$\sum_{p\in\wp}\sum_{t\in\mathbb{T}} K_{pn}\left[\sum_{m\in\mathcal{N}_o} \eta_{ptmn} L_{pm} f_{pt} + \sum_{m\in\mathcal{N}} \eta_{ptmn} r_{pmt}\right] \le \ell_n, \qquad \forall n \in \mathcal{N}_d. \tag{3.6}$$

Evacuation flow f_{pt} is considered in Constraint (3.6) only if the following condition holds

$$(t - \theta_{p\bar{a}}) + \theta_{p\bar{a}} + \tau_{\bar{a}} \le DT_{\bar{a}}, \qquad \forall \bar{a} \in \mathcal{A} \textit{ between the source node and destination node of path } p \in \wp.$$

Hence, starting from the origin and moving towards the destination, if the flow of an evacuee is not interrupted ($\eta_{ptmn} = 1$ where $m \in \mathcal{N}_o$ and $n \in \mathcal{N}_d$), it is counted in Constraint (3.6). Similarly, the rerouted flow r_{pmt} is considered to use the capacity of the destination node only if no incident affects the flow from node m $\in \mathcal{N}$ (the point it had been inserted on the path) to the destination node $n \in \mathcal{N}_d$ ($\eta_{ptmn} = 1$).

Finally, non-negativity and integrality of decision variables are reflected, respectively, as

$$r_{pnt} \in \mathbb{Z}^+, hc_{nt} \in \mathbb{Z}^+, \qquad \forall p \in \wp, n \in \mathcal{N}, t \in \mathbb{T}. \tag{3.7}$$

3.2.2 Algorithms to Calculate Key Model Parameters and Network Clearance Time

Upon examining the problem characteristics, we realized that the computational efforts for solving the problem can be significantly reduced if some key parameter values are determined prior to solving the model. Some of these parameters are identified, and their values are determined using two pre-processing algorithms introduced in this section. If these pre-processing algorithms were not proposed, developing an optimization model for the described rerouting problem was computationally challenging. For instance, to calculate the amount of disturbed flow (H_{pnt}) on node $n \in \mathcal{N}$ of path $p \in \wp$ at time $t \in \mathbb{T}$, instead of using equation $H_{pn(t+\hat{\theta}_{pn})} = \mathrm{V}_{pnt} f_{pt}$ we needed to add the following constraint

$$H_{np(t+\hat{\theta}_{pn})} \geq f_{pt}\gamma_{na}\delta_{pa}\frac{\left|t+\theta_{pa}+\tau_a-DT_a\right|}{t+\theta_{pa}+\tau_a-DT_a} - \left(\sum_{\acute{n}\in N_{pn}} \gamma_{n\acute{a}}\delta_{p\acute{a}}\frac{\left|t+\theta_{p\acute{a}}+\tau_{\acute{a}}-DT_{\acute{a}}\right|}{t+\theta_{p\acute{a}}+\tau_{\acute{a}}-DT_{\acute{a}}} + \left|N_{pn}\right|\right)M, \qquad \forall p \in \wp, n \in \mathcal{N}, t \in \mathbb{T},$$

where N_{pn} is the set of all preceding nodes to node $n \in \mathcal{N}$ of path $p \in \wp$ and M is a large number. The big challenge, however, was to develop constraints illustrating calculation of the amount of remaining disturbed flow (hc_{nt}), arc capacity limitation, destination node capacity restriction, and rerouting procedure. Hence, the following processing algorithms are developed and used prior to solving the proposed $RPBM$ formulation to simplify the computation.

(i) Methodology to Calculate Parameters Associated with Disruptions

Parameter V_{pnt} indicates whether or not flow f_{pt} on path $p \in \wp$ departing at time $t \in \mathbb{T}$ would be stalled on node $n \in \mathcal{N}$. *Algorithm 3.1* is developed to calculate the value of V_{pnt}. First, we calculate W_{pnt} to define whether f_{pt} is stopped on node $n \in \mathcal{N}$ regardless of any possible disturbances that may have surfaced during the flow passage up to node $n \in \mathcal{N}$. Accordingly, we initialize disruption times of preceding arcs to node $n \in \mathcal{N}$ to be infinity. We disregard disturbances of the preceding arcs and only take into account the time of incident (DT_a) of the arc that emerges from node $n \in \mathcal{N}$, arc transit time (τ_a), and the time to transport from the origin of the route to arc $a \in \mathcal{A}$ (θ_{pa}). If a flow departs on path $p \in \wp$ at time $t \in \mathbb{T}$, it reaches arc $a \in \mathcal{A}$ at time $t + \theta_{pa}$. Also, it takes τ_a unit of time for the flow to completely pass through the arc. Therefore, if $t + \theta_{pa} + \tau_a$ is greater than the disruption time of the arc (DT_a), the flow is interrupted, and W_{pnt} takes value 1.

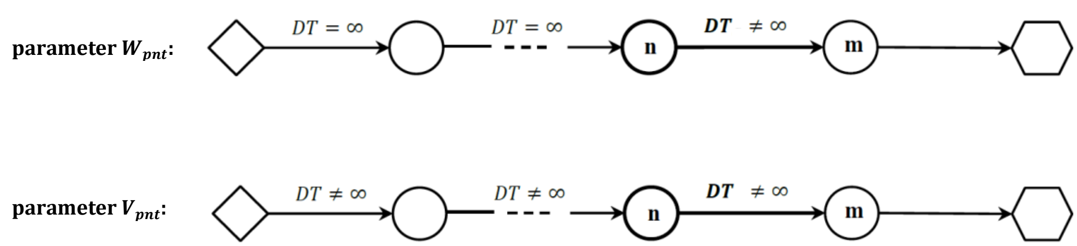

Figure 3.6: Defining parameters W_{pnt} and V_{pnt}

Next, we calculate the value of V_{pnt} and subsequently, take into account incident times of preceding arcs to arc $a \in \mathcal{A}$. The value of V_{pnt} equals 1 only if the flow f_{pt} experiences no interruption while moving toward node $n \in \mathcal{N}$ (i.e., $\sum_{m \in \mathcal{N}} W_{pmt} = 0$) and is disturbed on node $n \in \mathcal{N}$ of path $p \in \wp$ (i.e., $W_{pnt} = 1$). Else $V_{pnt} = 0$.

Algorithm 3 . 1

Inputs:

An evacuation network $\mathcal{G}$ consisting of a set of nodes $\mathcal{N}$ and a set of arcs $\mathcal{A}$.

Disruption Time of Arcs

Calculating V_{pnt}:

```
for all paths p ∈ ℘ do
    for all time slots t ∈ 𝕋 do
        for all arcs that belong to path p ∈ ℘ do
            if t + θ_pa + τ_a − DT_a > 0 then
                W_pnt = 1 (n is upstream node of arc a)
            else if t + θ_pa + τ_a − DT_a ≤ 0 then
                W_pnt = 0
            end if
            for all preceding nodes m ∈ N to arc a on path p do
                if ∑_{m∈N} W_pmt = 0 and W_pnt = 1 then
                    V_pnt = 1 (n is upstream node of arc a)
                else then
                    V_pnt = 0
                end if
            end for
        end for
    end for
end for
```

A numerical example for calculating the value of V_{pnt}:

The following example is used to illustrate the calculation of parameter V_{pnt}. Consider the path, disruption times, and arc transit times shown in Figure 3.7. When an evacuee departs from node i at time $t = 1$, the evacuee can pass through arc (i, j) because the disruption on arc $DT_{(i,j)} = 4$ occurs after the flow has reached node j (i.e., time $t = 2$). This evacuee can also pass through arc (j, k) with no interruption, as the time it arrives at node k (i.e., time $t = 2 + 5 = 7$) is earlier than the time of the incident on arc $DT_{(j,k)} = 8$. Accordingly, this flow is not disturbed on either of the arcs (i, j) or (j, k) and $V_{pi(t=1)} = V_{pj(t=1)} = 0$. Now, let us consider a flow starting on the path at time $t = 3$. It will arrive at the origin of the arc (j, k) at time $t = 4$ with no disturbance. The arc transit time for arc (j, k) is 5 units of time. Thus, it cannot pass through the arc because the incident occurred prior to the projected arrival at the location, *i.e.*, $4 + 5 > 8$. Associated values of V_{pnt} will be $V_{pi(t=3)} = 0$ and $V_{pj(t=3)} = 1$, as the disturbed flow is only affected on node j. Similarly, for the departure time $t = 5$, we would have $V_{pi(t=5)} = 1$ because the flow was not affected as the incident occurred prior to the departure time.

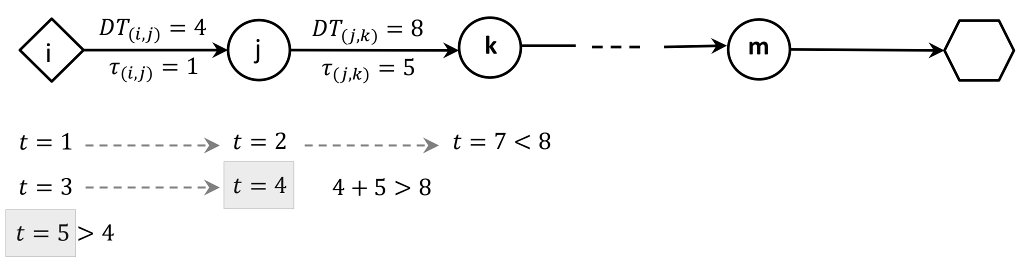

Figure 3.7: Example of parameter v_{pnt}

Next, *Algorithm 3.2* is developed to determine whether a flow can pass through a specific location in the network and can reach another location without any interruptions.

For any path $p \in \wp$, we first derive the sequence of nodes composing the path called φ_p. Then, for any combination of node $m \in \mathcal{N}$ and $n \in \mathcal{N}$ in the set φ_p (when m is a precedence to node n), we calculate the summation of $\sum_{k=m}^{n-1} V_{pkt}$. If $\sum_{k=m}^{n-1} V_{pkt} = 0$, we can conclude that the flow on path $p \in \wp$ at time $t \in \mathbb{T}$ is neither interrupted on node $m \in \mathcal{N}$ nor is disturbed between node $m \in \mathcal{N}$ and node $n \in \mathcal{N}$. If this condition holds, then $\eta_{ptmn} = 1$. Otherwise, $\eta_{ptmn} = 0$.

Algorithm 3 . 2

Inputs:

An evacuation network $\mathcal{G}$ consisting of a set of nodes $\mathcal{N}$ and a set of arcs $\mathcal{A}$, and v_{pnt}.

Calculating $\boldsymbol{\eta_{ptmn}}$:

for all paths $p \in \wp$ **do**
  determine set φ_p as a sequence of nodes in path p
    for all time slots $t \in \mathbb{T}$ **do**
      for all preceding nodes $m \in \varphi_p$ to node $n \in \varphi_p$ **do**
        if $\sum_{k=m}^{n-1} v_{pkt} = 0$ **then**
          $\eta_{ptmn} = 1$
        else then
          $\eta_{ptmn} = 0$
        end if
      end for
    end for
end for

(ii) Rerouted Clearance Time Calculation

This section explains the procedure to calculate *rerouted clearance time* (RCT). The RCT is the minimum time to safely evacuate people to safe destinations considering route adjustments during the evacuation. A two-step procedure is developed to calculate RCT to expedite the computation. The first step is to quickly approximate the RCT for $RPBM$. Using this value as a starting solution, *Algorithm 3.3* finds the exact value of RCT as the final step. Let $\mathfrak{D}_{nt} = \sum_{p\in\wp}\sum_{m\in\mathcal{N}} L_{pn}\, H_{pmt}$ denote the demand (evacuees) on source node $n \in \mathcal{N}_o$ of path $p \in \wp$ at time $t \in \mathbb{T}$. We aim to reroute these evacuees through the marginal (residual) capacity of the roads and find the shortest amount of time to reach safe shelters. The residual capacity of the arcs ($\mathcal{Z}_{at}$) and the destination nodes ($ƀ_n$) are calculated as follows:

$$\mathcal{Z}_{at} = C_a - \sum_{p\in\wp}\sum_{n\in\mathcal{N}}\sum_{m\in\mathcal{N}} \eta_{p(t-\theta_{pa})mn}\mathfrak{I}_{pna}\left(1 - V_{pn(t-\theta_{pa})}\right) L_{pm} f_{p(t-\theta_{pa})}, \qquad \forall a \in \mathcal{A},\ t \in \mathbb{T} \ \& \ \mathrm{t} < DT_a, \tag{3.8}$$

$$ƀ_n = \sum_{p\in\wp}\sum_{t\in\mathbb{T}}\sum_{m\in\mathcal{N}_0} K_{pn}\eta_{ptmn} L_{pm}\, f_{pt}\,, \qquad \forall n \in \mathcal{N}_d. \tag{3.9}$$

Approximated RCT can be obtained by the solution of the following optimization model:

$$Min \quad Max_{p\in\wp, t\in\mathbb{T}}\left(\mathfrak{u}_{pt}(t + d_p)\right)$$

$$\text{S.t.} \quad \sum_{p\in\wp}\sum_{t\in\mathbb{T}} L_{pn}\, ꞙ_{pt} \geq \sum_{t\in\mathbb{T}} \mathfrak{D}_{nt}, \qquad \forall n \in \mathcal{N}_o, \tag{3.10}$$

$$\sum_{p\in\wp} \partial_{pn} L_{pn}\delta_{pa} ꞙ_{p(t-\theta_{pa})} \leq \mathcal{Z}_{at}, \qquad \forall a \in \mathcal{A},\ \forall t \in \mathbb{T}, n \in \mathcal{N}, \tag{3.11}$$

$$\sum_{p\in\wp}\sum_{t\in\mathbb{T}} K_{pn}\, ꞙ_{pt} \leq ƀ_n, \qquad \forall n \in \mathcal{N}_d, \tag{3.12}$$

$$M\, \mathfrak{u}_{pt} \geq ꞙ_{pt}, \qquad \forall p \in \wp, \forall t \in \mathbb{T}, \tag{3.13}$$

$$ꞙ_{pt} \in \mathbb{Z}^+, \mathfrak{u}_{pt} \in \{0,1\}, \qquad \forall p \in \wp, \forall t \in \mathbb{T}. \tag{3.14}$$

Variable $ꞙ_{pt}$ is the amount of flow from the source node of path $p \in \wp$ at time $t \in \mathbb{T}$.

The objective function aims to minimize the maximum time in which a flow reaches its destination. Constraints (3.10)-(3.14) are used to reroute $\mathfrak{D}_{nt}$ from source nodes $\mathcal{N}_o$ through the residual capacity of the network. According to Constraint (3.13), binary variable $\mathfrak{u}_{pt}$ receives value 1 if the flow is reassigned to path $p \in \wp$ at time $t \in \mathbb{T}$. For $\mathfrak{u}_{pt} = 1$, the associated flow reaches the destination d_p unit of time later during time interval $(t + d_p)$, where d_p is the duration time of the path.

Let $\mathfrak{X}$ represent the solution of the above optimization model. Time value of $\mathfrak{X}$ is used in *Algorithm 3.3* to expedite the RCT calculation process. The algorithm has two main steps: RCT bound generation and value calculation. In bound generation, if $\sum_{n\in\mathcal{N}}\sum_{t\in\mathbb{T}} I_{nt} > 0$, it means there still remains some disturbed evacuees in the network, and the system is not cleared; hence, it provides a lower bound to RCT. If $\sum_{n\in\mathcal{N}}\sum_{t\in\mathbb{T}} I_{nt} \leq 0$, it means the system has been cleared. However, we are aiming to find the minimum amount of time required to clear the system; hence, we consider $\mathfrak{X}$ as a lower bound to RCT. In the second part of the algorithm to calculate RCT, the RPBM is solved considering T and $T - 1$ as the planning horizon, where $T = (\mathrm{LB_{RCT}} + \mathrm{UB_{RCT}})/2$. If the objective value at $\mathrm{T} - 1$ is positive (i.e., the system is not cleared) and becomes zero at time T (i.e., the system is cleared), the minimum time to clear the network is achieved at T; $RCT = T$. If both objective values are positive, the system cannot be cleared at time T. Hence, we update the lower bound of RCT to $LB_{RCT} = T$ if $T > LB_{RCT}$. If both objective values equal zero, it means that the system has been cleared at $\mathrm{T} - 1$. This triggers updating the upper bound to $UB_{RCT} = T - 1$ if $T - 1 < UB_{RCT}$. The algorithm continues until RCT value is found.

Algorithm 3 . 3: Calculating Clearance time of the reroute plan

Inputs:

$RPBM$ and $\mathfrak{X}$.

put CT of the evacuation network with no disruption as LB_{RCT}

put $UB_{RCT} = 2\ LB_{RCT}$

Calculating a tight bound for *RCT*:

put $\mathbb{T} = \{0, 1, \dots, \mathfrak{X}\}$ as the planning horizon

solve $RPBM$

if $\sum_{n \in \mathcal{N}} \sum_{t \in \mathbb{T}} I_{nt} > 0$ **then**

$LB_{RCT} = \mathfrak{X}$

else then

$UB_{RCT} = \mathfrak{X}$

end if

Calculating *RCT Value*:

put $\mathbb{T} = \{0, 1, \dots, T\}$ as the planning horizon

While $\psi \neq 1$ **do**

put $T = (LB_{RCT} + UB_{RCT})/2$

Solve $RPBM$ for $\mathbb{T} = \{0, 1, \dots, T\}$ and $\mathbb{T} = \{0, 1, \dots, T - 1\}$

if one objective value is a positive value and the other is equal to zero **then**

put $RCT = T$ and

$\psi = 1$

else if both objective values are positive and $T > LB_{RCT}$ **then**

put $LB_{RCT} = T$

else if both objective values are equal to zero and $T - 1 < UB_{RCT}$ **then**

put $UB_{RCT} = T - 1$

end if

end while

3.3 Computational Results

The computational experiments presented in this study focus on the impact of network arc disruptions on evacuation plans and the performance of the proposed recovery strategy. First, the performance of $RPBM$ is investigated on a small sample network in generating alternative routes. Then, the same experiment is conducted on a real evacuation network involving a large metropolitan area. The optimization models are solved using CPLEX 12.5.1, while experiments are performed on a PC with a 3.07 GHz Intel Core i7 processor having 24GB RAM and running Ubuntu 10.04.3.

3.3.1 Numerical experiments to illustrate the proposed approach

Experimental studies are conducted on the sample network shown in Figure 3.8 (Lim et al., 2012). The test network includes three source nodes ($\mathcal{N}_1$, $\mathcal{N}_2$, and $\mathcal{N}_3$), five intermediate nodes ($\mathcal{N}_4$,..., $\mathcal{N}_8$) and two destination nodes ($\mathcal{N}_9$ and $\mathcal{N}_{10}$). These nodes are connected through 22 arcs. Arc transit times (τ_a) as well as arc capacities (C_a) are shown above each arc of the network.

Demand on the source nodes (number of evacuees that are present at the source nodes) are assumed to be $D_1 = 110$, $D_2 = 120$, and $D_3 = 167$, and the capacity of each of the destination nodes are assumed to be 750. First, all possible paths between all origin and destination (O-D) pairs are enumerated using the solution pool feature of *CPLEX* for the shortest path problem. Next, a total of 42 shortest paths are selected as the candidate paths with 13 paths originating from source node $\mathcal{N}_1$, while 14 paths (P_{14}-P_{27}) originate from the second node, and 15 paths (P_{28}-P_{42}) originate from the third node. For instance, P_{12} follows the sequence of $\mathcal{N}_1 \rightarrow \mathcal{N}_5 \rightarrow \mathcal{N}_6 \rightarrow \mathcal{N}_8 \rightarrow \mathcal{N}_{10}$. These candidate paths are used as input data to the path-based evacuation model for the purpose of generating an initial evacuation plan.

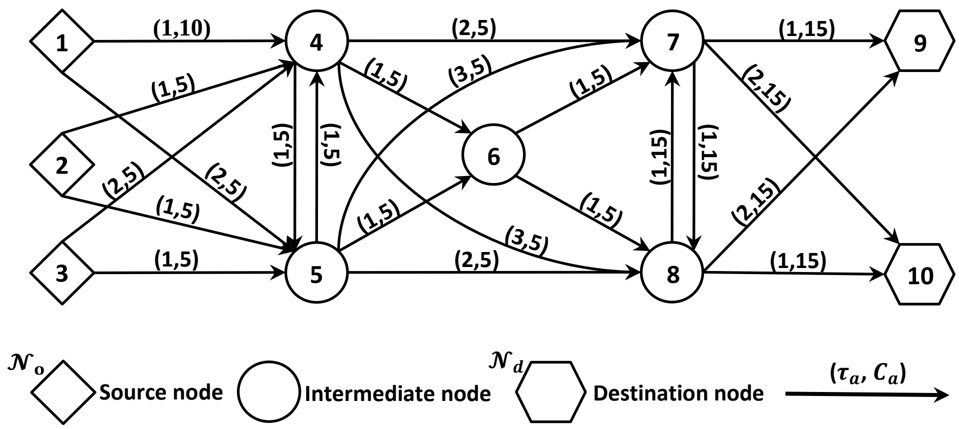

Figure 3.8: Evacuation test network

The path-based evacuation optimization model provides both the optimal pre-disruption route assignment and flow schedule f_{pt} for the test case as in Table 3.1. For example, as shown in the first row of the Table, five evacuees ($f_{P9,t2} = 5$) commence the evacuation by leaving node 1 following path P_9 at time $t = 2$. The evacuation rate varies during time $t = 3$, $t = 4$, and $t = 8$: $f_{P9,t3} = 2$, $f_{P9,t4} = 5$, and $f_{P9,t8} = 5$. The corresponding clearance time is 22 time units.

Suppose that three incidents occurred on different roads during the evacuation. The disturbed roads (i.e., arcs) are labeled as $A^{disturbed} = \{(2,5), (4,5), (4,7)\}$. Incidents are assumed to occur at different times: $DT_{a(2,5)} = 4$, $DT_{a(4,5)} = 6$, and $DT_{a(4,7)} = 8$. While monitoring the progress of the disaster, emergency management agencies received data on the network condition and attempted to develop revised plans accordingly. As the process of collecting information and rerouting plan generation takes time, it is assumed that agencies can implement the revised schedule immediately after the plan updating time $t_{updating} = 10$. Hence, before $t = 10$, no rerouting itinerary is planned and the corresponding variable ($\mathcal{R}_{pnt}$) remains at zero.

Disruptions on arcs (2,5), (4,5), and (4,7) partially affect several paths $\{P_{17}, P_{18}, P_{19}, P_{21}, P_{22}, P_{23}, P_{27}, P_{31}, P_{41}, P_{42}\}$. For example, flow $f_{p23,t2} = 2$ was scheduled to arrive at arc (4,7) at time $t + \theta_{p23,a(4,7)} = 2 + 1 = 3$. It takes $\tau_{a(4,7)} = 2$ time units for the flow to pass through this arc. Since the arc is supposed to fail at time $DT_{a(4,7)} = 8$, the flow $f_{p23,t2} = 2$ is not affected. Now, flow $f_{p23,t9} = 5$ is scheduled to reach arc (4,7) at time $t + \theta_{p23,a(4,7)} = 9 + 1 = 10$, but the arc is already blocked at time $t = 8$. So, there will be a flow accumulation on node 2 at time $t = 10$, and it is denoted by $H_{p23,n4,t10} = 5$.

Table 3.1: An initial evacuation plan for the sample network (f_{pt})

	Time Slots																	
Paths	***t1***	***t2***	***t3***	***t4***	***t5***	***t6***	***t7***	***t8***	***t9***	***t10***	***t11***	***t12***	***t13***	***t14***	***t15***	***t16***	***t17***	***t18***
P9		5	2	5				5										
P10	5	5		5		5	5	5	5	5	5	5		5		5	5	
P11	5						5	3		5	5					5		
P16																		5
P17													5	5				
P18						5												
P19		2		5												5		
P21		3																
P22					5		5				5	5	5			5	5	
P23		2	2	5				5	5	5				5	5			
P24	5		3			5												
P27		3																
P28																		5
P30		3																
P31	3					5				5					5	5	5	
P33				5							5	5						
P35															5			
P36						5		5	5	5			5	5		5		
P37		2	5	5	5		5					5					5	
P39	5																	
P40											5							
P41	2	5	5		5		2	5					5					
P42														5				

The magnitude, location, and interruption time of the disturbed flow H_{pnt} are demonstrated in Table 3.2.

Table 3.2: Amount of disturbed flow (H_{pnt})

Paths		Time Slots 4	6	7	8	9	10	11	12	13	14	15	16	17	18	19	Total
P17	***n2***									5	5						
P18	***n2***		5														**25**
P19	***n2***	5											5				
P22	***n4***		5		5				5	5	5			5	5		
P23	***n4***					5	5	5				5	5				
P31	***n4***				5				5					5	5	5	**107**
P41	***n4***			5		2	5					5					
P42	***n4***												5				

According to Table 3.2, 132 evacuees out of 392 are constrained at different locations of the transportation network between time periods $t = 4$ and $t = 19$. Hence, the proposed RPBM model is used to generate new paths to accommodate the disturbed flow.

Table 3.3 shows the rerouting schedule for the disturbed flow r_{pnt} provided by $RPBM$. The first row of the table shows the flow that should be reassigned to P_{21} from node 2. The remaining rows show route assignments from node 4 onto alternative paths $\{P_2, P_8, P_9, P_{10}, P_{15}, P_{16}, P_{25}, P_{26}, P_{33}\}$. This plan was able to reroute all interrupted flow and redirect them to safe shelters within 35 time intervals. Therefore, the rerouted clearance time (RCT) is equal to 35 time units. During this time period, a total of 25 evacuees are evacuated from node 2, and 132 evacuees are rerouted from node 4.

Table 3.3: Rerouting plan (r_{pnt})

		Time Slots 13	15	18	19	20	21	22	23	24	25	26	27	28	29	30	31	Total
P21	**n2**								5	5		5	5			5		**25**
P2											2							
P8												5						
P9																5		
P10		5		5	5	5	5					5		5		5		
P15	**n4**												5	5			5	**132**
P16								5										
P25					5	5	5		5									
P26			5					5	5	5	5		5		5			
P33									5									

Earlier, Table 3.2 showed that only 107 evacuees experience congestion on node 4 as a result of the incidents. However, the plan provided by $RPBM$ assigns 132 evacuees from this node onto new pathways. This is due to the fact that, in $RPBM$, disrupted flow could still reach disrupted arcs after its reroute assignment and thus add to the accumulated flow behind the failed arcs. Consequently, the overall amount of disturbances calculated in $RPBM$ shown in Table 3.4 could be higher than that of the associated amount shown in Table 3.2.

According to Table 3.4, 132 disturbed evacuees are associated with the pre-disruption flow ($H_{pn(t+\hat{\theta}_{pn})}$), and 25 disturbed evacuees highlighted in the table (from time $t = 24$ to $t = 31$) belong to the disrupted rerouted flow ($W_{pnt} \sum_{m\in\mathcal{N}} \eta_{ptmn} r_{pmt}$). The disruptions on the rerouted flow happened on Path 21 and created traffic congestion behind Node 4 during time slots 24, 25, 27, 28, and 31. As shown in Table 3.3, these disturbed flows have been previously rerouted onto Path 21 (through node 2) at time slots 23, 24, 26, 27, 30. Note that the node sequence of Path 21 is 2-4-5-6-8-10. Hence, the starting flow from Node 2 reached Node 4 within one unit of time. Since it could not pass through arc (4,5), the flow is stalled behind Node 4 one time unit later at times 24, 25, 27, 28, and 31.

Table 3.4: Total amount of disturbed flow (hc_{pnt})

Paths		Time Slots																			
		4	***6***	***7***	***8***	***9***	***10***	***11***	***12***	***13***	***14***	***15***	***16***	***17***	***18***	***19***	***24***	***25***	***27***	***28***	***31***
P17	**n2**									5	5										
P18	**n2**		5																		
P19	**n2**	5											5								
P21	**n4**																5	5	5	5	5
P22	**n4**		5		5				5	5	5			5	5						
P23	**n4**					5	5	5				5	5								
P31	**n4**				5				5					5	5	5					
P41	**n4**			5		2	5					5									
P42	**n4**												5								

The performance of the proposed model is further investigated using four different test instances. Table 3.5 shows the input data for these instances and includes information regarding the set of disrupted arcs, corresponding disruption times, and updating times for the rerouting strategy.

Table 3.5: Test problems

	C1	C2	C3	C4
Disrupted arcs	(2,5),(4,5), (4,7),(6,7)	(5,4),(5,7), (6,8),(7,10)	(2,5),(4,5), (5,7),(8,7)	(2,5),(4,5),(4,6), (5,6),(8,7),(7,10)
Disruption time	{9,16,14,8}	{17,8,10,19}	{12,15,14,7}	{15,6,8,10,9,12}
Updating time	16	19	15	15

Figure 3.9 highlights the total amount of disturbed flow, the accumulated disturbed flow on the nodes, and the rerouted flow for both models as the time progresses.

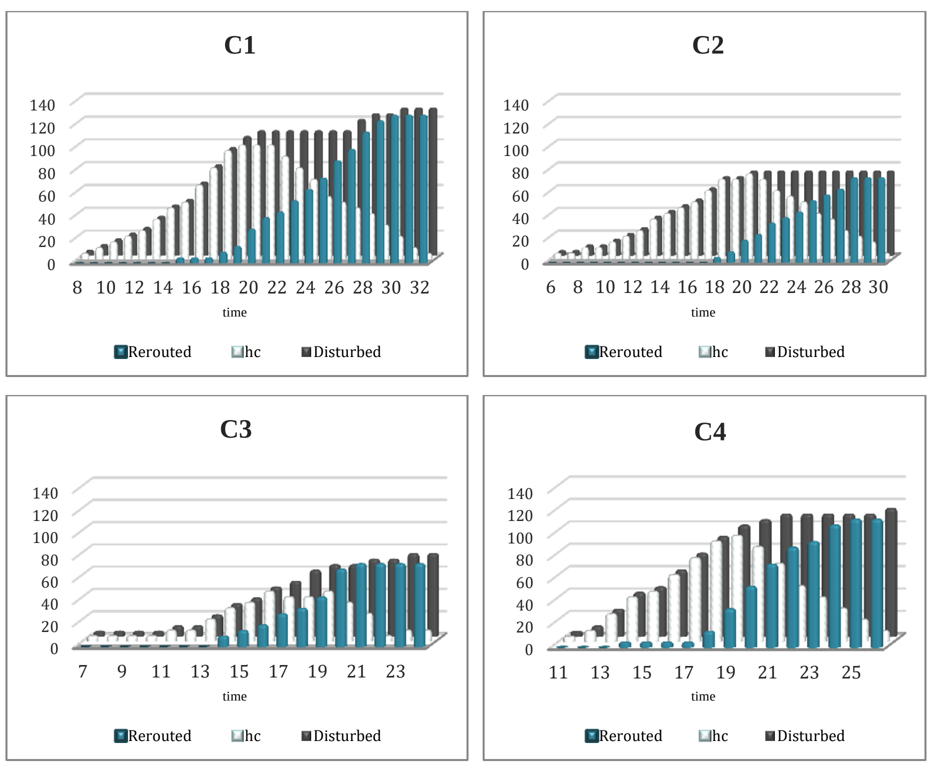

Figure 3.9: Rerouted, disturbed and accumulated remaining flow of sample problems

The accumulated disturbed flow gradually increases at early stages of the planning horizon. When the rerouting process begins, this flow is gradually decreased until there remains no disturbed flow to be rerouted. Once all evacuees reach the destination nodes, the system is cleared. The *rerouted clearance time* (*RCT*) for test problems C_1, C_2 , C_3, and C_4 are 34, 32, 25, and 29, respectively. The rerouted clearance times are different for each problem instance because the input data for the four cases are different in terms of the disrupted arcs, the arc disruption times, and the updating times. All of these factors have an influence on the amount of clearance time of the network. In the following, we provide a sensitivity analysis of the evacuation plans under different problem settings for these factors.

Effect of the network topology (disruption on arcs):

The effect of disruption on each arc is analyzed to determine which arc makes the network evacuation plan the most vulnerable by fixing the values of the other two factors. The clearance times of the rerouting plans, accounting for the disruption of each of the 22 arcs, are shown in Figure 3.10.

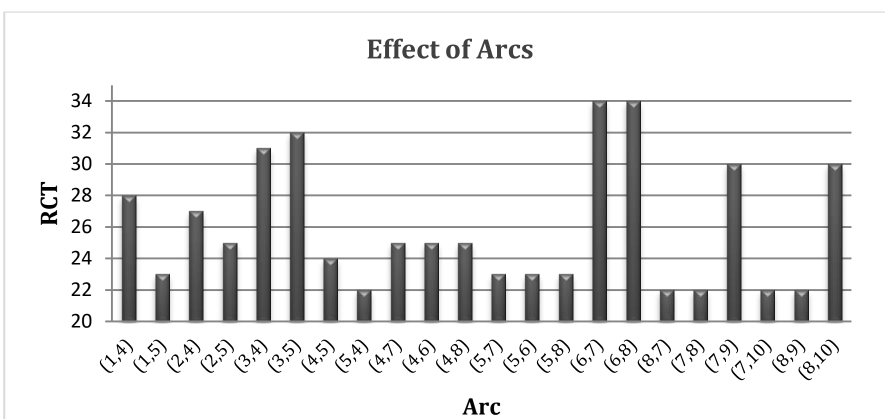

Figure 3.10: Effect of arc disruption on evacuation process

As shown, the most vulnerable arcs affecting the pre-disruption plan are (6,7) and (6,8). This is due to the fact that for these two arcs, it takes the longest time (RCT =34 time units) to reroute the disturbed flow and clear the network following their disruptions. The second most vulnerable arcs are (3,4), (3,5), (7,9) and (8,10) with a corresponding RCT ranging from 30 to 32. Finally, the least vulnerable arcs are (5,4), (8,7), (7,8), (7,10), and (8,9). Disruption on these arcs disturbs part of the flow; However, these disruptions do not change the RCT of the plan. The rerouting plan was able to use the residual capacity of the evacuation network to accommodate the disturbed flow onto alternate paths and redirect them to safe shelters within the same clearance time of the pre-disruption plan (CT=22 units of time). The amount of disturbed flow, the time range of flow disturbance as well as the rerouting time intervals, are shown in Table 3.6.

Table 3.6: Analysis of Less Vulnerable Arcs

Arc	**(5,4)**	**(8,7)**	**(7,8)**	**(7,10)**	**(8,9)**
Total disrupted	35	10	30	0	0
Flow disruption time	[9,17]	[11,14]	[9,18]	0	0
Arc capacity	5	15	15	15	15
Rerouting node	n5	n8	n7	-	-
Rerouting time	[11,17]	[11,17]	[11,20]	0	0

Note that the amount of disrupted flow is equal to the amount of rerouted flow. The rerouting node represents the upstream node of the disrupted arc from which the disturbed flow is rerouted. When arc (5,4) experiences a disturbance at time 9, it causes the disruption of 35 evacuees during the time intervals between 9 and 17. This amount of flow is gathered behind Node 5 and, consequently, is rerouted from the same node between time 11 and 17. Hence, the rerouting process ends before time 22, which also happens to be the CT of the pre-disruption plan. Cases for arcs (8,7) and (7,8) are similar. However, disruptions of arc (7,10) and (8,9) have no effect on the pre-disruption plan and no evacuees are disturbed. This is because the affected arcs are not associated with the paths used in the pre-disruption plan.

Effect of disruption times:

Next, the effect of arc disruption times on the evacuation process is studied. For this purpose, a set of disturbed arcs are chosen as $A^{disturbed} = \{(2,4),(4,8)\}$. The disruption times of the arcs are changed in the interval [1, 21], and an update will be triggered by one unit after arc disruption times. Figure 3.11 (a) shows the RCTs when the disruption time of the arcs changes between time 1 and time 21. As can be seen, the rerouting CT is higher when the disruption time occurs earlier in the planning horizon. This is not surprising because as a disruption happens earlier on the road, more evacuees are affected, and more time is required to reroute them and clear the system.

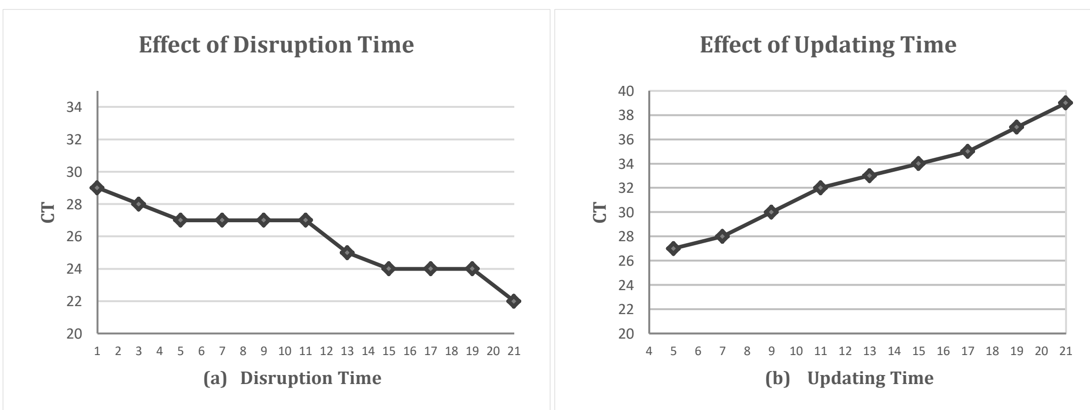

Figure 3.11: Effect of disruption time and updating time on the evacuation process

Effect of information (updating time):

When disruption happens within the network, it takes some time for the interruption to be noticed in addition to the extraneous time required to (1) analyze the situation, (2) make decisions on the rerouting strategy, and (3) implement the plan accordingly. In our approach, we assume that the rerouting process takes place after updating time $t_{updating}$. The effect of $t_{updating}$ on the evacuation process is shown in Figure 3.11 (b). The more delay there is in receiving updated information on the network situation, the longer the clearance time of the network after disturbed flow reassignments. Note that the computational times of all experiments on the small network of Figure 3.8 are less than a second.

3.3.2 Numerical Experiments on a Large-Scale Network

We continue the experiments on an evacuation network of the Greater Houston area (Lim et al., 2012). Houston, Texas, the fourth largest city in the U.S., is known to be one of the most vulnerable metropolitan cities situated on the Gulf Coast and has been severely affected by hurricanes and floods for several decades. The Houston network (Figure 3.12) comprises a total of 42 nodes and 107 arcs. The first thirteen nodes represent source nodes ($\mathcal{N}_1$ -$\mathcal{N}_{13}$), and the last four nodes ($\mathcal{N}_{39}$ -$\mathcal{N}_{42}$) represent safe destination nodes. For the purpose of demonstrating our proposed evacuation rerouting approach, we used the same input data for this network as it was reported in Lim et al., 2012. Hence, the total number of evacuees (i.e., evacuation vehicles) on the source nodes are assumed to be 56,600, in which each of source nodes 1-6 has 100 evacuees, 3,500 for each of nodes 7-10, and 14,000 evacuees each for nodes 11-13. The transit times are defined to be multiplies of $\tau = 30$ minute intervals. Using the PBM model, we first generate the pre-disruption evacuation plan using 140 candidate paths to be selected in the optimization model. The resulting pre-disruption plan distributed the evacuation flow over 52 selected paths, and it took 129τ to clear the network.

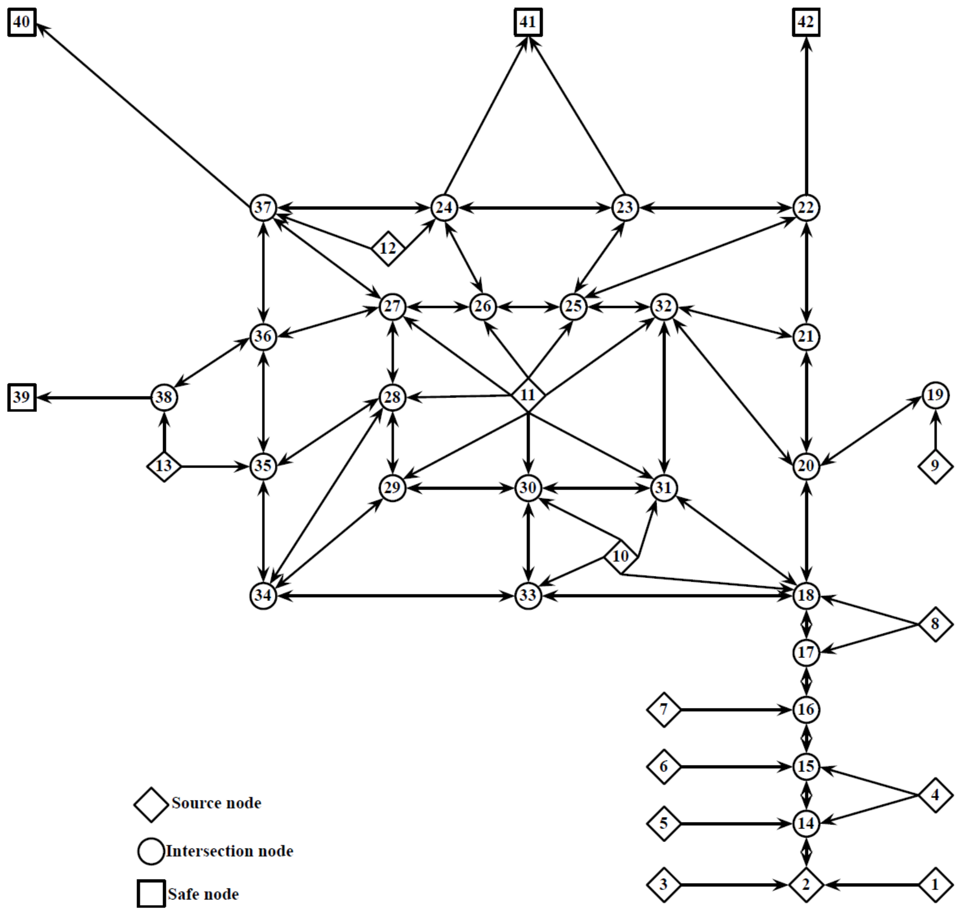

Figure 3.12: City of Houston transportation network

Disruptions are triggered on arcs (22,42), (20,32), (11,27), and (35,34) at times 56, 69, 67 and 48, respectively. These road disruptions affect flows on 11 paths and result in 10,966 evacuees being stranded behind nodes 11, 20, 22, and 35. Among these evacuees, 600 are on node 11, 1,675 on node 20, 7,331 on node 22, and 1,360 on node 35. The $RPBM$ is used to provide a reroute plan for the disturbed flow. The total combined computation time of running both *Algorithm 3.1* and *Algorithm 3.2* was 67.91 seconds, while it took 52.41 seconds to solve the $RPBM$. The corresponding reroute plan is shown in Figure 3.13. In the figure, the amount of rerouted flow from each node during different time intervals are illustrated. The total time taken to move all disturbed flow to safe shelters was 162τ. This means that our model required approximately 16 hours to adjust the plan and rearrange 251,850 disturbed evacuees to safe shelters through the residual capacity of the Houston network after disruption.

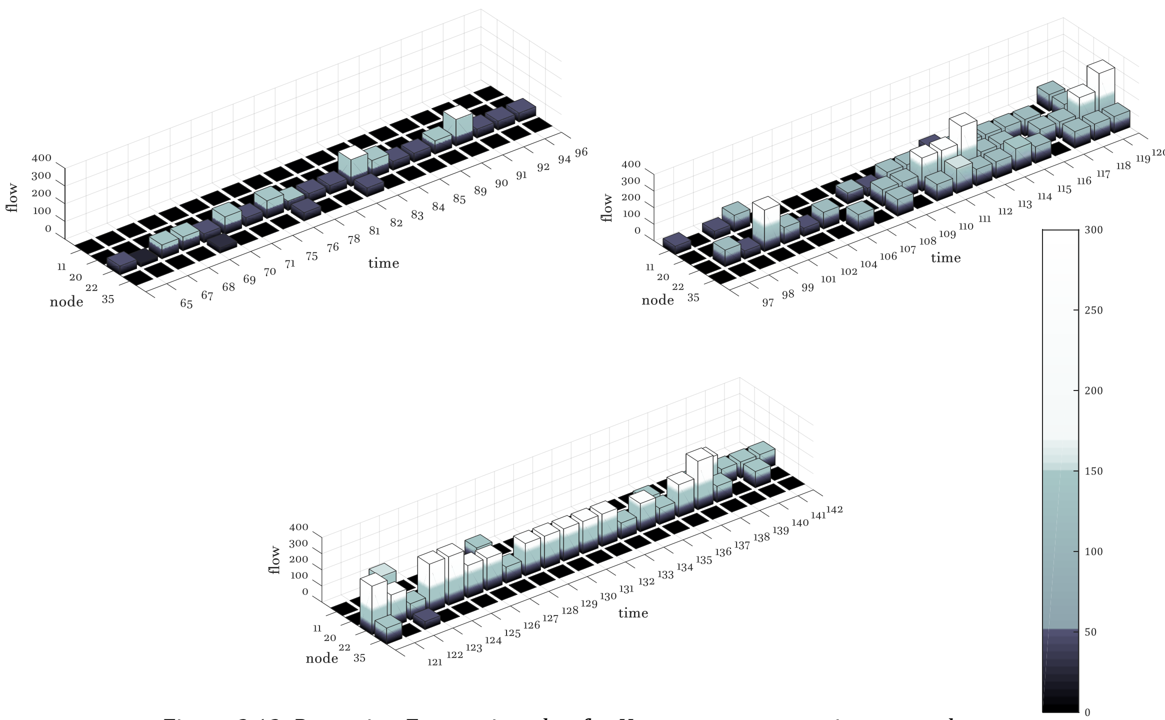

Figure 3.13: Rerouting Evacuation plan for Houston transportation network

3.4 Conclusion

During the course of an evacuation, real-time incidents occur and can disrupt the initial evacuation plan process. Providing an efficient recovery strategy to quickly respond to these unforeseen events and minimize the risk of evacuees stranded on transportation roads in the system cannot be overemphasized. Therefore, this paper introduced a real-time rerouting evacuation strategy that can be applied to post network disruption networks to minimize evacuation clearance time in response to the occurrence of real-time incidents. For this purpose, a dynamic network flow optimization model formulation ($RPBM$) was introduced, in which variable evacuation flow rates are allowed for the alternative paths to achieve more practical, effective evacuation plans. We have developed a rerouting clearance time calculation algorithm to efficiently calculate the minimum amount of time required to mobilize disturbed evacuees to safe shelters. Numerical experiments were thoroughly conducted to study the performance of the proposed $RPBM$ under different problem configurations. Three incident-related factors (location, time of occurrence, and plan updating time) have been investigated to better understand their effects on the rerouting process. As expected, more flow is disturbed as the incident occurs earlier during the evacuation, this leads to a greater amount of time to reroute the affected flow and clear the system. When the time for plan updates was delayed (i.e., the rerouting process takes place later), the clearance time of the network would increase accordingly. This emphasizes the importance of making quick decisions for fast response to incidents as it is crucial in an efficient evacuation rerouting plan. The proposed approach has also been tested on a large-scale evacuation network, and the results showed that it is capable of making rerouting decisions in a timely manner.

Chapter 4

Two-Stage Stochastic Model: Adjusting the Plan Robustness under Possible Road Disruptions

4.1 Introduction

To the best of our knowledge, there is no study that presents a proactive plan for short-notice evacuation which considers evacuees' rerouting as an option in response to the uncertainty of road disruption. This work is devoted to bridging the gap by investigating the effects of uncertain road closures on traffic dynamics in a system-optimal setting in order to provide a resilient pro-active evacuation plan while considering a recovery strategy (rerouting) to compensate negative effects of the disruption. We develop a mathematical framework that would address the following questions: What optimal real-time rerouting and rescheduling can be adopted in each disruption scenario so as to avoid chaos and further delay in clearance time? (Here disruption scenarios represent the simultaneous possibility of different road closures at various times). How do we prepare a pro-active plan to minimize disturbed evacuees and clearance time while reducing the possible degree of rerouting and rescheduling in the case of disruption?

In our proposed two-stage stochastic model, potential road disruptions are defined to be uncertain incidents that can disturb the evacuation plan. An evacuation plan is designed in the first stage of the model and the reroute plan as a mitigation strategy in the second stage of the model. The two-stage stochastic program only minimizes the expected value of the loss function, is a risk neutral-approach and has no control over any potential large deviations from the expected value under specific scenarios. To resolve the issue by using a risk-averse approach, an additional risk measure is added to the objective function of the model to control and minimize the large deviation in the disruption consequences. We further note that the solution obtained by the two-stage stochastic model with worst-case scenarios can be too conservative. In practice, there may be certain cases where the decision-maker is willing to add more resources under occurrences of specific scenarios. For instance, emergency managers might consider road capacity extension approaches such as contra-flow to add to the available capacity of certain roads during specific times if it can significantly improve the evacuation process. Conversely, the decision-maker may be willing to take a risk and to allow deviations from constraints under specific low probability worst-case scenarios. In all of these cases, the level of solution conservatism is reduced in order to achieve more desirable solutions in terms of optimality. This comes from the fact that, although optimal solutions are mathematically the best possible feasible solutions, if feasibility violations are allowed to a certain extent for specific scenarios, far better solutions can be achieved. To facilitate this concept, Mulvey et al. (1995) introduced the following two definitions:

Solution robustness: *The optimal solution of a two-stage stochastic program will be robust with respect to optimality if it remains "close" to optimal for any realization of a scenario in the scenario set*

Model robustness: *The solution is also robust with respect to feasibility if it remains "almost" feasible for any realization of a scenario in the scenario set*

These two concepts are used to assess solution optimality and solution feasibility deviations under the disruption scenario set and provide the decision-maker with a controller to make a trade-off between the solution robustness and model robustness.

In the following subsections, a mathematical formulation of the two-stage stochastic program for the evacuation planning problem under uncertainty of network disruption is presented. Algorithms to compute disruption-related parameters are introduced and numerical analysis to study the efficiency of our model is conducted. Finally, a detailed conclusion of our study is presented in Section 4.4.

4.2 Problem Description

The problem on the other hand addresses evacuation planning in an evacuation network that is susceptible to road disruptions.

An evacuation network is presented as a directed weighted graph $\mathcal{G} = (\mathcal{N}, \mathcal{A})$, where a set of nodes $\mathcal{N}$ correspond to intersections, a set of arcs $\mathcal{A}$ presents road segments, and weights τ_a are estimated arc travel times. Node set $\mathcal{N}$ is composed of a set of origin nodes ($\mathcal{N}_o$), a set of intermediate nodes, and a set of destination nodes ($\mathcal{N}_d$). To better capture traffic flow evolution and its changes due to disturbances, a dynamic network flow optimization model is proposed. This model allows variable flow rates to be assigned to paths throughout the evacuation process. Set $\mathbb{T} = \{0, 1, \dots, T-1\}$ is defined as time slots showing equal intervals of the time horizon.

In general, simultaneous decisions on evacuation route selection and flow schedule might be computationally intractable for large scale evacuation problems (Bretschneider and Kimms 2011, Kim et al. 2008, Lim et al. 2012). Moreover, in a short-notice emergency evacuation, authorities often define evacuation paths *a priori*. The concern would then shift to route assignment and schedule of the traffic flow to evacuate the area. The path-based approach (Lim et al., 2012) is applied to reduce the computational burden. In this approach, path formation is separated from the flow assignment by generating possible paths between origin-destination (O-D) pairs and using it as an input parameter to the model. Also, *PBM* is able to address specific desirable functions that can help managers in traffic control. For instance, it can impose limitations on the number of used routes for the evacuation, erase the negative effects of traffic hold-back in each road, or eliminate high duration pathways in the plan.

Two assumptions on the uncertain road disturbances are considered: (i) disruptions can happen on multiple roads, and (ii) the disruption time of each road can be different from each other. The set of disruption scenarios is denoted as S and contains possible combinations of arc closures. Given the number of evacuees/demand at the source nodes (D_n), the goal is to select a set of evacuation paths from the existing path pool ($\wp$) and assign variable flow rates (f_{pt}) to each selected path in order to obtain a pro-active evacuation plan. The following mathematical notation is used throughout the paper:

Sets:

$\mathcal{N}$	Set of all nodes in the evacuation network
$\mathcal{N}_{\mathrm{o}}$	Set of all origin nodes
$\mathcal{N}_{\mathrm{d}}$	Set of all destination nodes
$\mathbb{T}$	Set of all time slots
$\wp$	Set of all paths
$\wp_{\mathrm{n}}^{+}$	Set of paths originating from source node n
$\wp_{\mathrm{n}}^{-}$	Set of paths terminated at destination node n
S	Set of all disruption scenarios

Decision Variables:

Design variables (First Stage)	
f_{pt}	Flow on path p that is dispatched from the source at time t
β_n	Undispatched demand from source node n
Recourse variables (Second Stage)	
r_{pnts}	Rerouted flow of scenario s from node n to alternate route p which is assumed to start on this path at time t (behind node n, its amount is considered as a dummy)
h_{pnts}	Disturbed flow on node n of path p at time t at scenario s
hc_{nts}	Total disrupted flow at time t which has accumulated behind node n at scenario s

Parameters:

Free of noise parameters	
θ_{pa}	Transit time from the origin of path p to reach arc a
C_a	Capacity of arc a
D_n	Demand of source node n
τ_a	Transit time on arc a
L_{pn}	Takes value 1 if node n is the source node of path p, otherwise 0
$\acute{\theta}_{pn}$	Transit time from origin of path p to reach node n
δ_{pa}	Takes value 1 if arc a belongs to path p, otherwise 0
γ_{na}	Take value 1 if node n is the upstream (origin) node of arc a, otherwise 0
Auxiliary parameters (noise relevant)	
W_{pnts}	Takes value 1 if flow that starts at time t on path p regardless of disruption times of its preceding arcs is disturbed and gets stuck behind node n in scenario s, otherwise 0
η_{ptmn}	Takes value 1 if starting flow on path p at time t does not get stuck on node m and also is not disturbed between node m and node n (m is behind n) in scenario s, otherwise 0

V_{pnts}	Takes value 1 if flow that starts at time t on path p is disturbed and gets stuck behind node n in scenario s, otherwise 0

4.2.1 Two-Stage Stochastic Optimization for Evacuation Planning

Our mathematical framework has two distinctive components: a structural component and a control component. The structural component is fixed and free of any variation (noise). The control component is subject to variations due to the uncertainty of incidents.

Design variables f_{pt} and β_n are free of noise variables that are used to develop a pro-active evacuation plan that works well under disruption scenarios S. The recourse variables respond and react to uncertain incidents (variations). These variables take a value after the realization of each disruption scenario $s \in S$ and represent (i) the number of disturbed evacuees at each node during each time interval (h_{pnts}), (ii) the remaining number of disturbed evacuees on each node (hc_{nts}), and (iii) a reroute strategy for the incident-affected evacuees (r_{pnts}) under each scenario s ∈ S.

The parameters related to disruptions are W_{pnts}, V_{pnts}, and η_{ptnns}. These parameters play a crucial role in developing mathematical formulation with a linear structure. For the calculation of these parameters, two distinctive algorithms are proposed and will be explained later in the paper.

A loss function ξ_s is defined that showcase evacuees that are left behind and stranded on roads due to incidents defined for each scenario $s \in S$. This function is illustrated as

$$\xi_s = \sum_{n \in \mathcal{N}_O} \beta_n + \sum_{n \in \mathcal{N}} hc_{nTs}, \qquad \forall\, s \in S. \tag{4.1}$$

The variable (ξ_s) represents the addition of the total number of evacuees (β_n) that have not been evacuated from the source nodes ($\mathcal{N}_o$) and the disturbed flow (hc_{nTs}) under scenarios $s \in S$ that have not been rerouted due to high congestion in alternative pathways. In other words, ξ_s is the flow that has not reached the destination by the end of the planning horizon (T^F), given that incidents depicted in scenario $s \in S$ have occurred.

Hence, a two-stage stochastic framework for the path-based model (*TSPBM*) is proposed as follows:

$$Min \quad \sum_{s \epsilon S} P_s \xi_s \qquad\qquad \textbf{\textit{TSPBM}}$$

First Stage (Design Stage)

$$\sum_{p \in \wp_n^+} \sum_{t \in \mathbb{T}} f_{pt} + \beta_n \geq D_n, \qquad \forall n \in \mathcal{N}_o, \tag{4.2}$$

$$\sum_{p \in \wp} \delta_{pa} f_{p(t-\theta_{pa})} \leq C_a, \qquad \forall a \in \mathcal{A},\ \forall t \in \mathbb{T}, \tag{4.3}$$

Second Stage (Recourse Stage)

$$h_{\mathrm{pn}(t+\dot{\theta}_{pn})s} = \mathrm{V}_{pnts} f_{pt} + W_{pnts} \sum_{m \in \mathcal{N}} \eta_{ptmns} r_{pmts}, \qquad \forall p \in \wp, n \in \mathcal{N}, t \in \mathbb{T}, s \in S, \tag{4.4}$$

$$hc_{n(t=1)s} = \sum_{p \in \wp} h_{pn(t=1)s}, \qquad \forall\, n \in \mathcal{N}, s \in S, \tag{4.5}$$

$$\begin{aligned} hc_{\mathrm{n(t+1)}s} = hc_{\mathrm{nts}} + \sum_{p \in \wp} h_{\mathrm{pn}(t+1)s} \\ - \textstyle\sum_{a \in \mathcal{A}} \sum_{p \in \wp} \delta_{pa} \gamma_{na} (1 - W_{pn(t-\theta_{pa})s}) r_{\mathrm{pn}(t-\theta_{pa})s}, \end{aligned} \qquad \forall\, n \in \mathcal{N}, t \in \mathbb{T}/\{1\}, s \in S, \tag{4.6}$$

$$\begin{aligned} \sum_{p \in \wp} \sum_{n \in \mathcal{N}} \sum_{m \in \mathcal{N}} \delta_{pa} \gamma_{na}\, \eta_{p(t-\theta_{pa})mns} \Big[(1 - \mathrm{V}_{pn(t-\theta_{pa})s}) L_{pm} f_{p(t-\theta_{pa})} \\ + (1 - W_{pn(t-\theta_{pa})s}) r_{pm(t-\theta_{pa})} \Big] \leq C_a, \end{aligned} \qquad \begin{aligned} \forall a \in \mathcal{A}, \\ t \in \mathbb{T}, s \in S, \end{aligned} \tag{4.7}$$

$$f_{pt} \in \mathbb{Z}^+, \beta_n \in \mathbb{Z}^+, \qquad \forall p \in \wp, t \in \mathbb{T}, n \in \mathcal{N}_o, \tag{4.8}$$

$$r_{pnts} \in \mathbb{Z}^+, h_{pnts} \in \mathbb{Z}^+, hc_{nts} \in \mathbb{Z}^+, \ \ \beta_n \in \mathbb{Z}^+, \qquad \forall p \in \wp, n \in \mathcal{N}, t \in \mathbb{T}, s \in S. \tag{4.9}$$

The objective function of the model aims to minimize the expected value of the number of evacuees that are left behind in the system at the end of the planning horizon. Constraints (4.2) and (4.3), being first-stage specific constraints, are free of noise and include the design variables to define the pro-active evacuation plan. Constraint (4.2) states that the total amount of flow that has left source node $n \in \mathcal{N}_o$ plus the unmet demand of the node (β_n) should be equal to the initial number of evacuees on the node (D_n). The unmet demand of a source node represents the number of evacuees left behind on that node. Constraint (4.3) guarantees that the capacity of the arc restricts the total flow that reaches arc $a \in \mathcal{A}$.

The remainder of the constraints presented here belongs to the second stage of the program, containing both the design and recourse variables. In constraints (12), the amount of disturbed flow on path $p \in \wp$ congested on node $n \in \mathcal{N}$ at time $t \in \mathbb{T}$ is calculated under scenario $s \in S$. This amount is equal to the sum of: (i) the total flow interrupted by an incident and is stuck on the node ($V_{npts}f_{pt}$), and (ii) the total rerouted flow which again becomes disturbed and is idled on the node ($W_{pnts}\sum_{m\in\mathcal{N}}\eta_{ptmns}r_{pmts}$). Remember that r_{pmts} shows the reassigned flow on path $p \in \wp$ from node $\acute{n} \in \mathcal{N}$. In constraints (4.4), parameter η_{mnpts} is used to guarantee that r_{pmts} is being considered in the calculations only if (i) node $n \in \mathcal{N}$ comes after node $m \in \mathcal{N}$ on the path, and (ii) the rerouted flow does not receive any disturbances on intermediate arcs connecting node m $\in \mathcal{N}$ to n $\in \mathcal{N}$.

The remaining amount of flow to be rerouted at time $t \in \mathbb{T}$ on node $n \in \mathcal{N}$ is defined by constraints (4.5) and (4.6) under each scenario $s \in S$. Constraints (4.5) show that the remaining amount of affected flow during time interval $t = 1$ is equal to the amount disturbed during the exact same time interval. Constraints (4.6) show the remaining amount of affected flow when $t > 1$. Accordingly, $hc_{n(t+1)s}$ is equal to: (i) the remaining affected flow in the previous period (hc_{nts}), plus (ii) the currently disturbed flow ($\sum_{p \in \mathcal{p}} h_{pn(t+1)s}$), minus (iii) the rerouted flow during the previous time interval ($\sum_{a \in \mathcal{A}} \sum_{p \in \mathcal{p}} \delta_{pa} \gamma_{na} (1 - W_{pn(t-\theta_{pa})s}) r_{pn(t-\theta_{pa})s}$).

Constraints (4.7) ensure that the total flow simultaneously passing through arc $a \in \mathcal{A}$ does not exceed the capacity of the arc. The passing flow is equal to the amount of flow $f_{p(t-\theta_{pa})}$ that has not been disrupted on the way to arc $a \in \mathcal{A}$, plus the rerouted flow $r_{pm(t-\theta_{pa})}$ which safely passes from node $m \in \mathcal{N}$ to node $n \in \mathcal{N}$ and reaches arc $a \in \mathcal{A}$. Finally, constraints (4.8) and (4.9) reflect the non-negativity and integrality of our design and recourse variables, respectively.

4.2.2 Solution and Model Robustness Measures

The loss function ξ_s is used in order to develop solution robustness and model robustness terms. *Mulvey et al.* suggested solution robustness $\sigma(.)$ as

$$\sigma(.) = \sum_{s \epsilon S} P_s \xi_s + \lambda \sum_{s \epsilon S} P_s \left(\xi_s - \sum_{s \epsilon S} P_s \xi_s \right)^2. \tag{4.10}$$

where the first term is the expected value of ξ_s, and the second term is λ multiplied by the variance of the loss function. The quadratic structure of the second term requires substantial computational efforts (Yu and Li, 2000). Therefore, Yu and Li (2000) suggested the use of an absolute loss function deviation from its expected value.

Solution robustness measure: Solution robustness function is as

$$\sigma(.) = \sum_{s\epsilon S} P_s \xi_s + \lambda \sum_{s\epsilon S} P_s \left| \xi_s - \sum_{s\epsilon S} P_s \xi_s \right|. \tag{4.11}$$

This function measures whether a solution of our model remains "close" to optimal for any realization of the disruption scenario $s \in S$. The first term $\sum_{s\epsilon S} P_s \xi_s$ represents the expected value of the loss function (4.1) and calculates the expected number of evacuees that are left behind in the evacuation network due to the inability to reach a destination by the end of the planning horizon. The second term $\sum_{s\epsilon S} P_s |\xi_s - \sum_{s\epsilon S} P_s \xi_s|$ is the variability in the loss function (4.1), and λ is used as a weight parameter to control this variability.

Model robustness measure: Model robustness measure aims to check if a solution remains "almost" feasible for any realization of scenario $s \in S$. Among our set of constraints, constraints (4.2) and (4.3) are related to the design stage and include no noise. Constraints (4.4)-(4.6) belong to the second stage. They include the resource variables and are under the influence of disruption. However, these constraints exist mainly for calculation purposes and do not impose resource restrictions on the variables. Hence, deviations in these constraints will not be considered within the interest of this problem. Constraints (4.7) place an arc capacity limitation on the amount of both initial and rerouted flow (recourse) reaching an arc. The purpose is to study violations in these constraints. Our model robustness term is defined as in equation

$$p(.) = \sum_{a\in\mathcal{A}} \sum_{t\in\mathbb{T}} \sum_{s\in S} P_s \zeta_{ats}, \tag{4.12}$$

where $\zeta_{ats} \geq 0$, to assess positive violations of the capacity constraints. This specific equation serves to present the expected value of arc capacity violations. Variable ζ_{ats} represents violations from the capacity constraints (4.7) under each disruption scenario $s \in S$ on arc

$a \in \mathcal{A}$ during time interval $t \in \mathbb{T}$.

Using these measures in the objective function of the two-stage stochastic program (*TSRPBM*), solution robustness and model robustness can be assessed, and their levels pertaining to the problem can be adjusted. *TSRPBM* is formulated as following:

$$\text{Min} \quad \sum_{s \epsilon S} P_s \xi_s + \lambda \sum_{s \epsilon S} P_s \left| \xi_s - \sum_{s \epsilon S} P_s \xi_s \right| + \omega \sum_{a \in \mathcal{A}} \sum_{t \in \mathbb{T}} \sum_{s \in S} P_s \zeta_{ats} \qquad \textbf{\textit{TSRPBM}} \tag{4.13}$$

$$\text{s.t.} \quad (10) - (14), (16) - (17), \tag{4.14}$$

$$\begin{aligned} \sum_{p \in \wp} \sum_{n \in \mathcal{N}} \sum_{\acute{n} \in \mathcal{N}} \delta_{pa} \gamma_{na} \eta_{p(t-\theta_{pa})mns} \Big[(1 - \mathrm{v}_{pn(t-\theta_{pa})s}) L_{p\acute{n}} f_{p(t-\theta_{pa})} & \qquad \forall a \in \mathcal{A}, \\ + (1 - W_{pn(t-\theta_{pa})s}) r_{pm(t-\theta_{pa})} \Big] - \zeta_{ats} \leq C_a, & \qquad t \in \mathbb{T}, s \in S, \end{aligned} \tag{4.15}$$

$$\zeta_{ats} \geq 0, \qquad \forall a \in \mathcal{A},\ t \in \mathbb{T}, s \in S. \tag{4.16}$$

In this formulation, controller omega (ω) is used to adjust the importance level of the solution robustness and model robustness in the objective function and make a trade-off between these measures. In order to capture the deviations of capacity constraints, variable ζ_{ats} is introduced to capacity constraints (4.7) to form constraints (4.15). Constraints (4.16) show the non-negativity condition of these variables.

Note that the objective function is not linear because of the term $|\xi_s - \sum_{s \epsilon S} P_s \xi_s|$. To make it easier to solve, the term can be converted into linear by applying a goal programming approach in which two types of positive decision variables and a set of constraints are added to the model. However, this approach adds an undesirable amount of decision variables to the model. To reduce the number of variables resulting from linearization and remain efficient in terms of computational complexity, an approach proposed by Li (1996) and developed by Yu and Li (2000) is utilized as described below.

Model Linearization

The objective function (4.13) can be substituted by the objective function and the constraints as follows:

$$\text{Min} \quad Z = \sum_{s \epsilon S} P_s \xi_s + \lambda \sum_{s \epsilon S} P_s [\left(\xi_s - \sum_{s \epsilon S} P_s \xi_s \right) + 2\vartheta_s] + \omega \sum_{a \in \mathcal{A}} \sum_{t \in \mathbb{T}} \sum_{s \in S} P_s \zeta_{ats} \tag{4.17}$$

S.t:

$$\xi_s - \sum_{s \epsilon S} P_s \xi_s + \vartheta_s \geq 0, \qquad \forall s \in S, \tag{4.18}$$

$$\vartheta_s \geq 0, \qquad \forall s \in S. \tag{4.19}$$

Proof. Suppose that $\xi_s - \sum_{s \epsilon S} P_s \xi_s \geq 0$. Hence, $\vartheta_s = 0$ and Z will be

$$Z = \sum_{s \epsilon S} P_s \xi_s + \lambda \sum_{s \epsilon S} P_s \left(\xi_s - \sum_{s \epsilon S} P_s \xi_s \right) + \omega \sum_{a \in \mathcal{A}} \sum_{t \in \mathbb{T}} \sum_{s \in S} P_s \zeta_{ats}. \tag{4.20}$$

On the other hand, if $\xi_s - \sum_{s \epsilon S} P_s \xi_s < 0$, then $\vartheta_s = \sum_{s \epsilon S} P_s \xi_s - \xi_s$ and Z will be equal to

$$Z = \sum_{s \epsilon S} P_s \xi_s + \lambda \sum_{s \epsilon S} P_s \left(\sum_{s \epsilon S} P_s \xi_s - \xi_s \right) + \omega \sum_{a \in \mathcal{A}} \sum_{t \in \mathbb{T}} \sum_{s \in S} P_s \zeta_{ats}. \tag{4.21}$$

Thus, the non-linear robust model can efficiently be converted into a linear robust model with fewer auxiliary variables and constraints.

4.2.3 Methodology to Calculate Noise Related Parameters

Parameters (W_{pnts}, V_{pnts}, η_{ptmns}) reflect the effect of each disruption scenario $s \in S$ on the evacuation road and on the flow (based on the topology of the network and disruption time). These parameters are calculated prior to solve *TSPBM/TSRPBM.*

Algorithm 4.1 is introduced to calculate values of parameters W_{pnts} and V_{pnts}. First, the value of W_{pnts} is calculated to determine if the flow that leaves the origin of route $p \in \wp$ at time interval $t \in \mathbb{T}$ would be affected by the incident associated with node $n \in \mathcal{N}$ regardless of the possibility of its disturbance on the preceding arcs. In the process of calculating W_{pnts}, disruption times of the preceding arcs to node $n \in \mathcal{N}$ are neglected and only the effect of disruption time of the arc originating from node $n \in \mathcal{N}$ on the flow is investigated. When evacuees start moving along path $p \in \wp$ during time interval $t \in \mathbb{T}$, they arrive at arc $a \in \mathcal{A}$ at time $t + \theta_{pa}$. It takes τ_a unit of time for the flow to completely pass through the arc. Therefore, if $t + \theta_{pa} + \tau_a$ is greater than the incident time on arc $a \in \mathcal{A}$ (denoted by DT_{as}), the flow is affected by the incident and W_{pnts} takes value 1. Else, it takes the value 0.

Parameter $\widehat{v_{pnts}}$ shows whether the starting flow on path $p \in \wp$ at time $t \in \mathbb{T}$ would be disturbed and trapped on node $n \in \mathcal{N}$. Unlike W_{pnts}, the disruption time of the preceding arcs is taken into account to calculate this value. This is due to the fact that if the flow is disturbed on another arc before reaching node $n \in \mathcal{N}$, it will not get stuck on node $n \in \mathcal{N}$ regardless of the disruption time DT_{as}. Hence, the flow will be stuck on node $n \in \mathcal{N}$ ($V_{pnts} = 1$) only when (i) the flow is not troubled during its journey to arc $a \in \mathcal{A}$ ($\sum_{m \in \mathcal{N}} W_{pmts} = 0$), and when (ii) the required time to pass arc $a \in \mathcal{A}$ is greater than its total time of disruption ($W_{pnts} = 1$). Else, $V_{pnts} = 0$.

Also, it is important to know if a flow on a path can pass from a specific node and reach another node without being affected by any disturbances. Parameter η_{ptmns} demonstrates whether the flow that is leaving path $p \in \wp$ at time $t \in \mathbb{T}$ would experience a disturbance on one of the arcs connecting node $m \in \mathcal{N}$ to $n \in \mathcal{N}$. *Algorithm 4.2* is introduced to calculate this parameter.

Algorithm 4.1

Inputs:

An evacuation network $\mathcal{G}$ consisting of a set of nodes $\mathcal{N}$ and a set of arcs $\mathcal{A}$.

Disruption scenarios S.

Calculating $\boldsymbol{V_{pnts}}$:

for all paths $p \in \wp$ **do**

  for all time slots $t \in \mathbb{T}$ **do**

    for all scenarios $s \in S$ **do**

      for all arcs that belong to path $p \in \wp$ **do**

        if $t + \theta_{pa} + \tau_a - DT_{as} > 0$ **then**

          $W_{pnts} = 1$ (n is upstream node of arc a)

        else if $t + \theta_{pa} + \tau_a - DT_{as} \leq 0$ **then**

          $W_{pnts} = 0$

        end if

        for all preceding nodes $m \in \mathcal{N}$ to arc a on path p **do**

          if $\sum_{m \in \mathcal{N}} W_{pnts} = 0$ and $W_{pnts} = 1$ **then**

            $V_{pnts} = 1$ (n is upstream node of arc a)

          else then

            $V_{pnts} = 0$

          end if

        end for

      end for

    end for

  end for

end for

First, for each path $p \in \wp$, the sequence of nodes belonging to the path is derived, which is denoted by φ_p. Then for any combination of node $m \in \mathcal{N}$ and $n \in \mathcal{N}$ in set φ_p, where $m \in \mathcal{N}$ takes precedence over node $n \in \mathcal{N}$, the summation $\sum_{k=m}^{n-1} V_{pkts}$ is calculated. If $\sum_{k=m}^{n-1} V_{pkts} = 0$, the flow is not interrupted when traveling from node $m \in \mathcal{N}$ to node $n \in \mathcal{N}$ ($\eta_{ptmns} = 1$). Otherwise, $\eta_{ptmns} = 0$.

Algorithm 4.2

Inputs:

An evacuation network $\mathcal{G}$ consisting of a set of nodes $\mathcal{N}$ and a set of arcs $\mathcal{A}$, and parameter V_{pnts}.

Calculating $\boldsymbol{\eta_{ptmns}}$:

```
for all scenarios s ∈ S do
  for all paths p ∈ 𝓅 do
     determine set φ_p as a sequence of nodes in path p
     for all time slots t ∈ 𝕋 do
        for all preceding nodes m ∈ φ_p to node n ∈ φ_p do
           if Σ_{k=m}^{n-1} V_pkts = 0 then
               η_ptmns = 1
           else then
               η_ptmns = 0
           end if
        end for
     end for
  end for
end for
```

4.3 Computational Results

In this section, the performance of our two-stage stochastic evacuation planning model under various disruption scenarios is illustrated. The model is solved using CPLEX

12.5 and all experiments are made on a PC with 3.07 GHz Intel Core i7 processor having 24GB RAM and running Ubuntu 10.04.3. The test evacuation network shown in Figure 3.8 is used for the computational experiments. This network contains three source nodes ($\mathcal{N}_1$, $\mathcal{N}_2$, and $\mathcal{N}_3$) and two destination nodes ($\mathcal{N}_9$ and $\mathcal{N}_{10}$). Arc transmit times (τ_a) as well as arc capacities (C_a) are shown for each arc.

First, all paths between origin-destination (O-D) nodes of the network are enumerated by using the CPLEX pool feature to solve the shortest path problem. Some undesired paths with long durations are discarded and candidate paths are selected to form the set of paths $\wp$. Following Procedure 4.1, experiments are made to compare the performance of TSPBM with the performance of a well-known path-based deterministic model (Rungta et al., 2012). First, disruption scenarios and their probability of occurrence are defined. The disruption scenarios are assumed to follow an exponential distribution since the road disruption probability increases as time passes. For disruption scenarios S, parameters W_{pnts}, V_{pnts}, and η_{ptmns} are calculated using Algorithm 4.1 and Algorithm 4.2. Various demand cases examined in this study are tabulated in each row of Table 4.1. For each demand case, DPBM is solved, and its resulting plan is used as a benchmark for model performance comparisons. The flow rate and schedule f_{pt}^{DPBM} provided by DPBM is considered as an input parameter and is inserted into TSPBM to calculate the expected value of the loss function ($\sum_{n\in\mathcal{N}_S}\beta_n + \sum_{s\in S}[P_s \times \sum_{n\in\mathcal{N}} hc_{nT^{CT}s}]$). This amount represents the expected value of the number of evacuees that were left behind in the system at the end of the planning horizon when the DPBM plan is used.

Procedure 4 . 1: Output generation for model comparison

Inputs:

An evacuation network $\mathcal{G}$ consisting of a set of nodes $\mathcal{N}$ and a set of arcs $\mathcal{A}$.

Disruption scenarios $s \in S$ and their occurrence probabilities P_s

Calculated parameters W_{pnts}, V_{pnts} and η_{ptmns}.

Step 1: Initialization

Randomly generate demand distribution on source nodes, $D_n, \forall n \in \mathcal{N}_o$.

Step 2: Obtain the expected value of loss function under the deterministic plan

Step 2.a: Obtain the deterministic plan

Solve the deterministic model (*DPBM*) introduced by Rungta et al. (2012) to obtain deterministic evacuation plan f_{pt}^{DPBM}

Step 2.b: Calculate the expected value of loss function

Feed deterministic plan f_{pt}^{DPBM} as an input parameter to the *TSPBM*

Calculate $\sum_{n \in \mathcal{N}_s} \beta_n + \sum_{s \in S} [P_s \times \sum_{n \in \mathcal{N}} hc_{nT^{CT}s}]$ for this plan

Step 3: Obtain the expected value of loss function under the stochastic plan

Solve *TSPBM* to obtain stochastic evacuation plan f_{pt}^{TSPBM}

Calculate $\sum_{n \in \mathcal{N}_s} \beta_n + \sum_{s \in S} [P_s \times \sum_{n \in \mathcal{N}} hc_{nT^{CT}s}]$ for this plan

Step 4: Comparison

Compare the expected value and computation time of deterministic program (*DPBM*) with introduced *TSPBM*

Next, we solved TSPBM for the same data and measured the number of evacuees remaining in the system. In order to make a fair and clear comparison between the deterministic approach (DPBM) and our approach (TSPBM), we only compared the expected value of the loss function and ignored the variability and infeasibility penalty functions. These functions were investigated separately using TSRPBM to solve a sample test problem and study their effects on the evacuation plan, to be described later in this section.

In Table 1, the results of applying *Procedure 4.1* under different demand cases are tabulated. Each row of the table represents a demand case. The amount of demand for the three source nodes, the clearance time (*CT*) of the deterministic plan, the expected value of the loss function (Obj), the solution times for *DPBM* and *TSPBM*, and the amount of Obj improvement under *TSPBM* are shown in each column of the table. As indicated in the first row (*Case 1*), when the demand on the source nodes $\mathcal{N}_1$, $\mathcal{N}_2$, and $\mathcal{N}_3$ were equal to 75, 76, and 65, the expected value of the loss function for *DPBM* was 11.66. For this plan, $\sum_{n\in\mathcal{N}_s}\beta_n$ was equal to zero; this indicates that all the evacuees on the source nodes had been evacuated. Hence, the planning horizon, equaling 12, also serves as the clearance time (*CT*) of the deterministic plan. The clearance time for an evacuation plan is defined by the time at which all evacuees have safely evacuated from dangerous areas or have reached safe shelters. The *CT* of *DPBM* under all demand cases are shown in the column "*CT*". Using this time as the planning horizon duration, *TSPBM* is solved, and the expected value of the loss function is recorded. *CT* of *DPBM* is used as the planning horizon for *TSPBM* in order to fix the factor of competition time for the pro-active plan according to the completion time of the benchmark plan (provided by *DPBM*). Thus, the comparisons of the model results would be fair. For Case 1, the expected value for *TSPBM* was 9.2, or in other words, a 21.10% improvement over *DPBM*. As is clear, *TSPBM* outperformed *DPBM* in all cases tested in Table 4.1 in terms of reducing the expected value of the loss function.

Moreover, in the pro-active plans provided by *TSPBM* under each demand scenario, $\sum_{n\in\mathcal{N}_s}\beta_n$ was equal to zero; hence, *CT* of *TSPBM* was the same as *CT* of the *DPBM* plan. This means that after the disruptions, a fewer number of disrupted evacuees are expected to remain in the system while the clearance time of the proposed pro-active plan does not face any increase.

Table 4.1: Objective Value Comparison of DPBM and TSPBM under CT of DPBM

	Demand				*DPBM*		*TSPBM*		*Obj Improvement*
	N1	*N2*	*N3*	*CT*	*obj*	*time*	*obj*	*time*	
Case1	75	76	65	12	11.66	0	9.2	2.81	21.10%
Case2	72	71	94	14	12.1	0.02	5.83	3.16	51.82%
Case3	91	99	74	14	15.77	0.02	10.43	3.39	33.86%
Case4	124	137	137	19	32.66	0	20.37	3.22	37.63%
Case5	136	107	121	17	26.8	0.01	22.13	2.81	17.43%
Case6	116	102	142	19	23.67	0	11.37	3.41	51.96%

*TF: Time Frame, *obj: Expected value of loss function *time: computation time (seconds)

Detailed information on the plan provided by *DPBM* and *TSPBM* under the *CT* of *DPBM* can be found in Table 4.2. In this table, the number for disturbed flow represents the amount of flow from the plan that experienced a disturbance after the realization of disruption scenarios. Note that this amount is different from the amount given from the loss function. Our defined loss function shows the amount of disturbed flow that remains in the system after all possible rerouting and recovery actions are taken.

Table 4.2: Detailed Comparison of DPBM and TSPBM under CT of DPBM

		Case1	**Case2**	**Case3**	**Case4**	**Case5**	**Case6**
DPBM	#disturbed flow (EX, Max)	(21,110)	(22.1,129)	(29.3,158)	(50.3,225)	(42.9,231)	(50.5,205)
	#effective scenario	12	12	13	18	17	17
	rerouting CT (EX, Max)	(14.3, 20)	(16, 23)	(17.1, 24)	(25.1, 32)	(22.07,30)	(23.3, 29)
TSPBM	#disturbed flow (EX, Max)	(12.2,110)	(13.7,117)	(15.5,126)	(45.3,197)	(30.8,179)	(34.9,186)
	#effective scenario	6	8	8	15	14	15
	rerouting CT (EX, Max)	(13, 19)	(15.4, 21)	(15, 23)	(23.8, 31)	(21.1, 30)	(22.8, 29)

*EX: Expected value of disturbed flow *Max: Maximum value of disturbed flow

Contrarily, the values shown in Table 4.2 demonstrate how many people were initially affected by the incidents (before implementing a recovery strategy). Additionally, the number of effective scenarios in Table 4.2 showcases the number of scenarios in which the occurrence of the scenario affected the plan and disturbed its flow. Finally, the rerouting CT stands for the clearance time of the rerouted flow occurring after the disruptions. Rerouting CT shows the amount of time needed to reroute the disturbed evacuees and clear the network.

As seen in Table 4.2, for Case 1 using DPBM, the expected value of the disturbed flow and the maximum value pertaining to the worst-case scenario is 21 and 110 evacuees, respectively. Contrarily, the expected value of 21 is reduced to the expected value of 12.2 disturbed evacuees when TSPBM is used. After rerouting strategies are implemented, the expected number of evacuees to remain in the system based on the DPBM solution is 11.66 out of 21, while TSPBM reduces the number to 9.21 (see Table 4.1)—a 21.1% improvement over DPBM. Furthermore, TSPBM plans performed well under various disruption scenarios. The number of disruption scenarios that affected the DPBM evacuation plan is 12, and this number is reduced to 6 under TSPBM. Moreover, in TSPBM, the expected value of the rerouting CT is 13. In comparison to the corresponding value of 14.33 in DPBM, the TSPBM outcome demonstrates a reduction in the expected rerouting process time. This decrease in rerouting duration time is a result of the decrease in the amount of disrupted flow as well as the decrease in the number of effective scenarios. This has happened for all demand cases (Case 1 to Case 6). TSPBM makes an active attempt to minimize the number of disturbed evacuees that remain in the system. Hence, TSPBM expedites the rerouting process of the disturbed flow.

In most demand cases, the maximum amount of rerouting CT is also decreased as observed in Cases 1 - 4. This is mainly due to the decrease in the amount of worst-case disturbed flow. However, in Case 1, the maximum amount of disturbed flow for both models is the same (110 evacuees). The maximum rerouting CT is decreased when using TSPBM. This is because the maximum disturbed flow shown in the table is in fact the total amount of disturbed flow over all nodes of the evacuation network. As this amount is dispersed between different nodes, the number of evacuees on the node, the location of the node, and its distance to destination nodes could affect the rerouting CT.

To further analyze the performance of our model, we tabulated the improvement percentages in the expected value of the loss function under different time frames (dissimilar to *CT* of *DPBM*) in Table 4.3.

Table 4.3: Comparison of DPBM and TSPBM under Different Time Frames

	Case1	***Case2***	***Case3***	***Case4***	***Case5***	***Case6***
TF	13	15	15	20	18	20
obj	5.13	4.43	6.56	14.66	15.46	8.97
Improv	56.00%	63.39%	58.40%	55.11%	42.31%	62.10%
TF	14	16	16	21	19	21
obj	3.9	3.3	5.1	11.3	11	7.23
Improv	66.55%	72.73%	67.66%	65.40%	58.96%	69.46%
TF	15	17	17	22	20	22
obj	2.9	2.3	4.1	9.2	8.6	6.06
Improv	75.13%	80.99%	74.00%	71.83%	67.91%	74.40%
TF	16	18	18	23	21	23
obj	1.9	1.3	3.1	7.53	6.93	4.9
Improv	83.70%	89.26%	80.34%	76.94%	74.14%	79.30%

*TF: time frame, *obj: Expected value of loss function *Improv: objective function improvement

As shown in Table 4.3, when the time frame is greater than the clearance time of *DPBM*, *TSPBM* provides a more reliable plan that leads to fewer evacuees being severely affected by the network disruption. For instance, in Case 1, when the evacuation time is increased by one unit of time and reaches 13, the improvement in the expected value of the loss function increases from 21.1% to 56%. This amount reaches 66.55% when the evacuation process time is 14. Thus, this instance demonstrates that by compromising the evacuation time, we can far better reduce the negative consequences resulting from disruptions.

In the previous experiments, the probability distribution parameter $\lambda_{exp} = 10T$ is used for the disruption scenario generations. To further study the results, comparisons between *DPBM* and *TSPBM* under different values of λ_{exp} are made as shown in Table 4.4.

Table 4.4: Comparison of DPBM and TSPBM under Different Parameter for Disruption Scenario

	$\boldsymbol{\lambda_{exp}}$	***DPBM obj***	***TSPBM obj***	***Obj Improvement***
Case 1	14	9.5	7.36	22.53%
	12	10	8.2	18.00%
	10	11.66	9.2	21.10%
	8	14	11.1	20.71%

	$\boldsymbol{\lambda_{exp}}$	***DPBM obj***	***TSPBM obj***	***Obj Improvement***
Case 2	14	8.8	4.46	49.32%
	12	9.97	4.96	50.25%
	10	12.1	5.83	51.82%
	8	15.33	7.4	51.73%

	$\boldsymbol{\lambda_{exp}}$	***DPBM obj***	***TSPBM obj***	***Obj Improvement***
Case 3	14	11.93	8.3	30.43%
	12	13.06	9.13	30.09%
	10	15.77	10.43	33.86%
	8	19.93	13.13	34.12%

	$\boldsymbol{\lambda_{exp}}$	***DPBM obj***	***TSPBM obj***	***Obj Improvement***
Case 4	14	21.47	14	34.79%
	12	24.47	15.6	36.25%
	10	32.66	20.37	37.63%
	8	41.7	29.3	29.74%

	$\boldsymbol{\lambda_{exp}}$	***DPBM obj***	***TSPBM obj***	***Obj Improvement***
Case 5	14	18.6	15.63	15.97%
	12	20.97	17.6	16.07%
	10	26.8	22.13	17.43%
	8	30.07	24.7	17.86%

	$\boldsymbol{\lambda_{exp}}$	***DPBM obj***	***TSPBM obj***	***Obj Improvement***
Case 6	14	16.37	8.23	49.73%
	12	18.33	9.06	50.57%
	10	23.67	11.37	51.96%
	8	30.13	16.03	46.80%

We observe that as λ_{exp} decreases, the amount of disturbed flow remaining in the system increases. This is due to the fact that by decreasing λ_{exp}, the average arc disruption time increases. As a result, there could be an increase in disruptions and disturbed flow, as well as an increase in the expected value of the disturbed evacuees that remain in the system. Results also indicate that under different amounts of λ_{exp}, we experienced improvement in the value of the loss function yielded by *TSPBM*.

In the previous experiments, we focused on the expected value of the loss function in order to make the comparisons between *TSPBM* and *DPBM*. In the following experiments, we illustrate that *TSRPBM* can be used to control variations in the loss function as well as make a tradeoff between solution and model robustness. Consequently, compared to *TSPBM,* we show that *TSRPBM* can provide even better results in terms of the loss function reduction.

We consider an evacuation problem with the demand distribution on the source nodes as $D_1 = 102$, $D_2 = 130$, and $D_3 = 167$. Using various values of omega (the weight controller of the robustness measures) and $\lambda = 1$ (the weight of the loss function variation), we make a tradeoff between the solution and the model robustness of the evacuation plan generated using the network sample of Figure 3.8. Results are shown in Table 4.5 and Figure 4.1.

In Table 4.5, the solution robustness includes the expected value of the loss function as well as its variation. Figure 4.1 shows that critical points for omega are $\omega = 2.821$, $\omega = 2.841$, and $\omega = 2.91$. When ω was less than 2.841, we observed that the expected value and variations in the loss function took no value and were at their minimum level (zero), meaning all evacuees were cleared. The reason for this is that the objective function puts less emphasis on the feasibility of the solution and more on reducing the loss function. Consequently, we obtain the maximum amount of deviation from the capacity constraints (4.7) and increased redundant capacity for rerouting actions, and a lesser amount of disturbed evacuees remained in the system.

Table 4.5: Solution and Model Robustness

Omega (ω)	***Solution Robustness***		***Model Robustness***
	expected value	***variations***	***(infeasibility)***
1	0	0	5.55
2	0	0	5.55
2.82	0	0	5.55
2.821	2	3.64	3.55
2.84	2	3.64	3.55
2.841	5	9.16	0.55
2.85	5	9.16	0.55
2.9	5	9.16	0.55
2.91	5.55	11	0
3	5.55	11	0
7	5.55	11	0
9	5.55	11	0

Deviation (which is noted by ζ_{ats}) from the capacity constraint makes it possible for the system to accommodate and reroute more disturbed evacuees through the roads by considering a redundant capacity. This redundant capacity does not actually exist in the system unless evacuation managers decide to expand the capacity of the roads. When ω exceeded 2.821, the infeasibility of the capacity constraint adds more expenses to the objective function, leading to a reduced value for both infeasibilities and consequently model robustness terms.

Overall, we see that as the value of omega (ω) increases, the value of model robustness decreases. This happens because more emphasis is put on the model robustness rather than the solution robustness. Since the influence of the solution robustness on the objective value is decreased, the value of the solution robustness increases. When the objective function is influenced more by the constraint infeasibility, the model provides plans that are feasible under more disruption scenarios.

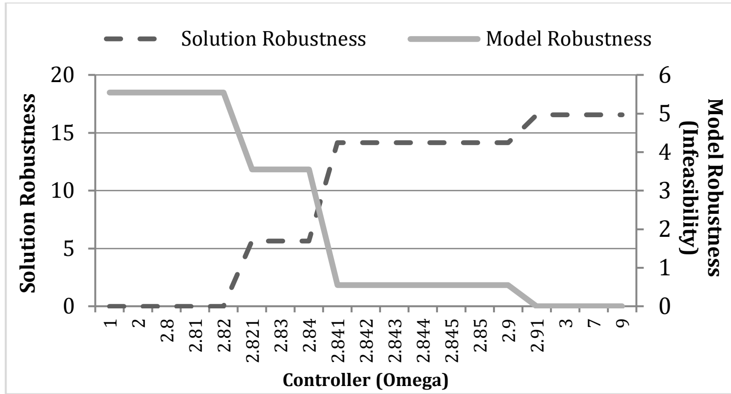

Figure 4.1: Tradeoff between Solution and Model Robustness using Controller (Omega)

The feasibility of capacity constraints under more scenarios restricts rerouting processes. Thus, in more scenarios, we observe disturbed evacuees remaining in the system. When ω exceeds 2.91, the model robustness equals zero. Thus, the infeasibility in the capacity constraint under all disruption scenarios amount to zero. This means that the model provides a solution that is feasible under all scenarios, including the worst-case scenarios.

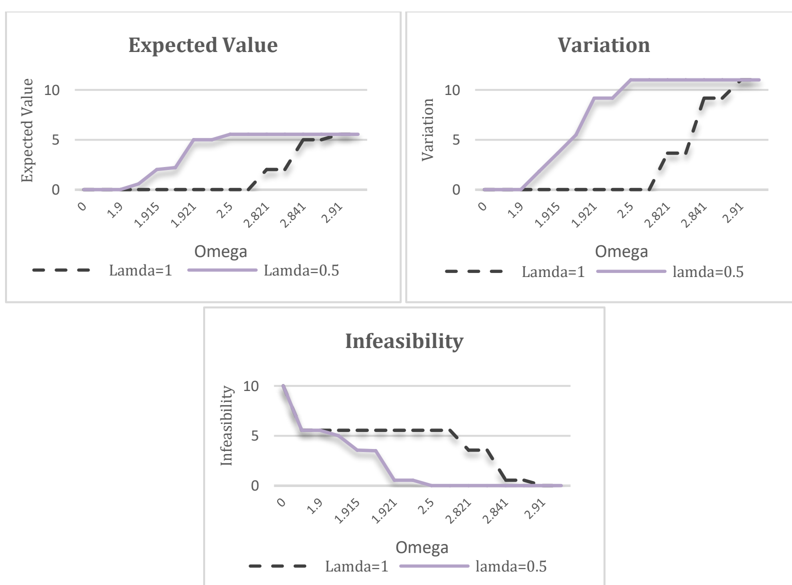

Figure 4.2: Expected Value, Variation, and Infeasibility Values under Different values of Lamda and Omega

The most conservative solution of this model occurs when ω exceeded 2.91 and leads to the lowest amount of solution robustness (expected value and deviation in the loss function). As a result, by using the controller omega, evacuation managers can make an appropriate tradeoff between the solution and model robustness and control the degree of conservatism of an evacuation plan. By changing the λ value with respect to ω, we are able to better trade-off between the expected value of the loss function, its variation, and its deviations in the road capacity constraints (infeasibility). Figure 4.2 shows these variations over different values of λ and ω.

The evacuation managers can also make a decision on whether to use road capacity improvement techniques such as a contra-flow approach (Wolshon, 2001) to make redundant capacity in specific roads at specific times to improve the solution robustness, or to accept the increase in the amount of loss function. For any specific value of omega, we can detect critical roads in the network as well as the amount of excess capacity that, if provided, could make an efficient enhancement in the solution robustness. In Figure 4.3, the amount of road capacity deviation (infeasibility) over different time slots of the planning horizon, arcs (roads) of the network, and the disruption scenarios under differing amounts of ω considering $\lambda = 1$ are shown. When $\omega = 1$, we see deviations occurring on arcs $a4$, $a5$, $a6$, $a19$, $a2$, and the time at which the road expansion is highly needed ranges from $t4$ to $t18$. By increasing the value of ω to 2.821 and 2.841, we observe fewer violations over time.

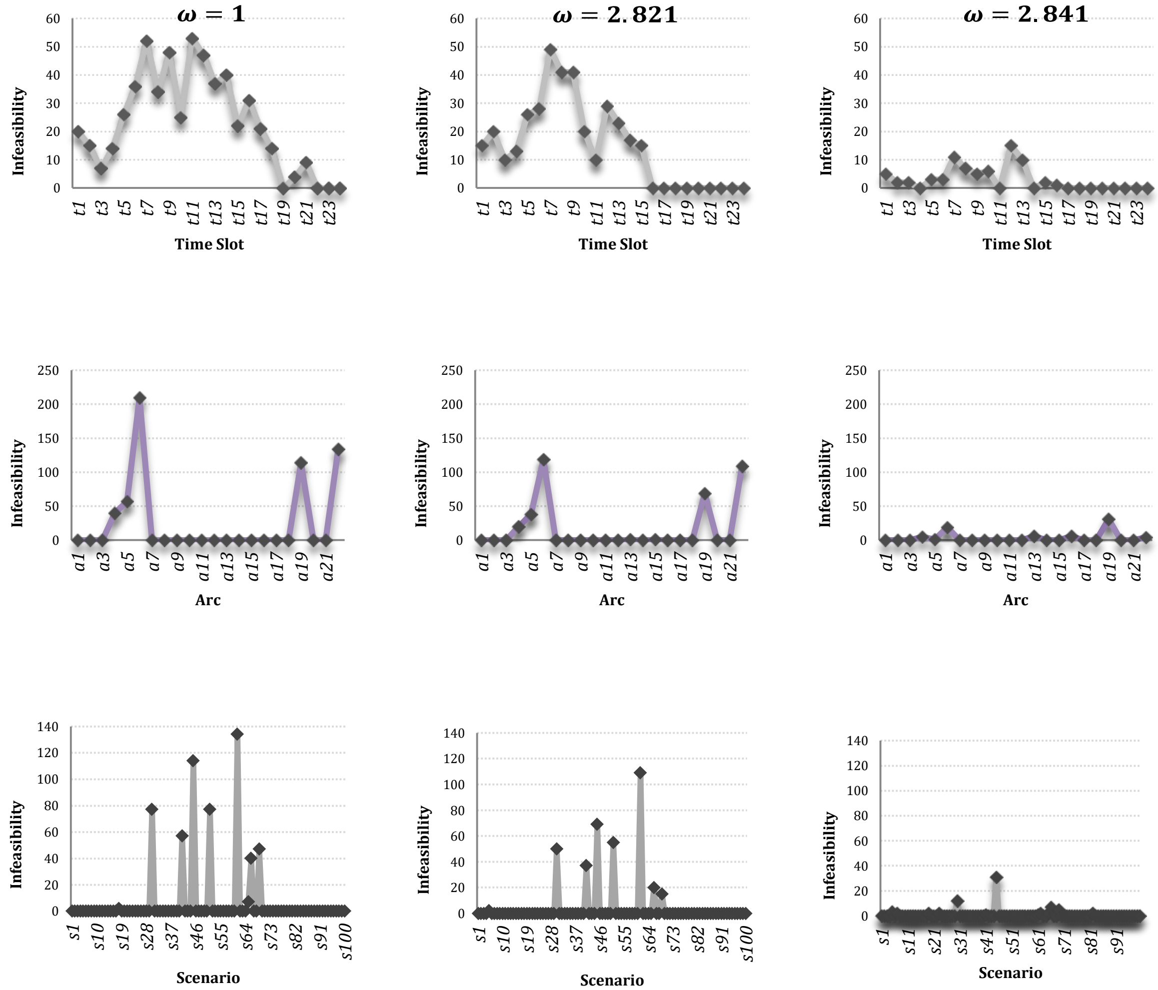

Figure 4.3: Infeasibility of the arc capacity constraint under panning intervals, roads, and disruption scenarios

4.4 Conclusion

In this work, we presented a two-stage stochastic optimization model to provide reliable plans when there is a possibility of several road closures during an evacuation. Two innovative algorithms were introduced to calculate noise-related parameters that ultimately helped to develop a linear structured model. The first stage of our model presents the reliable evacuation plan, while the second stage defines actions and a recovery plan to be implemented after the occurrence of road disruptions. The goal of the two-stage stochastic program (*TSPBM*) is to reduce the expected value of the number of evacuees that cannot reach a destination by the end of the planning horizon (considered as a loss function). Furthermore, to adjust and evaluate the level of plan conservatism, two robustness measures were introduced: optimality and feasibility. The optimality term aims to evaluate whether the provided evacuation plan is close enough to evacuation plans that are optimum for each disruption scenario. The feasibility term is considered as the penalty function of any violation of capacity constraints that relates to evacuation resources. By using goal programming, the decision-makers are given the opportunity to make a trade-off between these two terms in order to adjust the plan.

Using numerical experiments, the performance of our *TSPBM* is compared to the performance of a deterministic path-based model *DPBM* presented in the literature. As observed in all test cases, the results supported that the introduced *TSPBM* outperforms *DPBM* in terms of generating a more reliable evacuation route plan and schedule in the face of network disruptions. Moreover, using *TSPBM*, we were able to provide a better route plan if the evacuation process time was compromised. The plan conservativeness was further adjusted by using the introduced robustness measures. Results showed that when decision-makers focus on the feasibility of a solution under all disruption scenarios, the plan becomes too conservative and deviates further from improving the solution robustness. On the other hand, when decision-makers allow a certain amount of violations from the capacity constraints, they can achieve far better solutions in terms of reducing the negative consequences of disruptions. We conclude that using the *TSRPBM* model results in better solutions with respect to *TSPBM* in terms of reducing the loss function and negative consequences of road disruptions in the initial evacuation plan.

Chapter 5

Data-Driven Robust Optimization Approach Using Support Vector Clustering (SVC)

5.1 Introduction

The rate of participation of would-be evacuees during an emergency evacuation depends on a number of factors including the nature of the disaster (e.g., natural/man-made), the type of dwellings involved (e.g., permanent versus mobile homes), the region of impact, the time of impact, and the evacuees' perception of their risk. Here, in this research, we aim to develop proactive evacuation plans to reduce consequences arising from variations in demand (number of evacuees at each source node such as a ZIP code).

Large-scale evacuations are rare events and because of their uniqueness, limited data regarding them is available. Most often, demand approximations are based on limited available data or on expert's judgments. Hence, difficulties can arise during implementing an evacuation plan when there are inconsistencies in estimations. In some special cases, predictions using limited historical data may suffice to form the so-called expected-value problem. However, in most cases, especially in the context of mass-evacuations in which many unexpected events occur, using the expected-value plan may lead to many unwanted outcomes and dramatically damage the efficiency of the plan. This has urged us to study evacuation planning under uncertainty of input demand parameter. On the robust optimization concept, usually "worst-case" demand scenario is considered (Wolshon, 2009) and a single-scenario evacuation problem is solved. However, this approach can increase the clearance time of the system. Clearance time is the time required to evacuate all evacuees and get them to safe shelters. The first uncertainty set is built using support vector clustering (SVC) which is most often used in machine learning techniques. The second uncertainty set is obtained by the intersection of the previous uncertainty set with box uncertainty set (mostly used in robust optimization). In the following subsections, the proposed approaches are explained and through conducting numerical experiments their performances are studies.

5.2 Problem Statement

we adopt dynamic network flow optimization to capture evacuation traffic dynamics over the evacuation planning horizon and use a directed network $\mathcal{G} = (\mathcal{N}, \mathcal{A})$ to represent the evacuation network. T discrete time periods $\mathbb{T} = \{0, 1, \ldots, \mathrm{T} - 1\}$ are assumed as the planning horizon to complete the movement of people and reach all evacuees to the destination nodes. The status of evacuation flow at a specific time $t \in \mathbb{T}$ is shown by a static network, and the dynamic network flow is constructed through multiple static networks associated with each time $\in \mathbb{T}$. The evacuation flow assignment on this network requires a representation of a series of flows that are limited and affected by the capacity of evacuation roads intersections at various times in the attempt to meet the evacuation demand. The following notations are used throughout the paper.

Sets:

$\mathcal{N}$	Set of all nodes
$\mathcal{N}_{\mathrm{o}}$	Set of all source nodes
$\mathcal{N}_{\mathrm{d}}$	Set of all destination nodes
$\mathbb{T}$	Set of all time slots
$\mathcal{p}$	Set of all paths

M_l	Set of demand zones at source node $l \in \mathcal{N}_o$
$\wp_l^+$	Set of paths emerging from source node $l \in \mathcal{N}_o$
$\wp_l^-$	Set of paths reaching destination node $l \in \mathcal{N}_d$
SV_l	support vectors (SV) for demand data of source node $l \in \mathcal{N}_o$
BSV_l	boundary support vectors (BSV) for demand data of source node $l \in \mathcal{N}_o$

Decision Variables:

f_{pt}	Assigned flow to path $p \in \wp$ scheduled to depart at time $t \in \mathbb{T}$
β_l	Unsatisfied demand related to source node $l \in \mathcal{N}_s$
x_{lk}	An auxiliary variable

Parameters:

S_{lk}	Demand of zone $k \in M_l$ at source node $l \in \mathcal{N}_o$
C_a	Capacity of arc $a \in \mathcal{A}$
ℓ_l	Capacity of destination node $l \in \mathcal{N}$
τ_a	Transit time on arc $a \in \mathcal{A}$
θ_{pa}	Transit time from the origin of path $p \in \wp$ to arc $a \in \mathcal{A}$
S_{lk}	The nominal value of uncertain demand $\widetilde{S_{lk}}$
u_{lk}	Normalized random variable of uncertain demand $\widetilde{S_{lk}}$
$\widehat{S_{lk}}$	Variation amplitude of uncertain demand $\widetilde{S_{lk}}$
R_l	Radius of the sphere obtained by SVC covering demand data of source node $l \in \mathcal{N}_o$
p_l	Center of the sphere obtained by SVC covering demand data of source node $l \in \mathcal{N}_o$
L_{lk}	Width parameter associated to demand data of source node $l \in \mathcal{N}_o$

5.2.1 Path-Based Model

We begin by briefly describing the deterministic path-based model (DPBM) for the evacuation planning problem, which is the base-model for developing the proposed data-driven optimization model in the next section. The mathematical formulation of DPBM is presented as follows:

$$\text{Minimize} \quad \sum_{l \in \mathcal{N}_o} \beta_l \qquad \textit{(DPBM)} \tag{5.1}$$

$$\text{Subject to:} \quad \sum_{p \in \wp_l^+} \sum_{t \in \mathbb{T}} f_{pt} + \beta_l \geq \sum_{k \in M_l} S_{lk}, \qquad \forall l \in \mathcal{N}_o, \tag{5.2}$$

$$\sum_{p \in \wp} \delta_{pa} f_{p(t-\theta_{pa})} \leq C_a, \qquad \forall a \in \mathcal{A},\ \forall t \in \mathbb{T}, \tag{5.3}$$

$$\sum_{p \in \wp_l^-} \sum_{t \in \mathbb{T}} f_{pt} \leq \ell_l, \qquad \forall l \in \mathcal{N}_d, \tag{5.4}$$

$$f_{pt} \in \mathbb{Z}^+, \qquad \forall p \in \wp, \forall t \in \mathbb{T}, \tag{5.5}$$

$$\beta_l \in \mathbb{Z}^+, \qquad \forall l \in \mathcal{N}_o. \tag{5.6}$$

The *DPBM* aims to minimize any evacuees left behind (β_l) for the given planning horizon T, which ultimately maximizes the total flow leaving the evacuation network within time T. Objective function (5.1) is used to make sure that the assignments of evacuation flow rates (f_{pt}) to the selected set of paths $\wp$ are in such a way that the total remaining evacuees on all source nodes ($\sum_{l \in \mathcal{N}_o} \beta_l$) are minimized by the end of the planning horizon. Constraint (5.2) is to ensure that the total outflow departing from a source node $l \in \mathcal{N}_o$ and any remaining residents in the node (unserved demand β_l) meets the total number of available evacuees in each source node. Constraint (5.3) is the arc capacity constraint to accommodate the simultaneous use of an arc $a \in \mathcal{A}$ by multiple paths. However, it places a limitation on the total amount of flow reaching an arc $a \in \mathcal{A}$ at a specific time $t \in \mathbb{T}$ and ensures that the flow is less than the capacity of the road C_a. Similarly, the total amount of flow reaching the destination node $l \in \mathcal{N}_o$ is restricted by its capacity as in Constraint (5.4). Non-negativity and integrality conditions of the variables are reflected in Constraints (5.5) and (5.6).

An estimate of the demand (S_{lk}) is used in constraint (5.2) of DPBM which can result in suboptimal or infeasible evacuation plans in face of uncertain demand variations. To avoid the complication and derive a better evacuation plan, we propose an approach by actively learning a data-driven uncertainty set from available data with the use of machine learning and robust optimization techniques.

5.2.2 Data-Driven Robust Path-Based Model for Evacuation Planning

Because the evacuation demand is uncertain, Constraint (5.2) of DPBM is reformulated as

$$\sum_{p\in\wp_l^+}\sum_{t\in\mathbb{T}} f_{pt} + \beta_l \geq \sum_{k\in M_l} \widetilde{S_{lk}}, \qquad \forall l \in \mathcal{N}_o. \tag{5.7}$$

The uncertainty parameter can be expressed as

$$\widetilde{S_{lk}} = S_{lk} + u_{lk}\widehat{S_{lk}}, \qquad \forall l \in \mathcal{N}_o,\ \forall k \in M_l.$$

where S_{lk} is the nominal value of uncertain demand $\widetilde{S_{lk}}$, u_{lk} is the normalized random variable whose center of support is at the origin, and $\widehat{S_{lk}}$is the variation amplitude of the uncertain parameter. An uncertainty set U_l for each source node $l \in \mathcal{N}_\mathrm{o}$ can be built upon the random vector $\boldsymbol{u_l} = [u_{1l}, u_{2l}, \dots, u_{kl}, \dots, u_{nl}]^T$. The feasibility of constraint (5.7) is ensured when it is satisfied under all possible realization within U_l as

$$\sum_{k\in M_l} S_{lk} + max_{u_l\in \mathrm{U}_l} \sum_{k\in M_l} u_{lk}\widehat{S_{lk}} \leq \sum_{p\in\wp_l^+}\sum_{t\in\mathbb{T}} f_{pt} + \beta_l, \qquad \forall l \in \mathcal{N}_o. \tag{5.8}$$

By introducing auxiliary variable $x_{lk} = \widehat{S_{lk}}$, the robust counterpart of the DPBM model under uncertainty set U_l can be formulated as follows:

$$\text{Minimize} \quad \sum_{l \in \mathcal{N}_o} \beta_l \tag{5.9}$$

$$\text{S.t:} \quad \text{(5.3)-(5.6)}, \tag{5.10}$$

$$max_{u_l \in \mho_l} \sum_{k \in M_l} u_{lk} x_{lk} \leq \sum_{p \in \mathcal{p}_l^+} \sum_{t \in \mathbb{T}} f_{pt} + \beta_l - \sum_{k \in M_l} S_{lk}, \quad \forall a \in \mathcal{A},\ \forall t \in \mathbb{T}. \tag{5.11}$$

5.2.2.1 Data-Driven Model with SVC-based Uncertainty Set

We use support vector clustering to construct uncertainty set $\mho_l$ for the robust optimization model (5.9)-(5.11). The SVC algorithm has been proposed by Ben-Hur *et al.* (2001) based on the theory of machine learning. It helps to determine a minimum volume enclosed hypersphere that covers all data points. Assume that $Ɗ_l$ denotes a set of N_l data samples $Ɗ_l = \{u^{(i)}{}_l\}_{i=1}^{N_l}$ for node $l \in \mathcal{N}_o$. The smallest enclosed hypersphere containing images of data sample for each node $l \in \mathcal{N}_o$ can be obtained by the following optimization model:

$$\text{Minimize} \quad R_l^2 + \frac{1}{N_l \nu_l} \sum_{i \in N_l} \varepsilon_{il} \tag{12}$$

$$\text{Subject to:} \quad \left\| \emptyset\left(\boldsymbol{u}^{(i)}{}_l\right) - p_l \right\|^2 \leq R_l^2 + \varepsilon_{il}, \qquad \forall i \in N_l, \tag{13}$$

$$\varepsilon_{il} \geq 0, \qquad \forall i \in N_l. \tag{14}$$

where the nonlinear mapping $\emptyset(\boldsymbol{u_l})$:$\mathbb{R}^n \longrightarrow \mathbb{R}^\kappa$ maps the original input space into a high dimensional feature space, $\|.\|$ is the Euclidean norm, R_l is the radius of the sphere and p_l is its center. Slack variables $\{\varepsilon_{il}\}$ are used in the objective function and the constraints to provide a soft margin for the sphere which allows some data points to be outside of the sphere. Furthermore, a trade-off between the number of data points laying outside of the hypersphere and the volume of the hypersphere is possible by adjusting amount of the controller parameter ν_l. To solve the optimization model (5.12)-(5.14), Lagrangian multipliers $\boldsymbol{\alpha_l}, \boldsymbol{\gamma_l} \geq \mathbf{0}$ are introduced and the Lagrangian function is constructed as

$$L(\boldsymbol{p_l}, R_l, \boldsymbol{\varepsilon_l}, \boldsymbol{\alpha_l}, \boldsymbol{\gamma_l}) = R_l^2 + \frac{1}{N_l \nu_l} \sum_{i \in N_l} \varepsilon_{il} - \sum_{i \in N_l} \alpha_{il} \left(R_l^2 + \varepsilon_{il} - \left\| \emptyset(\boldsymbol{u}^{(i)}{}_l) - p_l \right\|^2 \right) - \sum_{i \in N_l} \gamma_{il} \varepsilon_{il}. \tag{5.15}$$

Following Karush-Kuhn-Tucker (KKT) conditions, we take derivatives from the Lagrangian function (5.15) with respect to R_l, $\boldsymbol{p_l}$, $\boldsymbol{\varepsilon_l}$. Setting these derivatives equal to zero ($\frac{\partial \mathrm{L}}{\partial \mathrm{R_l}} = 0, \frac{\partial \mathrm{L}}{\partial \boldsymbol{p_l}} = 0$, and $\frac{\partial \mathrm{L}}{\partial \boldsymbol{\varepsilon_l}} = 0$) leads to the following equations:

$$\sum_{i \in N_l} \alpha_{il} = 0, \qquad \forall l \in \mathcal{N}_o, \tag{5.16}$$

$$\sum_{i \in N_l} \alpha_{il}\, \emptyset(\boldsymbol{u}^{(i)}{}_l) = \boldsymbol{p_l}, \qquad \forall l \in \mathcal{N}_o, \tag{5.17}$$

$$\alpha_{il} + \gamma_{il} = \frac{1}{N_l \nu_l}, \qquad \forall i \in N_l,\ \ \forall l \in \mathcal{N}_o. \tag{5.18}$$

According to the KKT complementarity condition, we have the following relations:

$$\left(R_l^2 + \varepsilon_{il} - \left\| \emptyset(\boldsymbol{u}^{(i)}{}_l) - p_l \right\|^2 \right) \gamma_{il} = 0, \qquad \forall l \in \mathcal{N}_o, \tag{5.19}$$

$$\alpha_{il} \varepsilon_{il} = 0, \qquad \forall i \in N_l,\ \ \forall l \in \mathcal{N}_o. \tag{5.20}$$

The position of each data point $u_l^{(i)}$ ($\forall i \in N_l$) relative to its corresponding hypersphere boundary can be determined by interpreting optimal value of γ_l. If $\varepsilon_{il} > 0$, then $\alpha_{il} = 0$ and $\gamma_{il} = \frac{1}{N_l \nu_l}$ and the point is considered to be a boundary support vector (BSV). If $0 < \gamma_{il} < \frac{1}{N_l \nu_l}$, then according to (5.16) $\alpha_{il} > 0$ and according to (5.18) $\varepsilon_{il} = 0$ which yields $\left\| \emptyset(\boldsymbol{u}^{(i)}{}_l) - p_l \right\|^2 = R_l^2$. This condition indicates that the corresponding point is considered to be a support vector (SV). Consequently, if $\gamma_{il} = 0$ then $\alpha_{il} = \frac{1}{N_l \nu_l}$ and $\left\| \emptyset\left(\boldsymbol{u}^{(i)}{}_l\right) - p_l \right\|^2 > R_l^2$ and the data point is regarded as an outlier.

By substituting (5.16)-(5.18) into the Lagrangian (5.15), the Wolfe dual problem which is a disciplined quadratic program can be induced for each source node $l \in \mathcal{N}_{\text{o}}$ as following:

$$\text{Maximize} \qquad \sum_{i \in N_l} \alpha_{il} K_l\left(\boldsymbol{u}^{(i)}{}_l, \boldsymbol{u}^{(i)}{}_l\right) - \sum_{i \in N_l} \sum_{j \in N_l} \alpha_{il} \alpha_{jl} K_l\left(\boldsymbol{u}^{(i)}{}_l, \boldsymbol{u}^{(j)}{}_l\right) \quad QP_{SVC} \tag{5.21}$$

$$\text{Subject to:} \qquad 0 \le \alpha_{il} \le 1/N_l \nu_l, \qquad \forall i \in N_l, \tag{5.22}$$

$$\sum_{i \in N_l} \alpha_{il} = 1, \tag{5.23}$$

where $K\left(\boldsymbol{u}^{(i)}{}_l, \boldsymbol{u}^{(j)}{}_l\right)$ is the kernel function. Hence, we can define the support vectors (SV) and boundary support vectors (BSV) by solving the dual program (5.21)-(5.23) and analyze the optimum values of α_{il} and construct the SV and BSV sets for each node $l \in \mathcal{N}_{\text{o}}$ can be determined based on

$$SV_l = \{i | \alpha_{il} > 0, \quad \forall i \in N_l\}, \qquad \forall l \in \mathcal{N}_{\text{o}}, \tag{5.24}$$

$$BSV_l = \{i | 0 < \alpha_{il} < 1/N_l \nu_l, \ \forall i \in N_l\}, \qquad \forall l \in \mathcal{N}_{\text{o}}. \tag{5.25}$$

Figure 5.1 demonstrates an example of a "SVC-based" uncertainty set, the support vectors, and the boundary support vectors. Motivated by Mercer's theorem (Steinwart and Scovel, 2012), the kernel function is equal to the dot product $(\emptyset\left(\boldsymbol{u}^{(i)}{}_l\right) . \emptyset\left(\boldsymbol{u}^{(j)}{}_l\right))$ in the feature space with multiple dimensions (Cristianini & Shawe-Taylor, 2000). This eases computations by being able to simply calculate the inner-products in high-dimensional spaces. The most well-known kernel functions $K(.,.)$ used in pattern recognition and machine learning are: (1) Polynomial kernel: $K(\boldsymbol{u}, \boldsymbol{v}) = (\boldsymbol{u}^T \boldsymbol{v} + 1)^d$, (2) radial basis function (RBF) kernel: $K(\boldsymbol{u}, \boldsymbol{v}) = \exp\{-\|\boldsymbol{u} - \boldsymbol{v}\|^2/2\sigma^2\}$, and (3) sigmoid kernel: $K(\boldsymbol{u}, \boldsymbol{v}) = \tanh(\gamma . \mathbf{u}^{\mathrm{T}}\boldsymbol{v} + r)$ (Hsu, et al. 2003).

In this study, we use a piece-wise linear kernel function in order to avoid complicated nonlinear terms in our data-driven robust optimization framework and provide a MIP model. The weighted generalized intersection kernel (WGIK) (Shang et al., 2017) is used for the demand data sample of source nodes of the evacuation problem as

$$K_l\big(\boldsymbol{u}^{(i)}{}_l, \boldsymbol{u}^{(j)}{}_l\big) = \sum_{k \in M_l} L_{lk} - \big\|\boldsymbol{Q}_{\boldsymbol{l}}(\boldsymbol{u}^{(i)}{}_l - \boldsymbol{u}^{(j)}{}_l)\big\|, \qquad \forall i \in N_l,\ \forall i \in N_l,\ \forall l \in \mathcal{N}_{\mathrm{o}}, \tag{5.26}$$

where L_{lk} is the width parameter for data sample related to node $l \in \mathcal{N}_{\mathrm{o}}$. This parameter is used to bound the uncertainty and prevent the inducing separating hyperplane to be distant and far from the center. To guarantee a positive-definite matric of kernel $K_l\big(\boldsymbol{u}^{(i)}{}_l, \boldsymbol{u}^{(j)}{}_l\big)$ and convexity of dual problem (5.21)-(5.23) the amount of L_{lk} is tuned according to

$$L_{lk} > max_{1 \le i \le N_l} \boldsymbol{Q}_{lk}^{\boldsymbol{T}} \boldsymbol{u}^{(i)}{}_l - min_{1 \le i \le N_l} \boldsymbol{Q}_{lk}^{\boldsymbol{T}} \boldsymbol{u}^{(i)}{}_l, \qquad \forall l \in \mathcal{N}_{\mathrm{o}},\ \forall k \in M_l. \tag{5.27}$$

Whitening matrix $\boldsymbol{Q}_{\boldsymbol{l}}$ is used in (5.26) to incorporate covariation information making each dimension of the transformed data $\boldsymbol{Q}_{\boldsymbol{l}}\boldsymbol{u}_{\boldsymbol{l}}$ to be isotropic and have the same effect on the kernel function. This matrix can be constructed based on unbiased estimation of the covariance matrix $\sum$ of the data samples as in $\boldsymbol{Q}_{\boldsymbol{l}} = \sum^{-\boldsymbol{1}/\boldsymbol{2}}$.

Since the index sets of all support vectors (SV) and boundary support vectors (BSV) have been defined as such in (5.24)-(5.25), the formulation of the data-driven uncertainty set under a general kernel function can be derived as

$$\mathcal{U}_l(\mathcal{D}_l) = \left\{ u_l \,\middle|\, K_l(\boldsymbol{u}_l, \boldsymbol{u}_l) - 2 \sum_{i \in N_l} \alpha_{il}\, K_l\big(\boldsymbol{u}_l, \boldsymbol{u}^{(i)}{}_l\big) + \sum_{i \in N_l} \sum_{j \in N_l} \alpha_{il}\, \alpha_{jl} K_l\big(\boldsymbol{u}^{(i)}{}_l, \boldsymbol{u}^{(j)}{}_l\big) \le R_l^2 \right\}. \tag{5.28}$$

By substituting the WGIK kernel function into the uncertainty set (5.28), we will have

$$\mathcal{U}_l(\mathcal{D}_l) = \left\{ u_l \,\middle|\, \sum_{i \in N_l} \alpha_{il} \left\| \boldsymbol{Q}_l\big(\boldsymbol{u}_l - \boldsymbol{u}^{(i)}{}_l\big) \right\|_1 \le \mathfrak{u}_l \right\}, \tag{5.29}$$

where $\mathfrak{u}_l = \sum_{i \in N_l} \alpha_{il} \left\| \boldsymbol{Q}_l\big(\boldsymbol{u}^{(j)}{}_l - \boldsymbol{u}^{(i)}{}_l\big) \right\|_1$, $\exists j \in BSV$. By introducing auxiliary variables $\boldsymbol{V}_l = [\boldsymbol{v}_{1l}, \dots, \boldsymbol{v}_{N_l l}]$ and matrix $\boldsymbol{W}_l^{(i)} = \boldsymbol{Q}_l \boldsymbol{u}^{(i)}{}_l$ the uncertainty set $\mathcal{U}_l(\mathcal{D}_l)$ can be linearized as in

$$\mathcal{U}_l(\mathcal{D}_l) = \left\{ u_l \,\middle|\, \begin{array}{c} \exists v_{ikl},\ i \in SV,\ k \in M_l \ \ s.t. \\ \displaystyle\sum_{i \in SV} \sum_{k \in M_l} \alpha_{il} v_{ikl} \le \mathfrak{u}_l \\ \displaystyle\sum_{h \in M_l} Q_{khl} u_{hl} - W_{kl}^{(i)} \le v_{ikl} \quad \forall k \in M_l \\ \displaystyle\sum_{h \in M_l} Q_{khl} u_{hl} - W_{kl}^{(i)} \ge -v_{ikl} \quad \forall k \in M_l \end{array} \right\}. \tag{5.30}$$

By introducing Lagrange multipliers η_l, $\boldsymbol{\mu}_l$, and $\boldsymbol{\lambda}_l$, and incorporating the linearized uncertainty set (5.30) into the worst-case constraint (5.11), we can derive the data-driven robust path-based model with SVC induced uncertainty set for our evacuation planning problem (*DSPBM*) as follows:

$$\text{Minimize} \quad \sum_{l \in \mathcal{N}_o} \beta_l \qquad \qquad (DSPBM) \tag{5.31}$$

$$\text{Subject to:} \quad (5.3) - (5.6) \tag{5.32}$$

$$\sum_{i\in SV}\sum_{k\in M_l}\left[W_{kl}^{(i)}(\mu_{ikl}-\lambda_{ikl})\right]+\eta_l\mathfrak{u}_l\leq \sum_{p\in\mathcal{P}_l^+}\sum_{t\in\mathbb{T}}f_{pt}+\beta_l-\sum_{k\in M_l}S_{lk},\qquad \forall l\in\mathcal{N}_o, \tag{5.33}$$

$$\sum_{i\in SV}\sum_{k\in M_l}\left[Q_{khl}(\lambda_{ikl}-\mu_{ikl})\right]-x_{lh}=0,\qquad \forall h\in M_l,\forall l\in\mathcal{N}_o, \tag{5.34}$$

$$\mu_{ikl}+\lambda_{ikl}=\eta_l\alpha_{il},\qquad \forall i\in SV,\ \forall k\in M_l,\forall l\in\mathcal{N}_o, \tag{5.35}$$

$$x_{lk}=\widehat{S_{lk}},\qquad \forall l\in\mathcal{N}_o,\ \forall k\in M_l, \tag{5.36}$$

$$\eta_l\geq 0,\mu_{ikl}\geq 0,\lambda_{ikl}\geq 0,\qquad \forall i\in SV,\ \forall k\in M_l,\forall l\in\mathcal{N}_o. \tag{5.37}$$

5.2.2.2 Data-Driven Model with Box+SVC-based Uncertainty Set

The SVC algorithm aims to find a minimum volume of hypersphere that encloses the data sample. As explained previously, by adjusting the amount of the regulator parameter ν, the decision-maker can adjust the volume of the hypersphere and accordingly adjust the coverage of the data point in the sample. When the parameter ν is increased, the hypersphere becomes tighter, more data points lay outside the boundary of the hypersphere, and solution conservatism is decreased (See Figure 5.1).

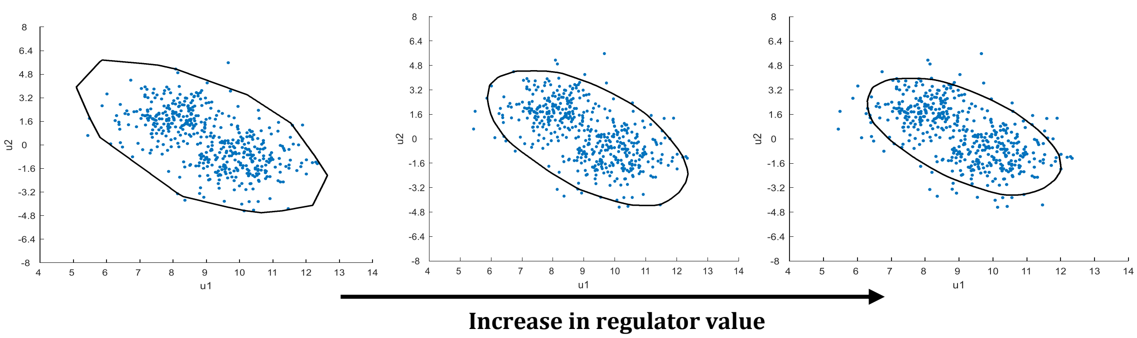

Figure 5.1: Data coverage of SVC-based uncertainty set

On the contrary, when the parameter ν is decreased, it leads to superfluous coverage by the induced uncertainty set (due to empty feature spaces covered by the hypersphere). As a method to reduce this superfluous coverage while maintaining the same sample data coverage (robustness), the “Box+SVC-based" uncertainty set is introduced to be used for each evacuation source demand data sample and, accordingly, the robust counterpart problem for the evacuation planning problem is derived.

The box uncertainty set used in robust optimization is derived by the ∞-norm of the random vector $\boldsymbol{u_l} = [u_{1l}, u_{2l}, \dots, u_{kl}, .., u_{nl}]^T$ as in

$$\mathrm{U}_l(\mathcal{D}_l) = \{u_l |\ \|u_l\|_\infty \leq \psi_l\} = \{u_l |\ \ |u_{kl}| \leq \psi_l, \quad \forall k \in M_l\ \}, \tag{5.38}$$

where the controller/budget parameter ψ_l is used to define the size of the box and restrict the covered area. Despite the ability to reduce the feature space coverage by adjusting the amount of parameter ψ_l, the box uncertainty set results in either extreme coverage of empty feature space or failure inappropriately covering the data sample (See Figure 5.2).

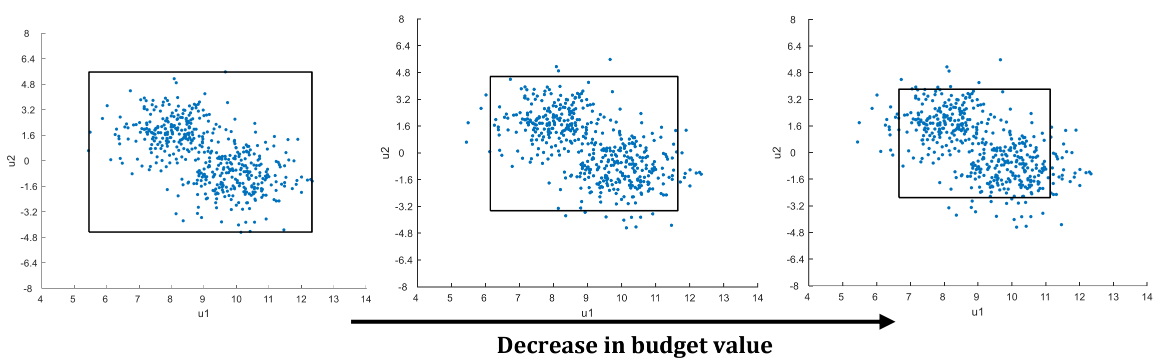

Figure 5.2: Data coverage of box uncertainty set

Hence, we first linearize the term $|u_{kl}| \leq \psi_l$ and project it as $-\psi_l \leq u_{kl} \leq \psi_l$. Next, we intersect the SVC induced uncertainty set (5.30) with the box uncertainty set (5.38) to construct a more appropriate and tighter uncertainty set as in

$$
\mho_l(\mathcal{D}_l) = \left\{ u_l \left| \begin{array}{ll} \exists v_{ikl},\ \ i \in SV,\ k \in M_l \quad s.t. & \\ \displaystyle\sum_{i \in SV} \sum_{k \in M_l} \alpha_{il} v_{ikl} \leq \mathfrak{u}_l & \\ \displaystyle\sum_{h \in M_l} Q_{khl} u_{hl} - W_{kl}^{(i)} \leq v_{ikl} & \forall k \in M_l \\ \displaystyle\sum_{h \in M_l} Q_{khl} u_{hl} - W_{kl}^{(i)} \geq -v_{ikl} & \forall k \in M_l \\ u_{kl} \leq \psi_l & \forall k \in M_l \\ u_{kl} \geq -\psi_l & \forall k \in M_l \end{array} \right. \right\}. \tag{5.39}
$$

Using the "Box+SVC-based" uncertainty set (5.39), the inner optimization problem (5.11) can be written as follows:

$$
\text{Maximize} \qquad \sum_{k \in M_l} u_{lk} x_{lk} \tag{5.40}
$$

$$
\text{Subject to:} \qquad \sum_{i \in SV} \sum_{k \in M_l} \alpha_{il} v_{ikl} \leq \mathfrak{u}_l, \tag{5.41}
$$

$$
\sum_{h \in M_l} Q_{khl} u_{hl} - W_{kl}^{(i)} \leq v_{ikl}, \qquad \forall k \in M_l, \tag{5.42}
$$

$$
\sum_{h \in M_l} Q_{khl} u_{hl} - W_{kl}^{(i)} \geq -v_{ikl}, \qquad \forall k \in M_l, \tag{5.43}
$$

$$
u_{kl} \leq \psi_l, \qquad \forall k \in M_l, \tag{5.44}
$$

$$
u_{kl} \geq -\psi_l, \qquad \forall k \in M_l. \tag{5.45}
$$

By introducing Lagrange multipliers η_l, μ_{ikl}, λ_{ikl}, ϑ_{kl}, and ω_{kl} the dual problem of (5.40)-(5.45) can be induced and substituted by worst-case constraint (5.11) to form the data-driven robust path-based model with "Box+SVC-based" uncertainty set for evacuation planning problem (*DBSPBM*) as follows:

$$
\text{Minimize} \qquad \sum_{l \in \mathcal{N}_o} \beta_l \qquad \textit{(DBSPBM)} \tag{5.46}
$$

$$
\text{Subject to:} \qquad (5.3) - (5.6), \tag{5.47}
$$

$$\sum_{i\in SV}\sum_{k\in M_l}\left[W_{kl}^{(i)}(\mu_{ikl}-\lambda_{ikl})\right]+\eta_l \text{ɩ}_l+\psi_l\sum_{k\in M_l}(\vartheta_{kl}+\omega_{kl}) \le \sum_{p\in\wp_l^+}\sum_{t\in\mathbb{T}} f_{pt}+\beta_l-\sum_{k\in M_l} S_{lk}, \qquad \forall l\in\mathcal{N}_o, \tag{5.48}$$

$$\sum_{i\in SV}\sum_{k\in M_l}\left[Q_{khl}(\lambda_{ikl}-\mu_{ikl})\right]+\vartheta_{hl}+\omega_{hl}-x_{lh}=0, \qquad \forall h\in M_l, \forall l\in\mathcal{N}_o, \tag{5.49}$$

$$\mu_{ikl}+\lambda_{ikl}=\eta_l\alpha_{il}, \qquad \forall i\in SV,\ \forall k\in M_l, \forall l\in\mathcal{N}_o, \tag{5.50}$$

$$x_{lk}=\widehat{S_{lk}}, \qquad \forall l\in\mathcal{N}_o,\ \forall k\in M_l, \tag{5.51}$$

$$\eta_l\ge 0, \mu_{ikl}\ge 0, \lambda_{ikl}\ge 0, \qquad \forall i\in SV,\ \forall k\in M_l, \forall l\in\mathcal{N}_o. \tag{5.52}$$

5.3 Computational Results

This section is designed to test the performance of the “SVC-based" uncertainty set, the “Box+SVC-based" uncertainty set, and the corresponding data-driven robust evacuation path-based models DSPBM and DBSPBM. All experiments are conducted on a sample evacuation network shown in Figure 3.8. The quadratic program QP_{SVC} is solved in MATLAB R2017b using CVX (Grant and Boyd, 2013), and the data-driven mixed-integer programs are solved by CPLEX 12.5.1 (IBM, 2013) on a PC with a 3.07 GHz Intel Core i7 processor having 24GB RAM and running Ubuntu 10.04.3. The test network in Figure 3 includes 22 arcs connecting three source nodes ($\mathcal{N}_1$, $\mathcal{N}_2$, and $\mathcal{N}_3$), five intermediate nodes ($\mathcal{N}_4$,..., $\mathcal{N}_8$) and two destination nodes ($\mathcal{N}_9$ and $\mathcal{N}_{10}$). Arc transit times (τ_a) as well as their capacities (C_a) are shown above each arc in the network. The solution pool feature of CPLEX for the shortest path problem is used to generate all possible paths between all origin and destination (O-D) pairs and 42 paths are selected as the candidate paths to be used in path-based models.

Demand (number of evacuees) at zones of each source node ($\widetilde{S_{lk}}$) is considered to be uncertain and 500 samples embodying correlations are generated for each source node ($\mathcal{N}_1$, $\mathcal{N}_2$, and $\mathcal{N}_3$). The value of each sample is decomposed to define the nominal value S_{lk}, variation amplitude $\widehat{S_{lk}}$, and a random amount u_{lk} of the sample. The nominal and amplitude values are presented in Table 5.1, and the random values are plotted in Figure 5.3.

Table 5.1: Nominal and magnitude value of data samples

		Node 1	Node 2	Node 3
Nominal value	Zone 1	7	10	5
	Zone 2	3	10	15
Magnitude	Zone 1	12	26	45
	Zone 2	20	14	12

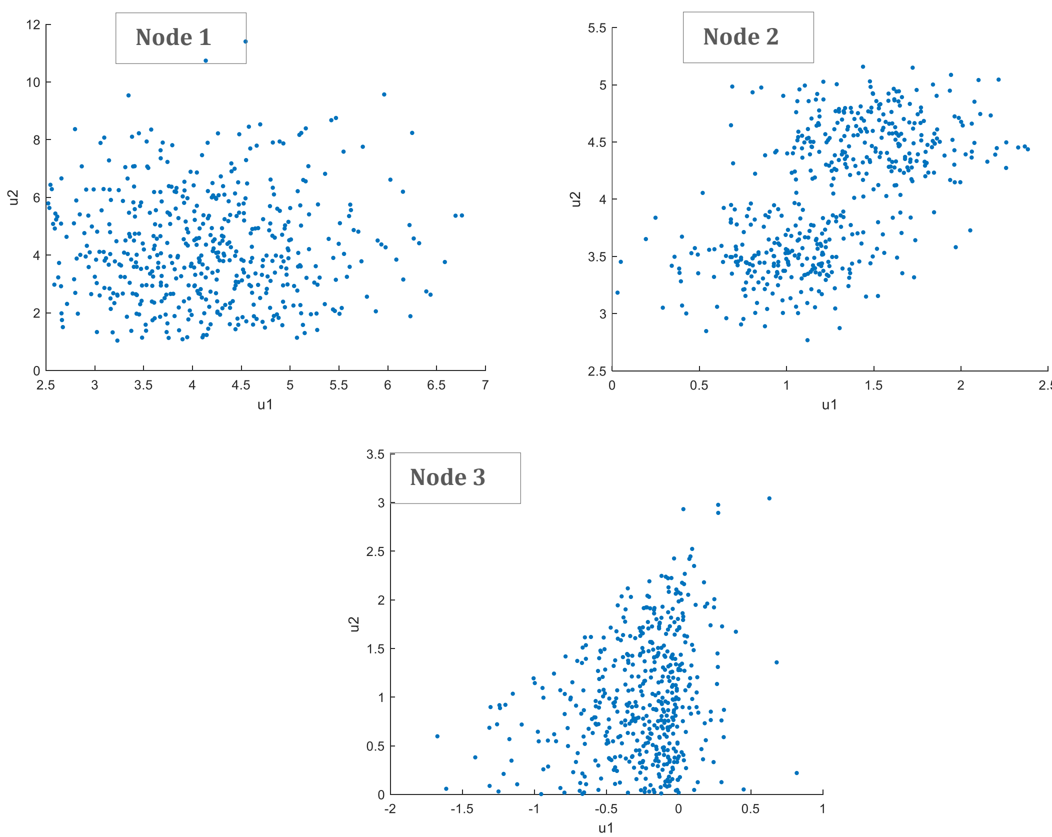

Figure 5.3: Scatter plot of random variables of demand samples under each source node

The “SVC-based" uncertainty sets are constructed for each data samples by solving the quadratic program QP_{SVC}, and the regularization parameter (ν_l) is used to adjust the conservatism of the uncertainty sets. The derived uncertainty sets were able to systematically cover complicated distributional geometries of the uncertain parameters. As an example, Figure 5.4 visualizes data coverage of the induced uncertainty sets for the data sample of node 3 under regularization parameters $\nu_3 = 0.01$, $\nu_3 = 0.03$, $\nu_3 = 0.05$, $\nu_3 = 0.07$, $\nu_3 = 0.09$, and $\nu_3 = 0.1$. The relationship between the regularization parameter and the number of support vectors (SV), the number of boundary support vectors (BSV), and the percentage of outliers are presented in Table 5.2.

Table 5.2: Number of SV, BSV, and Outliers under different regularization parameter

		Regulation Parameter (ν_l)						
		0.01	**0.02**	**0.03**	**0.04**	**0.05**	**0.06**	**0.07**
$\boldsymbol{\mathcal{N}_1}$	#SV	11	15	19	23	25	32	41
	#BSV	10	7	6	5	5	32	41
	Outliers%	1.80%	2.80%	3.40%	4.40%	5.40%	6.20%	8.00%
$\boldsymbol{\mathcal{N}_2}$	#SV	11	15	19	23	26	32	40
	#BSV	10	7	6	5	6	32	40
	Outliers%	2.00%	2.80%	3.60%	4.40%	5.60%	6.20%	7.80%
$\boldsymbol{\mathcal{N}_3}$	#SV	8	13	17	24	28	31	39
	#BSV	4	5	3	7	5	31	39
	Outliers%	1.40%	2.40%	3.20%	4.60%	5.40%	6.00%	7.60%

As observed in Table 5.2, when the value of the regularization parameter increases, the number of employed support vectors increases. For instance, changing ν_1 from 0.01 to 0.05 increases the number of support vectors used in the uncertainty set of node 1 from 11 to 28. More support vectors result in more hyperplanes in the uncertainty set. Therefore, the resulting uncertainty sets, which are the intersection of the hyperplanes, tend to be more and more smooth. Furthermore, when the regularization parameter increases, more demand data points reside outsight the constructed set. For instance, changing ν_1 from 0.01 to 0.05 increases the number of outliers by 4%. This is due to the fact that the uncertainty set becomes tighter and covers fewer areas of the feature space. This leads to less conservative evacuation plans.

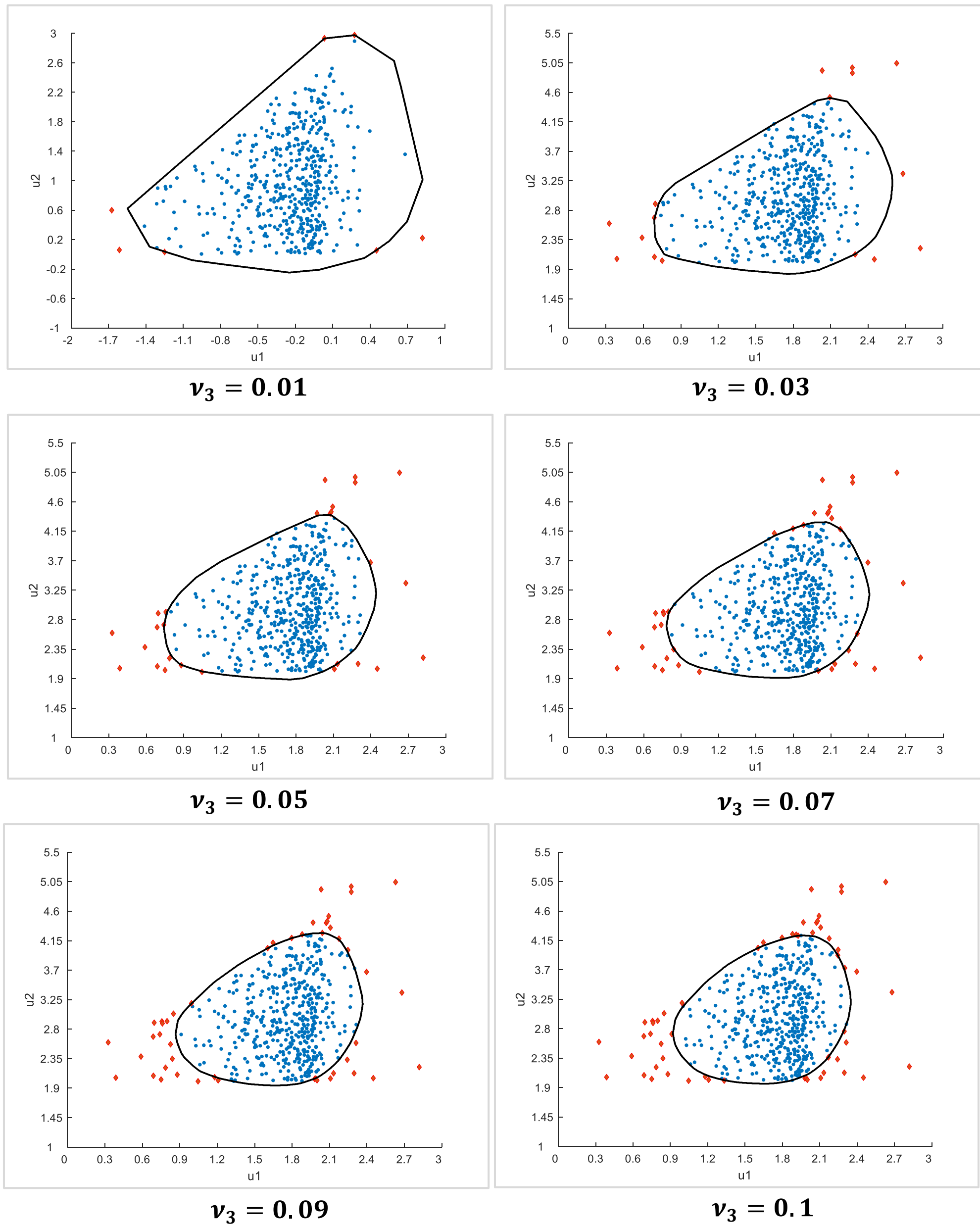

Figure 5.4: "SVC-Based" uncertainty sets for node 3 based on different regulation parameters

If the actual evacuation demand falls into a constructed set, then the evacuation plan and schedule are considered feasible (evacuation demand is met). Otherwise, the evacuation plan becomes infeasible and the excess amount of evacuees remains at the source nodes. Hence, it puts a toll on the emergency evacuation strategy as the incumbent evacuation plan becomes infeasible, and the need to consider a recovery strategy if an incident arises. If the uncertainty set covers most of the data points, the plan robustness increases, and the risk of plan infeasibility reduces. However, if the uncertainty set becomes loose, the assumed number of would-be evacuees in the planning phase becomes inflamed, leading to an overly conservative evacuation plan and unnecessary evacuation preparedness.

To obtain the optimal evacuation policies based on the constructed "SVC-based" uncertainty sets from the demand data samples, the induced data-driven robust evacuation planning counterparts DSPBM are solved. Table 5.3 demonstrates the amount of optimal evacuation flow obtained by DSPBM that planned to depart each of the source nodes. When ν_l increases, a smaller number of evacuees are considered to be evacuated from the source nodes and the plan robustness and conservatism reduces. For instance, when the regularization parameter changes from 0.01 to 0.05, the number of would-be evacuees on node 1 decreases by 14.7% from 285 to 243. However, as mentioned before, the percentage of outliers increases which adds to the risk of plan infeasibility.

Table 5.3: Optimal evacuation flow obtained by DSPBM

		Regulation Parameter (ν_l)						
		0.01	**0.02**	**0.03**	**0.04**	**0.05**	**0.06**	**0.07**
Flow	$\mathcal{N}_1$	285	268	259	249	243	240	239
	$\mathcal{N}_2$	152	149	149	149	149	147	145
	$\mathcal{N}_3$	192	185	178	172	171	170	170
Total		629	602	586	570	563	557	554

The solution time for solving the quadratic program QP_{SVC} and DSPBM under different values of regularization parameter (ν_l) are tabulated in Table 5.4. When the value of ν_l increases, the computational time of DSPBM appears to increase. This is because more support vectors are employed in the corresponding uncertainty set, a more complicated uncertainty set is obtained, and more constraints are embodied in DSPBM. However, on average, it only takes about 0.0002s to solve the quadratic programs and 0.052s to solve DSPBM integer programs, which are negligible.

Table 5.4: Solution time of QPSVC and DSPBM

			Regulation Parameter (ν_l)					
			0.01	**0.02**	**0.03**	**0.04**	**0.05**	**0.07**
Solution Time	***QP_{SVC}***	$\mathcal{N}_1$	0.0002	0.0003	0.0001	0.0002	0.0002	0.0003
		$\mathcal{N}_2$	0.0001	0.0001	0.0002	0.0002	0.0003	0.0002
		$\mathcal{N}_3$	0.0003	0.0002	0.0002	0.0002	0.0002	0.0002
	DSPBM		0.022	0.0299	0.0472	0.0553	0.0767	0.0811

To reduce the redundant coverage of the feature space by the uncertainty sets, the introduced “Box+SVC-based" uncertainty sets are investigated. Examples of the combination of a box uncertainty set with an “SVC-based" uncertainty set for each source node of the evacuation network is visualized in Figure 5.5. As is shown, the projected “Box+SVC-based" uncertainty sets are tighter compared to the associated “SVC-based" uncertainty sets while having the same number of outliers (Same level of plan conservatism).

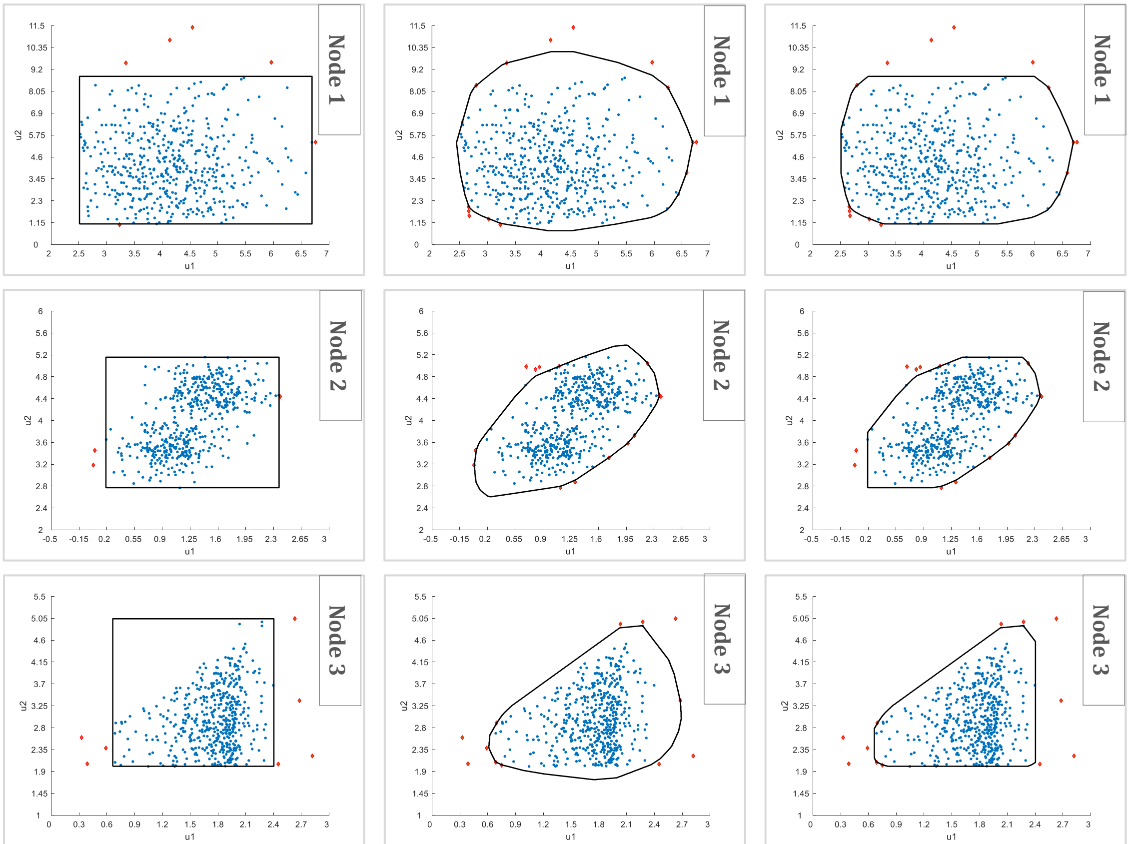

(a) Box **(b) SVC-based** **(C) Box+SVC-based**

Figure 5.5: "Box", "SVC-based" and "Box+Svc-based" uncertainty sets

Results of more investigations on the performance of the box uncertainty set, "SVC-based" uncertainty set, and "Box+SVC-based" uncertainty set are shown in Figure 5.6. The horizontal axes depict the level of plan conservatism defined by the percentage of data that lay outside of the corresponding uncertainty sets. Under each level of plan conservativeness, optimum numbers of evacuation flow are derived by solving the associated optimization model of the box, "SVC-based", and "Box+SVC-based" uncertainty set. The vertical axes depict these optimum flow values. It is noticeable that "SVC-based" uncertainty set optimization model (DSPBM) performs better than the robust optimization model built upon the uncertainty sets (RPBM) in most cases considered.

As the level of conservatism decreases (percentage of outliers increases), this performance distinction becomes more and DSPBM is able to provide solutions with less cost of robustness; meaning that it can provide evacuation plans that are prone to the same level of infeasibility risk but require less evacuation preparedness efforts since the optimum value of the assumed would-be evacuees is decreased.

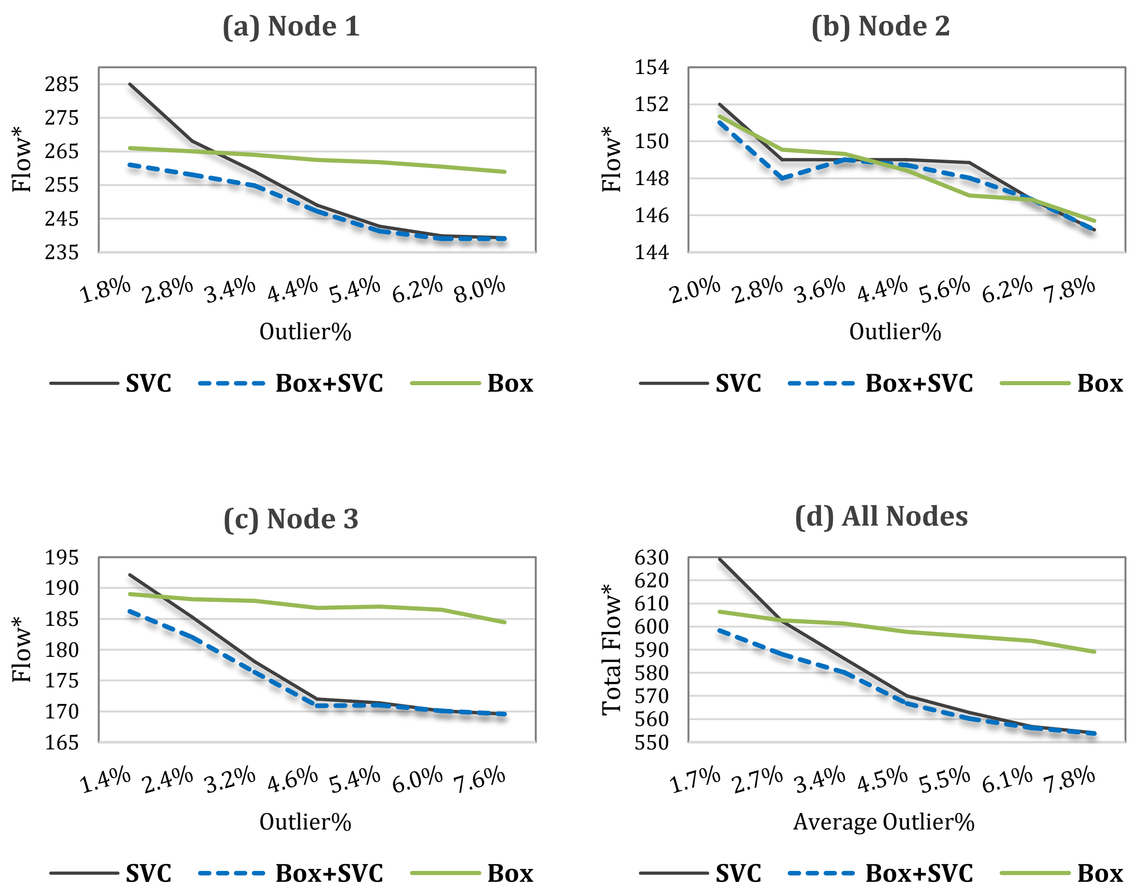

Figure 5.6: Optimal evacuation flow resulted from "Box", "SVC-based" and "Box+Svc-based" uncertainty sets

For instance, the optimum number of would-be evacuees on node 1 obtained by DSPBM under 8% level of conservatism equals 239, which is 8% less than 259 of RPBM (see Figure 5.6(a)). The data-driven optimization model built upon Box+SVC-based" uncertainty set (DBSPBM) performs slightly better DSPBM and is most beneficial if the level of conservatism is increased. However, compared to RPBM, in all cases, DBSPBM has been able to provide better solutions that require less amount of evacuation efforts.

5.4 Conclusion

This paper introduced a data-driven mixed-integer linear programming framework for evacuation route planning and traffic flow schedule under uncertain evacuation demand. The motivation behind the development of the data-driven framework is to be able to effectively capture the geometry of the uncertain demand (number of evacuees) data. A dynamic network flow optimization approach has been developed to capture the evacuation flow moving along the network over time. In order to make the optimization model scalable for large-scale transportation networks, a solution method was developed using a path-based model (PBM). An uncertainty set is defined based on support vector clustering (SVC) for the proposed data-driven robust optimization model. The "SVC-based" uncertainty set advantages from the benefits of nonparametric kernel learning methods; hence they do not require parameter adjustment. Moreover, it is reasonable for it to be adopted for complex data while substantially reducing the computational costs. Most kernel functions used in the literature provide a way to transform the feature space with the original coordinates into a lower-dimensional space. Since this transformation is nonlinear, developing a data-driven robust optimization counterpart with a linear structure is not possible. Hence, we proposed to use a piecewise linear kernel termed as the generalized intersection kernel to derive the MIP data-driven formulation for the evacuation problem (DSPBM). Furthermore, the intersection of the SVC-based uncertainty set and the conventional box uncertainty set is introduced to provide tighter uncertainty sets and reduce the conservatism. Consequently, a data-driven optimization approach (DBSPBM) corresponding to the new uncertainty set has been developed.

Numerical experiments were conducted to study the performance of the proposed data-driven models under different demand distributions on the source nodes of a sample transportation network. Results showed that the DSPBM is able to systematically integrate information from historical data into the evacuation planning and is capable of effectively leveraging information to handle complicated distributional geometries. The model is computationally tractable, and the computational times of all experiments made in this paper were negligible. We showed that the conservatism of the evacuation plan can be adjusted by a regulation parameter. Smaller values of the regulation parameter resulted in looser uncertainty sets, better data coverage, and, subsequently, more conservative evacuation plans. Further investigations were made on the performance of DSPBM, DBSPBM, and the robust optimization model based on box uncertainties. The results indicated that, in most cases, DSPBM and DBSPBM can provide evacuation plans with the same level of conservatism, but at a lower cost of robustness (evacuation efforts) compared to the traditional robust optimization model. Also, the DBSPBM outperformed the DSPBM in terms of reducing the cost of robustness, but the difference became less significant as the regulation parameter increased. Hence, it is more suitable to use DBSPBM when a higher level of plan conservatism is desirable.

Chapter 6

Distributionally Robust Chance-Constraint program: Unknown Probability Distribution of Network Disruption Times

6.1 Introduction

In this section, we describe the evacuation planning problem subject to the risk of multiple road disruptions. The purpose is to fill the gap in the literature by introducing a distributionally robust optimization model that ensures the constraints subject to parameter randomness are satisfied under actual distributions, consistent with the ambiguity set built on the distributions' moment information. Unlike previous studies, we introduce an improved framework that: (i) provides a proactive plan that is less interrupted by the occurrence of probable road disruptions; (ii) better projects traffic dynamics by employing a dynamic traffic network flow optimization approach, which allows for variation in flow rates over the planning horizon; (iii) provides more realistic results considering disruptions on roads (where roads are defined as a section of a path) instead of on an entire path in the evacuation network; (iv) assumes simultaneous disruptions on multiple roads in the evacuation network; (v) makes no assumptions regarding the type of uncertainty distributions and considers that the probability distribution functions of road disruption times are not fully known and that only partial information (the first two moments) is available.

In the context of stochastic programming, the most reliable way to account for demand uncertainty is to use chance-constraints, which have the following form:

$$\min\ f(x) \tag{6.1}$$

$$\text{s.t. } \mathbb{P}\big(F(x.\tilde{\xi}) \leq 0\big) \geq 1-\epsilon. \tag{6.2}$$

where $\tilde{\xi}$ is a random vector demonstrating uncertain parameters and $\mathbb{P}$ is the associated probability measure, f is the objective function of the program, and function F is related to performance measures representing constraints in a particular system. In our problem, $\tilde{\xi}$ is a random vector describing road disruption times in the evacuation network. We fix a risk level $\epsilon \in [0,1]$ so that the constraint (6.2) requires that the uncertain constraint $F(x.\tilde{\xi}) \leq 0$ be satisfied with a confidence level of at least $(1-\epsilon)$.

Generally, the way the problem is approached from an algorithmic perspective strongly depends on the form of F as well as the information that is available on the probability distribution of the uncertain parameters. In the above chance-constrained program, if the underlying random parameter is known, we may be able to provide a deterministic equivalent of it using the inverse of the cumulative distribution function (CDF) of the uncertain parameter. However, due to insufficient data available related to road disruption times and differences in the nature of disasters, accurately identifying the underlying distribution may be impossible. In some studies, the unknown distribution $\mathbb{P}$ in (6.2) has been replaced by crude estimate, like $\widetilde{\mathbb{P}}$, which can result in an overly optimistic solution that may not satisfy the chance-constraint under the "true" distribution $\mathbb{P}$. Approximating the probability in the chance-constraint requires making some assumptions about the probability distribution. A more realistic assumption is that we have limited information regarding $\mathbb{P}$, such as information about its first two moments. These assumptions consequently affect the optimal choice of evacuation routes and traffic flow in an evacuation plan.

In the following subsections, we develop a mathematical formulation representing a distributionally robust data-driven program for the evacuation planning problem under uncertainty of network disruption. Since the problem is intractable, we decompose the noise (uncertainty)-related constraint into three sets of constraints and reformulate the problem to obtain a Mixed Integer formulation. Moreover, we introduce a solution methodology to be employed for large-scale evacuations. Numerical experiments are conducted, and a detailed conclusion of our study is presented accordingly.

6.2 Problem Formulation

The evacuation network is represented as a directed graph $\mathcal{G} = (\mathcal{N}, \mathcal{A})$, which consists of a set of nodes $\mathcal{N}$ corresponding to intersections and a set of arcs $\mathcal{A}$ to project the evacuation road segments restricted by road capacities C_a and weighted by estimated arc travel times τ_a. Since a dynamic network flow optimization approach is employed, the traffic assignment is projected on a time-expanded network. Set $\mathbb{T} = \{0, 1, \dots, T-1\}$ shows time slots that represent equal intervals of the planning horizon. Using this approach, throughout the evacuation process, variable flow rates are assigned to the paths that connect the origin–destination nodes of the network.

A path-based approach is adopted, and set $\wp$ is used to demonstrate the set of all paths that have been chosen by authorities and are fed into the optimization evacuation model. Three sets of integer decision variables are used in the model, including: set $\mathrm{f}_{\mathrm{pt}} \in \mathbb{Z}^{+}$, to show the evacuation flow (evacuees) scheduled to depart on path $\mathrm{p} \in \wp$ at time $t \in \mathbb{T}$; set $\beta_n \in \mathbb{Z}^+$, representing unsatisfied demand on the source node $n \in \mathcal{N}_s$; and set $I_{pnt} \in \mathbb{Z}^+$, demonstrating the departed flow on path $p \in \wp$ at time $t \in \mathbb{T}$ that is interrupted due to road incidents and is jammed before node $n \in \mathcal{N}$. Note that the initial number of evacuees on a source node is denoted as demand D_n, and the number of evacuees who have not been evacuated by the end of the evacuation horizon is referred to as unsatisfied demand.

6.2.1 Scenario Analysis Associated with Disturbance Uncertainty

To develop the mathematical model, the first possible scenarios regarding the effect on time of multiple road/arc disruptions on a scheduled flow assigned to a path are investigated. Let the random variable $\widetilde{DT}_a$ represent the uncertain disruption time on arc $a \in \mathcal{A}$ of the transportation network. Considering disruption time of a specific arc $a \in \mathcal{A}$ ($\widetilde{DT}_a$) as well as disruption time of preceding arcs ($\widetilde{DT}_{\bar{a}}$) along path $p \in \wp$, three cases can occur for a scheduled flow f_{pt}.

Case 1: Flow is not disturbed before reaching arc $a \in \mathcal{A}$ and is only disturbed on arc $a \in \mathcal{A}$

In this case, disruption times of the arcs preceding $a \in \mathcal{A}$ cannot disrupt the flow, as shown by the following conditions:

$$\begin{aligned} & t + \theta_{p\bar{a}} + \tau_{\bar{a}} \leq \widetilde{DT}_{\bar{a}}, \\ \& \quad & t + \theta_{pa} + \tau_a > \widetilde{DT}_a, \end{aligned} \qquad \forall \bar{a} \in \mathcal{A} \textit{ preceding to } a \in \mathcal{A} \textit{ on } p \in \wp.$$

When a flow starts at time $t \in \mathbb{T}$, it takes $\theta_{p\bar{a}}$ amount of time for the flow to reach the arc $\bar{a} \in \mathcal{A}$. Passing through this arc requires $\tau_{\bar{a}}$ unit of time. If the disruption on the arc $\bar{a} \in \mathcal{A}$ happens after the flow has passed through the arc ($t + \theta_{p\bar{a}} + \tau_{\bar{a}}$), then flow is not affected by the disruption on the arc $\bar{a} \in \mathcal{A}$ at all. This situation can be shown by $t + \theta_{p\bar{a}} + \tau_{\bar{a}} \leq \widetilde{DT}_{\bar{a}}$. If the same thing happens for all arcs $\bar{a} \in \mathcal{A}$ that precede arc $a \in \mathcal{A}$, then the flow can successfully reach arc $a \in \mathcal{A}$. If the flow cannot safely pass through arc $a \in \mathcal{A}$ and the disruption time of arc a $\in \mathcal{A}$ is greater than the time needed for the flow to pass through the arc ($t + \theta_{pa} + \tau_a > \widetilde{DT}_a$), then the flow will be disrupted on arc $a \in \mathcal{A}$ and jammed on node $n \in \mathcal{N}$ (origin node of arc $a \in \mathcal{A}$).

Case 2: Flow is disturbed before reaching arc a $\in \mathcal{A}$

In this case, a preceding arc $\bar{a} \in \mathcal{A}$ interrupts the flow and prevents it from reaching arc a $\in \mathcal{A}$ which is shown by the condition

$$t + \theta_{p\bar{a}} + \tau_{\bar{a}} > DT_{\bar{a}}, \qquad \exists \bar{a} \in \mathcal{A} \text{ preceding to } a \in \mathcal{A} \text{ on } p \in \wp.$$

Case 3: Flow is not disturbed at all and can pass through arc a $\in \mathcal{A}$

The disruption times of the arcs preceding arc a $\in \mathcal{A}$, as well as arc a $\in \mathcal{A}$ itself, do not influence the flow, and the flow successfully reaches and passes through arc a $\in \mathcal{A}$. We show this case by the following conditions

$$\begin{aligned} t + \theta_{p\bar{a}} + \tau_{\bar{a}} &\leq DT_{\bar{a}}, \\ \& \quad t + \theta_{pa} + \tau_a &\leq DT_a, \end{aligned} \qquad \forall \bar{a} \in \mathcal{A} \text{ preceding to } a \in \mathcal{A} \text{ on } p \in \wp.$$

Given this understanding of possible scenarios regarding the influence of arc disruption times on a scheduled flow, an incident indicator ($\tilde{v}_{pnt}$) is introduced and will be employed in the problem mathematical formulation described in Section 3.2.

Incident Indicator ($\tilde{v}_{pnt}$): This parameter is a function of uncertain arc disruption times ($\widetilde{DT}_a$) and is defined as

$$\tilde{v}_{pnt} = \frac{\left|t + \theta_{pa} + \tau_a - \widetilde{DT}_a\right|}{t + \theta_{pa} + \tau_a - \widetilde{DT}_a}, \qquad \forall a \in \mathcal{A} \textit{ emerging from node } n \in \mathcal{N} \textit{ on path } p \in \wp.$$

If a scheduled flow on path $p \in \wp$ that departs at time $t \in \mathbb{T}$ is interrupted by disruption on emerging arc $a \in \mathcal{A}$ from node $n \in \mathcal{N}$, then disruption time of the arc ($\widetilde{DT}_a$) is greater than the time required for the flow to reach and pass through the arc ($t + \theta_{pa} + \tau_a$). In this case, since $t + \theta_{pa} + \tau_a - DT_a > 0$, we would have $\left|t + \theta_{pa} + \tau_a - \widetilde{DT}_a\right| / \left(t + \theta_{pa} + \tau_a - \widetilde{DT}_a\right) = 1$. Otherwise, if the flow can pass through the arc without any disturbances, then $\left|t + \theta_{pa} + \tau_a - \widetilde{DT}_a\right| / \left(t + \theta_{pa} + \tau_a - \widetilde{DT}_a\right) = -1$.

6.2.2 Path-Based Approach

The purpose of the evacuation model is to develop a reliable flow schedule and route assignment under the uncertainty of road disruptions such that that the evacuation plan is less negatively affected by the consequences of the disruptions. The following mathematical notation is used throughout the paper:

Sets:

$\mathcal{N}$	Set of all nodes in the evacuation network
$\mathcal{N}_o$	Set of all origin nodes
$\mathcal{N}_d$	Set of all destination nodes
$\mathcal{N}_{pn}$	Set of all preceding nodes to node n on path p
$\mathbb{T}$	Set of all time slots
$\mathcal{A}$	Set of all arcs
$\wp$	Set of all paths
$\wp_n^+$	Set of paths originating from source node n
$\wp_n^-$	Set of paths terminated at destination node n

Decision Variables:

f_{pt}	Flow on path p that is dispatched from the source at time t
β_n	Undispatched demand from source node n
I_{pnt}	Disturbed flow on node n of path p at time t

Parameters:

$\widetilde{DT}_a$	Uncertain disruption time of arc a
θ_{pa}	Transit time from origin of path p to arc a
C_a	Capacity of arc a
D_n	Demand of source node n
τ_a	Transit time on arc a
$\acute{\theta}_{pn}$	Transit time from the origin of path p to node n
δ_{pa}	If arc a belongs to path p
γ_{na}	If node n is upstream (origin) node of arc a
$\tilde{v}_{pnt}$	Incident indicator for a flow scheduled at time t that accumulates on node n of path p
$\varphi_{p\acute{n}n}$	Takes value 1 if node n is not behind the node $\acute{n}$ on path p, and otherwise 0
M	A large number

The mathematical formulation for the evacuation planning problem under uncertainty of road disruptions is as follows:

Minimize $$\sum_{n \in \mathcal{N}_o} \beta_n + \sum_{p \in \wp} \sum_{n \in \mathcal{N}} \sum_{t \in \mathbb{T}} I_{pnt} \qquad PBM \tag{6.3}$$

Subject to: $$\sum_{p \in \wp_n^+} \sum_{t \in \mathbb{T}} f_{pt} + \beta_n \geq D_n, \qquad \forall n \in \mathcal{N}_o, \tag{6.4}$$

$$\sum_{p \in \wp} \delta_{pa} f_{p(t-\theta_{pa})} \leq C_a, \qquad \forall a \in \mathcal{A},\ \forall t \in \mathbb{T}, \tag{6.5}$$

$$I_{np(t+\acute{\theta}_{pn})} \geq f_{pt}\tilde{v}_{pnt} - \left(\sum_{\acute{n}\in N_{pn}} \tilde{v}_{p\acute{n}t} + |N_{pn}|\right)M, \quad \forall p \in \wp, n \in \mathcal{N}, t \in \mathbb{T}, \tag{6.6}$$

$$f_{pt} \in \mathbb{Z}^{+}, \beta_n \in \mathbb{Z}^{+}, I_{pnt} \in \mathbb{Z}^{+}, \quad \forall p \in \wp, t \in \mathbb{T}, n \in \mathcal{N}_o. \tag{6.7}$$

The objective function (6.3) attempts to minimize the number of evacuees who are left behind on the source nodes ($\sum_{n\in\mathcal{N}_s}\beta_n$) and the total number disrupted evacuees ($\sum_{p\in\wp}\sum_{n\in\mathcal{N}}\sum_{t\in\mathbb{T}} I_{pnt}$) who are left in the evacuation network by the end of the planning horizon. Constraints (6.4) guarantee that the total number of evacuees departing from a source node $n \in \mathcal{N}_o$ into different paths over all time ($\sum_{p\in\wp_n^+}\sum_{t\in\mathbb{T}} f_{pt}$) plus the number of evacuees remaining on the source node (β_n) is greater than the initial number of evacuees on the node (D_n). Constraints (6.5) ensure that aggregated flow from all paths that reach arc $a \in \mathcal{A}$ at time $t \in \mathbb{T}$ is less than the capacity of the arc (C_a).

Using constraints (6.6), the amount of flow disturbed by disruptions and accumulated at time $t + \acute{\theta}_{pn}$ on node $n \in \mathcal{N}$ of path $p \in \wp$ is calculated. Indicator $\tilde{v}_{pnt}$ is equal to 1 if a flow that departs at time $t \in \mathbb{T}$ on path $p \in \wp$ due to disturbances is trapped on node $n \in \mathcal{N}$; otherwise it is equal to -1. If flow f_{pt} is only disturbed by an arc emerging from node $n \in \mathcal{N}$, since it is not interrupted by any preceding arc to the node, then $\sum_{\acute{n}\in N_{pa}} \tilde{v}_{p\acute{n}t} = -|N_{pn}|$ and $\tilde{v}_{pnt}$=1. Hence, $I_{np(t+\acute{\theta}_{pn})} = f_{pt}$ when the objective function is minimized. However, if Case 2 or Case 3 occurs, constraints (6.6) will be relaxed. The non-negativity and integrality conditions of variables are shown in constraints (6.7).

Model PBM is not deterministic as constraints (6.6) are influenced by the uncertain parameter $\tilde{v}_{pnt}$. The so-called individual chance-constraints, which can be presented as in (6.8), limit the infeasibility of each constraint by a violation level $\epsilon_i \in (0,1]$.

$$\mathbb{P}\left(I_{np(t+\acute{\theta}_{pn})} \geq f_{pt}\tilde{v}_{pnt} - \left(\sum_{\acute{n}\in N_{pn}} \tilde{v}_{p\acute{n}t} + |N_{pn}| \right) M \right) \geq 1-\epsilon_{pnt}, \quad \forall p \in \wp, n \in \mathcal{N}, t \in \mathbb{T}. \qquad (66.8)$$

By replacing $\tilde{v}_{pnt}$ as a function (6.3) of the uncertain disruption times, constraints (6.8) can be presented as:

$$\mathbb{P}\left(I_{np(t+\acute{\theta}_{pn})} \geq f_{pt}\gamma_{na}\delta_{pa}\frac{|t+\theta_{pa}+\tau_a-\widetilde{DT}_a|}{t+\theta_{pa}+\tau_a-\widetilde{DT}_a} - \left(\sum_{\acute{n}\in N_{pn}} \gamma_{n\acute{a}}\delta_{p\acute{a}}\frac{|t+\theta_{p\acute{a}}+\tau_{\acute{a}}-\widetilde{DT}_{\acute{a}}|}{t+\theta_{p\acute{a}}+\tau_{\acute{a}}-\widetilde{DT}_{\acute{a}}} + |N_{pn}| \right) M \right) \geq 1-\epsilon_{pnt}, \quad \forall p \in \wp,\ n \in \mathcal{N},\ t \in \mathbb{T}. \qquad (6.9)$$

Even if the probability distribution function $\mathrm{F}_{\widetilde{DT}_a}$ of the random parameters ($\widetilde{DT}_a s$) were known with certainty, deriving the deterministic equivalent of the chance-constraints (6.9) would not be possible, and the chance-constraints would be intractable. In our paper, the challenge is even greater since it is assumed that the distribution $\mathbb{P}$ of random variables ($\widetilde{DT}_a s$) is not known except for some assumed structural features. Hence, to be able to develop convex approximations for the probability constraints, the set of constraints (6.6) is reformulated, as described later in the section.

6.2.3 Decomposition of Probability Constraints

To make tractable approximations of the probability constraints, auxiliary variables w_{pnt}, and y_{pnt} are introduced and used to break down the set of constraints (6.6) into three different sets of constraints (6.10), (6.11), and (6.12) as follows:

$$\text{S.t.} \quad w_{pnt} \geq \frac{1}{M}\delta_{pa}\gamma_{na}\left(t+\theta_{pa}+\tau_a-\widetilde{DT}_a\right), \quad \forall p \in \wp, n \in \mathcal{N}, t \in \mathbb{T}, a \in \mathcal{A}, \qquad (6.10)$$

$$y_{pnt} \geq w_{pnt} - M \sum_{\acute{n} \in \mathcal{N}/\{\mathrm{n}\}} \varphi_{p\acute{n}n} w_{p\acute{n}t}, \qquad \forall p \in \wp, n \in \mathcal{N}, t \in \mathbb{T}, \tag{6.11}$$

$$I_{np(t+\theta_{pn})} = f_{pt} y_{pnt}, \qquad \forall p \in \wp, n \in \mathcal{N}, t \in \mathbb{T}. \tag{6.12}$$

Variable w_{pnt} takes value 1 if the flow that departs at time $t \in \mathbb{T}$ from the origin of path $p \in \wp$ has a disruption condition due to the disruption time ($\widetilde{DT}_a$) of the emerging arc from node $n \in \mathcal{N}$; otherwise, it takes 0. Variable y_{pnt}takes value 1 if the departed flow at time $t \in \mathbb{T}$ from the origin of path $p \in \wp$ does not disturb any preceding arcs to node $n \in \mathcal{N}$ and is only disturbed on $n \in \mathcal{N}$; otherwise, it takes 0. Constraints (6.10) ensure that the disruption condition for any departed flow on an arc is checked and the value of w_{pnt} is determined. Constraint (6.11) implies that a scheduled flow is considered to be disturbed on node n ($y_{pnt} = 1$) only if it has disruption condition on this node and does not have any disruption condition on any of the preceding nodes to the node ($\sum_{\acute{n} \in \mathcal{N}/\{\mathrm{n}\}} \varphi_{p\acute{n}n} w_{p\acute{n}t} = 0$). Constraints (6.12) determine the amount of disturbed evacuation flow, where the disturbed evacuees are located, and the time they are stopped and added to the remaining disturbed flow.

6.2.4 Distributionally Robust Approximation of Chance-Constraints

In the reformulated constraints, only constraints (6.10) are influenced by the uncertainty of parameter $\widetilde{DT}_a$. Hence, the chance-constraint of the reformulated probable with the desired confidence level $1 - \epsilon_i \in (0,1]$ can be presented as

$$\mathbb{P}\left(w_{pnt} \geq \frac{1}{M} \delta_{pa} \gamma_{na} \big(t + \theta_{pa} + \tau_a - \widetilde{DT}_a\big)\right) \geq 1 - \epsilon_{pnta}, \quad \forall p \in \wp, n \in \mathcal{N}, t \in \mathbb{T}, a \in \mathcal{A}. \tag{6.13}$$

To develop a data-driven approximation of this program, the individual chance-constraints (6.13) are rearranged and presented as in (6.14) such that the random variable $\widetilde{DT}_a$ is separate on the left-hand side of the inequality

$$\mathbb{P}\big(\widetilde{DT}_a \geq t + \theta_{pa} + \tau_a - Mw_{pnt}\big) \geq 1 - \epsilon_{pnta}, \qquad \begin{array}{l} if\ \delta_{pa}\gamma_{na} = 1, \\ \forall p \in \wp, n \in \mathcal{N}, t \in \mathbb{T}, a \in \mathcal{A}. \end{array} \tag{6.14}$$

Note: Condition $\delta_{pa}\gamma_{na} = 1$ is added to create the same feasible region as constraints (6.13) impose. If either $\delta_{\text{pa}} = 0$ or $\gamma_{\text{na}} = 0$, then the product will be $\delta_{\text{pa}}\gamma_{\text{na}} = 0$, and consequently $w_{pnt} \geq 0$, which is a surplus condition since w_{pnt} is already defined as a binary variable. Hence, we can ignore these cases ($\delta_{pa} = 0\ or\ \gamma_{na} = 0$) and consider the constraint only under $\delta_{pa}\gamma_{na} = 1$ condition as in

$$\mathbb{P}\left(w_{pnt} \geq \frac{1}{M}\delta_{pa}\gamma_{na}\big(t + \theta_{pa} + \tau_a - \widetilde{DT}_a\big)\right) = \mathbb{P}\left(\widetilde{DT}_a \geq t + \theta_{pa} + \tau_a - M\frac{1}{\delta_{pa}\gamma_{na}}w_{pnt}\right) =$$
$$= \mathbb{P}\big(\widetilde{DT}_a \geq t + \theta_{pa} + \tau_a - Mw_{pnt} | \delta_{pa}\gamma_{na} = 1\big).$$

If the probability distribution function of the uncertain parameters $F_{\widetilde{DT}_a}$ were known with certainty, then the deterministic equivalent of the chance-constraints (6.14) would be of the form

$$F^{-1}_{\widetilde{DT}_a}\big(\epsilon_{pnta}\big) \geq t + \theta_{pa} + \tau_a - Mw_{pnt}, \quad \text{if}\ \ \delta_{pa}\gamma_{na} = 1, \quad \forall p \in \wp, n \in \mathcal{N}, t \in \mathbb{T}, a \in \mathcal{A}. \tag{6.15}$$

However, knowing the probability distributions is rather unlikely due to scarce available data on link failures during evacuation emergencies. Hence, a robust tractable approximation of the chance-constraints is derived assuming the availability of partial information, such as first and second moments, on probability distributions of link disruptions. The proposed approach in this paper is related to Lim et al. (2019). However, the proposition differs from the above-published work based on the fact that the probability constraint is structurally different, and hence the distributionally robust constraints are derived by employing a different asymptotic estimation for inequalities. The purpose is to put restrictions on auxiliary variable w_{pnt} such that the chance-constraints (6.14) hold irrespective of the probability distribution of $\widetilde{DT}_a$.

Proposition 1. *Consider a family of distributions denoted by $\wp = (\overline{DT}, \Sigma)$, where $\overline{DT} = (\overline{DT}_a)_{a\in\mathcal{A}}$ is the mean vector and $\Sigma = diag(\sigma_a^2)_{a\in\mathcal{A}}$ is the covariance matrix of the random vector $\widetilde{DT}$. For all distributions included in $\wp$ (distributions that are compatible with the given moments), the chance-constraints (6.14) can be written as:*

$$\text{Minimize} \quad \sum_{n\in\mathcal{N}_O} \beta_n + \sum_{p\in\wp}\sum_{n\in\mathcal{N}}\sum_{t\in\mathbb{T}} I_{pnt} \tag{6.16}$$

$$\text{s.t} \quad \inf_{\widetilde{DT}\sim(\overline{DT},\Sigma)} \mathbb{P}\left(\widetilde{DT}_a \geq t + \theta_{pa} + \tau_a - Mw_{pnt} \middle| \delta_{pa}\gamma_{na} = 1\right) \geq 1 - \epsilon_{pnta}, \quad \forall p \in \wp, n \in \mathcal{N}, t \in \mathbb{T}, a \in \mathcal{A}, \tag{6.17}$$

$$w_{pnt} \in \{0,1\},\ y_{pnt} \in \{0,1\}, \quad \forall p \in \wp, n \in \mathcal{N}, t \in \mathbb{T}, \tag{6.18}$$

$$(6.4), (6.5), (6.7), (6.11), \& (6.12), \tag{6.19}$$

where constraints (6.17) can be approximated and replaced by a convex second-order cone constraint for the family of distribution $\wp = (\overline{DT}, \Sigma)$ as expressed in

$$t + \theta_{pa} + \tau_a - Mw_{pnt} \leq \overline{DT}_a - \sqrt{\frac{1-\epsilon_{pnta}}{\epsilon_{pnta}}}\sigma_a, \quad \text{if} \quad \delta_{pa}\gamma_{na} = 1, \quad \forall p \in \wp, n \in \mathcal{N}, t \in \mathbb{T}, a \in \mathcal{A}. \tag{6.20}$$

Proof. From Cantelli's inequality we can write a one-sided version of Chebyshev's inequality as

$$\mathbb{P}\left(\widetilde{DT}_a \leq \overline{DT}_a - \kappa\sigma_a\right) \leq \frac{1}{1+\kappa^2}, \tag{6.21}$$

which is equal to

$$\mathbb{P}\left(\widetilde{DT}_a \geq \overline{DT}_a - \kappa\sigma_a\right) \geq 1 - \frac{1}{1+\kappa^2}. \tag{6.22}$$

If inequality (6.21) holds, then we can conclude that

$$\mathbb{P}\left(\widetilde{DT}_a \geq t + \theta_{pa} + \tau_a - Mw_{pnt}\right) \geq \mathbb{P}\left(\widetilde{DT}_a \geq \overline{DT}_a - \kappa\sigma_a\right), \quad \text{if} \quad \delta_{pa}\gamma_{na} = 1. \tag{6.23}$$

Finally, from inequalities (21) and (22) we can conclude that

$$\mathbb{P}\left(\widetilde{DT}_a \geq t + \theta_{pa} + \tau_a - Mw_{pnt}\right) \geq 1 - \frac{1}{1+\kappa^2}, \qquad \text{if} \quad \delta_{pa}\gamma_{na} = 1. \tag{6.24}$$

The probability that each of these constraints is violated is more than $1/1+\kappa^2$. Setting $\kappa = \sqrt{\frac{1-\epsilon_{\text{pnta}}}{\epsilon_{\text{pnta}}}}$ yields the desired result, and the data-driven robust chance-constraint approximation (18) can be used. Clearly, when the risk level ϵ_{pnta} is decreased, the estimation of arc disruption time $(\widetilde{DT}_a)$ is decreased to reach the desired level of confidence, and the resulting proactive plan can better handle possible disruption times that occur earlier in the evacuation process, providing more conservative measures. When the risk level ϵ_{pnta} is increased, the estimated disruption times are increased, and the obtained plan becomes more vulnerable to change in the actual disruption times.

Model Linearization

The term $f_{pt}y_{pnt}$ in constraint (6.12) is nonlinear, and hence the resulting mathematical model is a mixed-integer nonlinear program (MINLP). In the product of two variables $I_{np(t+\theta_{pn})} = f_{pt}y_{pnt}$ in constraint (6.12), f_{pt} is an integer, and y_{pnt} is a binary variable. If f_{pt} is bounded below by zero and above by $\bar{\mathrm{f}}_{\mathrm{pt}}$, then we can linearize the nonlinear equation by substituting it with a set of inequalities

$$I_{np(t+\theta_{pn})} \leq \bar{f}_{pt} y_{pnt},$$

$$I_{np(t+\theta_{pn})} \leq f_{pt}, \qquad \forall p \in \wp, n \in \mathcal{N}, t \in \mathbb{T}. \qquad (6.25)$$

$$I_{np(t+\theta_{pn})} \geq f_{pt} - (1 - y_{pnt}) \bar{f}_{pt},$$

For defining the upper bound of the integer variable f_{pt}, we assume that at each time interval $t \in \mathbb{T}$, regardless of flow congestion in previous time intervals, we can dispatch a flow equal to the maximum capacity of the path $p \in \wp$. The maximum capacity of a path is defined by the capacity of its bottleneck arc, which is the arc in the path with the minimum capacity. Hence, we can have $\bar{f}_{pt} = min\{C_a \delta_{pa}, \ \forall a \in \mathcal{A}\}$. Replacing the set of constraints (6.12) with constraints (6.25), we will have a MIP formulation, presented in the following:

$$\text{Minimize} \quad \sum_{n \in \mathcal{N}_o} \beta_n + \sum_{p \in \wp} \sum_{n \in \mathcal{N}} \sum_{t \in \mathbb{T}} I_{pnt} \qquad DRPBM \qquad (6.26)$$

$$\text{s.t} \quad t + \theta_{pa} + \tau_a - M w_{pnt} \leq \overline{DT}_a - \sqrt{\frac{1 - \epsilon_{pnta}}{\epsilon_{pnta}}} \sigma_a, \qquad \text{if} \ \ \delta_{pa} \gamma_{na} = 1, \ \forall p \in \wp, n \in \mathcal{N}, t \in \mathbb{T}, a \in \mathcal{A}, \qquad (6.27)$$

$$I_{np(t+\theta_{pn})} \leq \bar{f}_{pt} y_{pnt}, \qquad \forall p \in \wp, n \in \mathcal{N}, t \in \mathbb{T}, \qquad (6.28)$$

$$I_{np(t+\theta_{pn})} \leq f_{pt}, \qquad \forall p \in \wp, n \in \mathcal{N}, t \in \mathbb{T}, \qquad (6.29)$$

$$I_{np(t+\theta_{pn})} \geq f_{pt} - (1 - y_{pnt}) \bar{f}_{pt}, \qquad \forall p \in \wp, n \in \mathcal{N}, t \in \mathbb{T}, \qquad (6.30)$$

(6.4), (6.5), (6.7), (6.11), & (6.18). (6.31)

The proposed DRPBM is a mixed-integer program (MIP) with a linear structure and is able to find solutions to small and medium-sized problems in a timely manner. To improve the solution procedure, reduce the complexity of the model, and reduce the computational time for large-scale problems, we introduce a heuristic methodology, to be discussed later in the section.

6.2.5 Heuristic Algorithm to Find Optimal Solutions

This section explains a heuristic solution procedure to expedite solution computation. A two-step procedure is developed including the following: (i) employing preprocessing Algorithm 6.1 to calculate values of a specific parameter ϑ_{pnt}. This parameter indicates the disturbance location of the flow f_{pt} based on the estimation of arc disruption times ($\widetilde{DT}_a$)s that belong to $p \in \wp$; (ii) feeding the obtained values ϑ_{pnt} into a reduced optimization model (6.32)–(6.34). Preprocessing Algorithm 6.1 has two main steps: (i) calculate ω_{pnt} value based on $\widetilde{DT}_a$ s Approximation, and (ii) calculate ϑ_{pnt} value based on ω_{pnt} of preceding arcs to node m $\in \mathcal{N}$.

In the first step, for a specific arc of a path, if $t + \theta_{pa} + \tau_a - \overline{DT}_a + \sqrt{\frac{1-\epsilon_{pnta}}{\epsilon_{pnta}}}\sigma_a > 0$, then according to the value of approximated $\widetilde{DT}_a$, scheduled flow f_{pt} cannot pass through the arc and is halted behind node n $\in \mathcal{N}$ (origin node of arc $a \in \mathcal{A}$); hence $\omega_{pnt} = 1$. Otherwise, if $t + \theta_{pa} + \tau_a - \overline{DT}_a + \sqrt{\frac{1-\epsilon_{pnta}}{\epsilon_{pnta}}}\sigma_a \leq 0$, the flow is not affected by the estimated disruption time of the arc and hence $\omega_{pnt} = 0$.

However, to define the exact disturbance location of the flow, we must also consider the effect of the disruption time of other arcs in paths on the flow. Thus, in the second part of the algorithm, values of ω_{pnt} associated with preceding arcs to node m $\in \mathcal{N}$ are considered in defining the value of the parameter ϑ_{pnt}. If $\sum_{m\in\mathcal{N}} \omega_{pmt} = 0$ for all preceding arcs of arc a $\in \mathcal{A}$ and $\omega_{pnt} = 1$ (where n $\in \mathcal{N}$ is the origin node of the arc), then the actual disturbance location of the flow f_{pt} is on node n $\in \mathcal{N}$ of path p $\in \wp$; Hence, $\vartheta_{pnt} = 1$. Otherwise, flow disturbance does not occur at all or occurs elsewhere in the network, and

$\vartheta_{\mathrm{pnt}} = 0$.

Preprocessing Algorithm 6 . 1

Inputs:

An evacuation network $\mathcal{G}$ consisting of a set of nodes $\mathcal{N}$ and a set of arcs $\mathcal{A}$

for all paths $p \in \wp$ **do**

for all time slots $t \in \mathbb{T}$ **do**

for all arcs that belong to path $p \in \wp$ **do**

Calculating $\boldsymbol{\omega_{pnt}}$ value based on $\widetilde{\boldsymbol{DT_a}}$ s Approximation:

if $t + \theta_{pa} + \tau_a - \overline{DT}_a + \sqrt{\frac{1-\epsilon_{pnta}}{\epsilon_{pnta}}}\sigma_a > 0$ **then**

$\omega_{pnt} = 1$ (n is origin node of arc a)

else if $t + \theta_{pa} + \tau_a - \overline{DT}_a + \sqrt{\frac{1-\epsilon_{pnta}}{\epsilon_{pnta}}}\sigma_a \leq 0$ **then**

$\omega_{pnt} = 0$

end if

Calculating $\boldsymbol{\vartheta_{pnt}}$ value based on $\boldsymbol{\omega_{pnt}}$ of preceding arcs to node $\boldsymbol{m} \in \boldsymbol{\mathcal{N}}$:

for all preceding nodes $m \in \mathcal{N}$ to arc a on path p **do**

if $\sum_{m\in\mathcal{N}} \omega_{pmt} = 0$ and $\omega_{pnt} = 1$ **then**

$\vartheta_{pnt} = 1$ (n is origin node of arc a)

else then

$\vartheta_{pnt} = 0$

end if

end for

end for

end for

end for

Having the value of the parameter ϑ_{pnt}, we can eliminate constraints that relate to the disruption time estimations and the effect of disruption times on the flow and reduce the model as follows:

$$\text{Minimize} \quad \sum_{n \in \mathcal{N}_O} \beta_n + \sum_{p \in \wp} \sum_{n \in \mathcal{N}} \sum_{t \in \mathbb{T}} I_{pnt} \qquad DRPBM_{Reduced} \qquad (6.32)$$

$$I_{np(t+\theta_{pn})} = f_{pt} \vartheta_{pnt}, \qquad \forall p \in \wp, n \in \mathcal{N}, t \in \mathbb{T}, \qquad (6.33)$$

s.t (6.4), (6.5), & (6.7). (6.34)

6.3 Computational Results

Computational experiments are conducted to evaluate the performance of the proposed distributionally robust data-driven model (DRPBM) as well as the introduced heuristic solution methodology under various test problems. First, investigations are conducted on a small sample network, the performance of DRPBM is compared to the result of the deterministic model DPBM, and the effect of the introduced heuristic solution methodology in reducing computational time is illustrated. Then, DRPBM is used to conduct experiments on a real evacuation network involving a large metropolitan area. The mathematical models are solved using CPLEX 12.5.1, heuristic algorithms are run using MATLAB R2017b, and experiments are performed on a PC with a 3.07 GHz Intel Core i7 processor and 24GB RAM and running Ubuntu 10.04.3.

6.3.1 Numerical Case Study

For the computational experiments in this section, the test evacuation network shown in Figure 3.8 is used. The network includes three source nodes ($\mathcal{N}_1$, $\mathcal{N}_2$, and $\mathcal{N}_3$) and two destination nodes ($\mathcal{N}_9$ and $\mathcal{N}_{10}$). Values of arc transmit times (τ_a) as well as arc capacities (C_a) are shown for each arc, and the disruption time of arcs is considered to be uncertain. Six different test samples (C1, C2, …, C6) are defined by considering a combination of two levels for source node demands and three levels for arc disruption times. Level 1 of source node demands includes the amounts of 91, 99, and 74 for the demand values on the nodes $\mathcal{N}_1$, $\mathcal{N}_2$, and $\mathcal{N}_3$, respectively. In Level 2 of source node demands, these amounts are 136, 157, and 121. For each level of arc disruption times, the first number of arcs that undergo disruption is randomly selected from the range [3–7]. According to these numbers, a set of arcs from the available 22 arcs of the network is selected. Next, the mean and standard deviation of the disruption time of each of the selected arcs are randomly chosen from the range [0.2CT– 0.7CT] and [0.05CT– 0.2CT], respectively. Here, CT is the clearance time obtained by the deterministic model DPBM and represents the minimum amount of time required to complete the evacuation process and clear the network under deterministic settings.

The CPLEX pool feature is used to enumerate and generate all possible paths between the origin–destination (O-D) nodes of the sample network. Paths with long durations are eliminated, and the remaining 42 candidate paths (see Appendix) are chosen to form a set $\wp$ of input paths. DRPBM has $5|\wp| + 5|\mathcal{N}| + 6|\mathbb{T}| + 2|\mathcal{A}| + |\mathcal{N}_o|$ constraints, $2|\wp| + |\mathcal{N}| + 2|\mathbb{T}| + |\mathcal{N}_o|$ integer variables, and $2|\wp| + 2|\mathcal{N}| + 2|\mathbb{T}|$ binary variables. These amounts are reduced in DRPBM$_{\text{Reduced}}$ to $3|\wp| + 3|\mathcal{N}| + 4|\mathbb{T}| + 2|\mathcal{A}| + |\mathcal{N}_o|$ constraints, $2|\wp| + |\mathcal{N}| + 2|\mathbb{T}| + |\mathcal{N}_o|$ integer variables, and $|\wp| + |\mathcal{N}| + |\mathbb{T}|$ binary variables. Table 6.1 illustrates the comparison between the number of constraints and variables in DRPBM and DRPBM$_{\text{Reduced}}$ for the sample network in Figure 3.8. As is shown, using DRPBM$_{\text{Reduced}}$, the number of constraints and the number of binary variables are reduced by 33.5% and 50%, respectively, indicating the effectiveness of DRPBM$_{\text{Reduced}}$ in reducing the complexity of the problem.

Table 6.1: Number of constraints and variables in DPRBM and DRPBM$_{Reduced}$

	Constraints	Variables		
		Binary	Integer	total
DRPBM	537	180	175	355
DRPBM$_{Reduced}$	357	90	175	265
Improvement%	33.5%	50.0%	0.0%	25.4%

DRPBM and the heuristic approach are used to solve the problem under the test samples C1, C2, …, C6. The solution time of the DRPBM model and the solution time of the heuristic algorithm, which included the computational time of the reduced model (DRPBM$_{Reduced}$) and the computational time of the heuristic preprocessing algorithm 6.1, are tabulated in Table 6.2. As shown, the computational time of Algorithm 6.1 is less than a second and hence negligible. However, in most cases (C2, C3, C4, C5), the total computational time of the heuristic approach overcomes the computational time of DRPBM due to the reduction in complexity of the DRPBM$_{Reduced}$ compared to DRPBM.

Table 6.2: Computational times of DRPBM and DRPBM-Heuristic

		Solution Time (sec)					
		C1	**C2**	**C3**	**C4**	**C5**	**C6**
DRPBM	**DRPBM**	0.06	989.02	1002.02	867.04	1007.16	0.09
DRPBM - Heuristic	**DRPBM$_{Reduced}$**	0.03	0.02	0.02	0.03	0.03	0.02
	Algorithm 6.1	0.05	0.05	0.06	0.05	0.06	0.06
	Total	0.08	0.07	0.08	0.08	0.09	0.08
Improvement%		-33.3%	100.0%	100.0%	100.0%	100.0%	11.1%

Procedure 6.1 is proposed to investigate the effectiveness of the DRPBM in comparison with the well-known path-based deterministic model (Rungta et al., 2012). We should mention that DRPBM and DRPBM$_{Reduced}$ provide the same evacuation plans,

and the only difference is in their computational time. In the first step of Procedure 1, for each test sample C1, C2, …, C6, the flow rate and schedule f_{pt}^{DPBM} are determined by solving the deterministic model DPBM.

Procedure 6.1: Output generation for model comparison

Inputs:

An evacuation network $\mathcal{G}$ consisting of a set of nodes $\mathcal{N}$ and a set of arcs $\mathcal{A}$.

Test samples *C1, C2, …, C6.*

Calculated parameter ϑ_{pnt}.

Step 1: Obtain the number of disturbed evacuees under the deterministic plan

Step 1.a: Obtain the deterministic plan

Solve the deterministic model (*DPBM*) introduced by Rungta et al. (2012) to obtain a deterministic evacuation plan f_{pt}^{DPBM}

Step 1.b: Calculate the number of disturbed evacuees

Feed deterministic plan f_{pt}^{DPBM} as an input parameter to the DRPBM

Generate 10 disruption scenarios

Use the plan f_{pt}^{DPBM} and calculate $\sum_{p\in\mathcal{p}}\sum_{n\in\mathcal{N}}\sum_{t\in\mathbb{T}} I_{pnt}$ under each disruption scenario

Step 2: Obtain the number of disturbed evacuees under the proposed plan

Solve DRPBM to obtain stochastic evacuation plan f_{pt}^{DRPBM}

Use the 10 previously generated disruption scenarios

Use the plan f_{pt}^{DRPBM} and calculate $\sum_{p\in\mathcal{p}}\sum_{n\in\mathcal{N}}\sum_{t\in\mathbb{T}} I_{pnt}$ under each disruption scenario

Step 3: Comparison

Compare the average and standard deviation of the percentage of disturbed evacuees under plans resulting from DPBM and DRPBM

For each test sample C1, C2, …, C6, 10 random disruption scenarios under uniform or normal distribution functions are generated. The mean and the variance of the uniform or normal distribution are considered to be inconsistent with the mean and variance previously used in each case C1, C2, …, C6. Next, f_{pt}^{DPBM} is considered as an input parameter and is inserted into DRPBM, and the number of disturbed evacuees $(\sum_{p\in\mathcal{P}}\sum_{n\in\mathcal{N}}\sum_{t\in\mathbb{T}} I_{pnt})$ is calculated for each of the generated disruption scenarios. Table 6.3 illustrates the average and the standard deviation of the percentage of disturbed evacuees over the generated disruption scenarios. In the second step of Procedure 1, the same procedure is conducted for DRPBM. First, the desired confidence level (1-ϵ_{pnta}) is selected, then DRPBM is solved under each test sample C1, C2, …, C6, and the corresponding flow and schedule f_{pt}^{DRPBM} are obtained. Next, a disruption scenario is considered, f_{pt}^{DRPBM} is inserted in DRPBM, and the number of disturbed evacuees $(\sum_{p\in\mathcal{P}}\sum_{n\in\mathcal{N}}\sum_{t\in\mathbb{T}} I_{pnt})$ under the realization of the considered disruption scenario is calculated. Table 6.3 tabulates the results and demonstrates the performance of the proposed DRPBM using 95%, 90%, and 80% confidence levels with the performance of the DPBM under the normal and uniform probability distribution function assumption for the road disruptions.

For each combination of confidence level, test sample, and underlying distribution function of the road disruptions, the average (Ave) and the standard deviation (STD) of the disturbed flow percentage are displayed. For instance, in test sample C1, using DRPBM with a 90% confidence level, the average amount of disturbed flow percentage equals 5.7%, with the standard deviation of 4.1% over the 10 generated disruption scenarios from the normal distribution function. These amounts rise to 11.7% for the average disturbed flow percentage and 6.7% for the standard deviation when DPBM is used.

Table 6.3: Percentage of disturbed flow associated with DRPBM and DPBM evacuation plans

Dist.	*Model*	*Confidence level* **(1- ϵ)**	*Ave (STD) per test sample*					
			C1	**C2**	**C3**	**C4**	**C5**	**C6**
Normal	**DRPBM**	**95%**	0.0% (0.0%)	9.3% (4.2%)	2.3% (1.9%)	12.4% (4.1%)	16.7% (3.0%)	4.0% (2.3%)
		90%	5.7% (4.1%)	9.5% (4.0%)	1.5% (1.2%)	12.9% (3.3%)	16.9% (3.3%)	2.9% (1.9%)
		80%	7.3% (4.5%)	12.4% (5.3%)	6.9% (1.2%)	16.3% (3.1%)	17.6% (2.9%)	4.3% (1.9%)
	DPBM		11.7% (6.7%)	11.7% (6.7%)	12.8% (6.9%)	7.0% (2.0%)	21.4% (6.7%)	24.9% (4.9%)
Uniform	**DRPBM**	**95%**	0.0% (0.0%)	8.0% (4.2%)	1.1% (1.3%)	12.1% (3.4%)	14.7% (3.7%)	1.9% (1.9%)
		90%	5.3% (4.0%)	10.6% (4.4%)	2.5% (2.1%)	12.7% (4.1%)	17.9% (3.0%)	3.0% (2.3%)
		80%	5.6% (4.1%)	12.9% (5.5%)	2.9% (2.4%)	13.0% (3.8%)	18.1% (3.0%)	4.5% (3.4%)
	DPBM		7.2% (5.1%)	7.2% (5.1%)	13.8% (3.7%)	5.2% (3.4%)	17.5% (6.1%)	23.58% (1.3%)

Ave: Average of disturbed flow percentage; *STD*: Standard deviation of disturbed flow percentage

The same results are obtained using a combination of other test samples with other distribution assumptions, indicating that compared to DPBM, the proposed DRPBM can provide evacuation plans with a lower percentage of disrupted evacuees. Note that the normal distribution shows a better result than the uniform distribution when DPBM is used. For instance, the average of the disturbed flow percentage resulting from the DPBM plan is 11.7% in test sample C1 under a normal distribution and drops to 7.2% under the uniform distribution. However, we did not find the same results for DRPBM plans.

We also observe that the average of the disturbed flow percentage under DRPBM with higher values of confidence level (1-ϵ_{pnta}) outperforms the DRPBM with lower confidence levels. For instance, under test sample C1, the average amount of disturbed flow percentage equals 0% when a confidence level of 95% is used. However, this average increases to 7.3% when the confidence level is reduced to 80%. This difference is due to the fact that by increasing the confidence level, the risk level ϵ_{pnta} decreases, resulting in a reduction in the estimated amount of disruption time $(\overline{DT}_a - \sqrt{\frac{1-\epsilon_{pnta}}{\epsilon_{pnta}}}\sigma_a)$. Figure 6.1 displays the estimated amounts of road disruption time for a set of arcs $(a_3, a_5, a_8, a_{10}, a_{12}, a_{14}, a_{16}$, and $a_{19})$ under different amounts of the risk level ϵ_{pnta}.

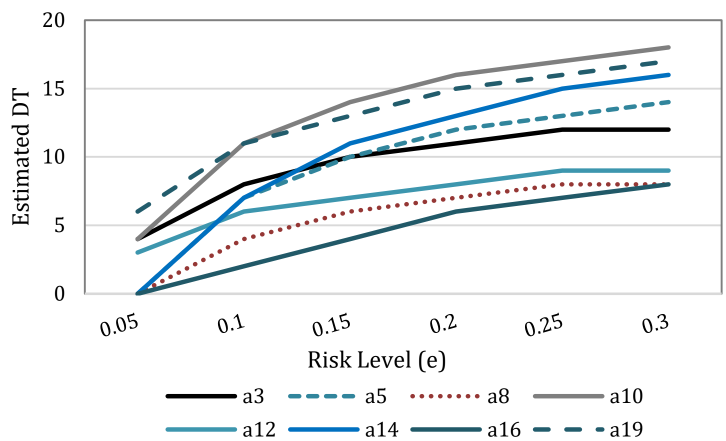

Figure 6.1: Estimation of DT under different values of ϵ

Through a reduction in the risk level, the produced evacuation plan, which is built on the lower values estimated for the disruption times, is less affected by the actual occurrence of early disruptions in the network. To better demonstrate the effectiveness of our proposed approach, in Figure 6.2 we display the percentage of reliability improvement of DRPBM with different confidence levels under different test samples. The reliability improvement percentage refers to the percentage reduction of disturbed evacuees when DRPBM is used in comparison to DPBM. As in our previous conclusion, DRPBM outperforms DPBM and improves the reliability of the evacuation plan, and the higher the confidence level of DRPBM, the more reliable the plan is in the face of possible road disruptions.

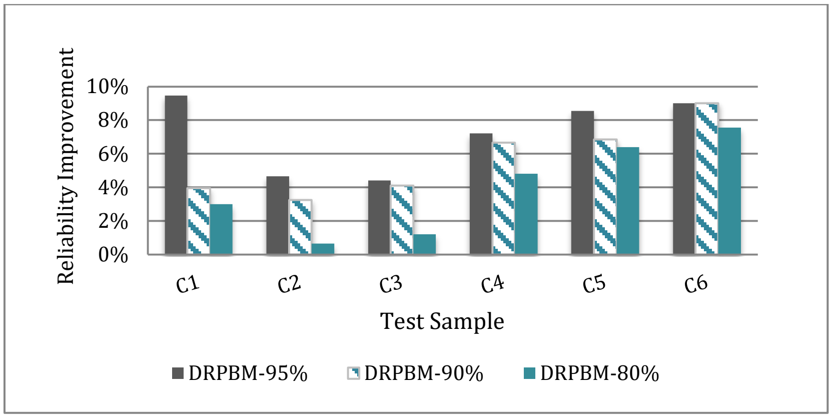

Figure 6.2: Reliability improvement by DRPBM under different confidence levels

6.3.2 Numerical Experiments on a Large-Scale Network

We continue the experiments on a large metropolitan area evacuation network. Figure 6.3 displays the transportation network of the Greater Houston area in Texas (Lim et al., 2012). The city, which is the fourth-largest city in the United States., is situated on the Gulf Coast and is one of the most vulnerable metropolitan cities in the area as it has experienced many severe hurricanes and floods over the past decades. In Figure 6.3, the endangered areas are represented by the 13 nodes ($\mathcal{N}_1 - \mathcal{N}_{13}$), and the destination and safe shelters are represented by the last four nodes ($\mathcal{N}_{39} - \mathcal{N}_{42}$). The rest of the nodes are intermediate nodes that connect the considered 107 roads displayed by directed arcs.

The input data used for this network is obtained from the work in Lim et al. (2012). The road transit times are considered to be multiples of $\tau = 30$-minute intervals. The total number of evacuation vehicles on the 13 source nodes is 779,400. To evacuate evacuees on each of the first six nodes ($\mathcal{N}_1 - \mathcal{N}_6$), 1,400 evacuation vehicles are required; for each source node ($\mathcal{N}_7 - \mathcal{N}_{10}$), 48,000 vehicles are needed, and for source nodes ($\mathcal{N}_{11} - \mathcal{N}_{13}$), 193,000 vehicles are required.

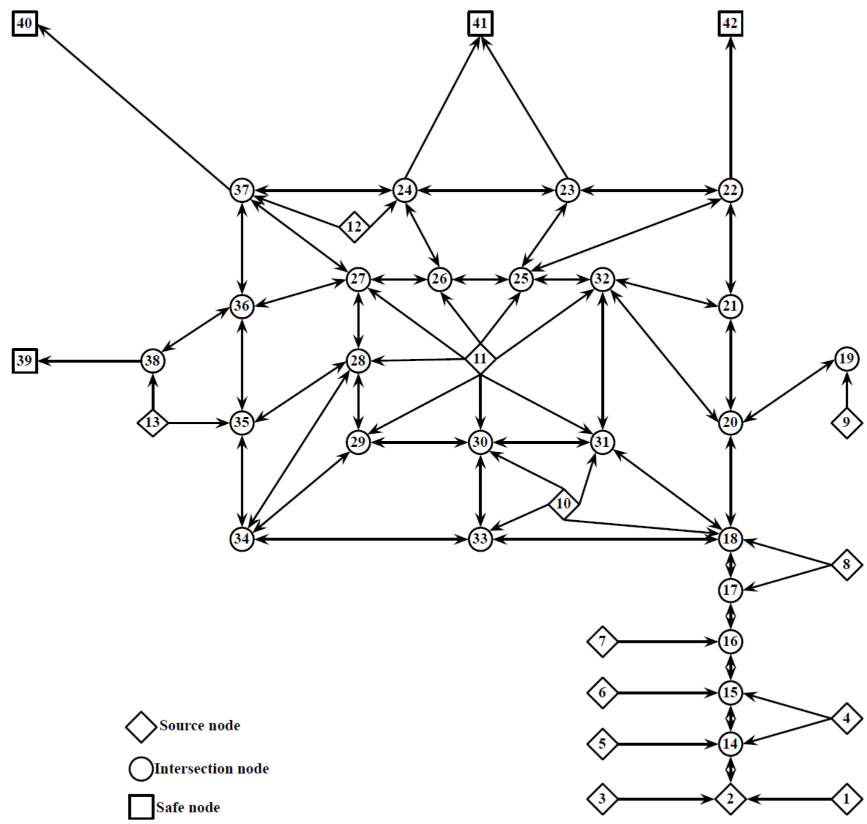

Figure 6.3: Houston transportation network

All possible paths between all O-D pairs are enumerated by using the solution pool feature of CPLEX, solving the shortest path problem for each O-D pair. The solution pool of paths is refined, and 140 candidate paths are selected to be used in the optimization model. The $\text{DRPBM}_{\text{Reduced}}$ is used to provide an evacuation plan for the Houston network. The computation time of running preprocessing Algorithm 1 was 61.23 seconds, while it took 5.78 seconds to solve the $\text{DRPBM}_{\text{Reduced}}$. The corresponding robust evacuation plan resulting from the heuristic approach is displayed in Figure 6.4. The horizontal axis displays the time intervals of the planning horizon, and the vertical axes illustrate the total number of evacuation vehicles that need to depart from the source nodes during each time interval. The total time required to complete the evacuation process and move approximately 1,792,600 evacuees to safe destinations was 167τ.

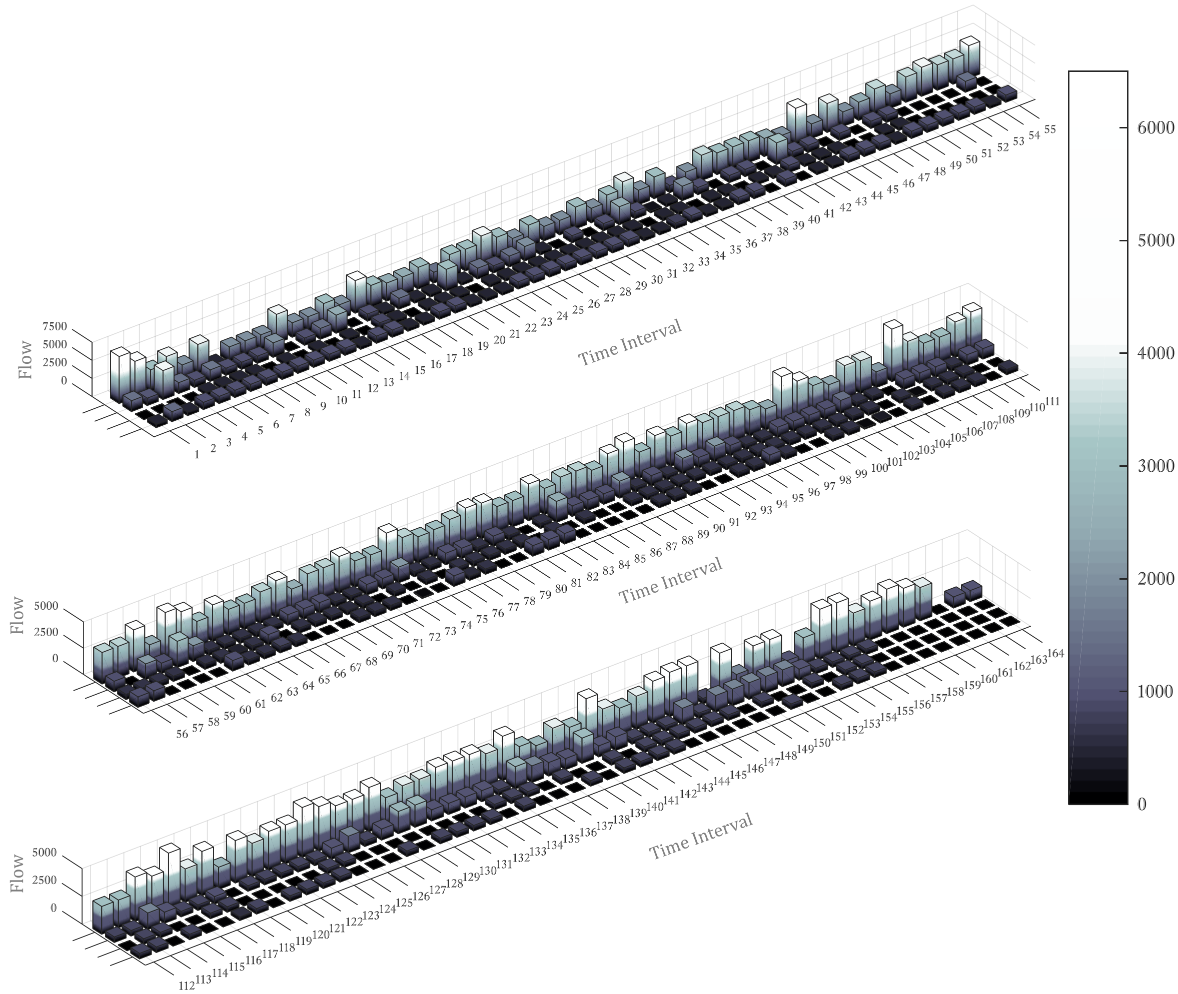

Figure 6.4: Robust evacuation plan for Houston transportation network

6.4 Conclusion

The study aims to investigate the hazard process with probable disruptions before the occurrence of a disaster to provide a proactive evacuation plan that is less affected by the actual realization of the road disruptions. It is assumed that since a proper database of disturbed roads in hazard situations is very unlikely to be available, accurate estimates of the disruption times are not possible to determine, and the probability distribution function of road incident times is unknown. However, partial information, such as the first and second moment of the probability distribution functions, is accessible through the data. Accordingly, we propose a distributionally robust data-driven evacuation planning problem with known first and second moments. Since the developed distributionally robust data-driven model is intractable, the model is reformulated and the constraint that is subject to uncertainty is decomposed into three different sets of constraints to construct a MIP model (DRPBM). Moreover, to reduce the computational time of the model, we introduce a preprocessing algorithm that defines the value of an introduced parameter based on the robust linear approximations of the constraint subjected to the disruption uncertainty and the departure times of the evacuation flow on the evacuation paths. Next, we directly use this parameter in a reduced optimization framework ($DRPBM_{Reduced}$) that provides the same results as DRPBM but in less computation time.

Numerical experiments were thoroughly conducted to compare the performance of the proposed DRPBM and $DRPBM_{Reduced}$ with the deterministic model in the literature (DPBM) under different sample tests and under different assumptions for the actual probability distribution of the disruptions. The percentage of disturbed evacuation flow due to road disruptions is used as a measure for the performance comparisons. Results showed that our proposed approach outperformed the DPBM in providing plans with more robustness in the face of road disruptions as it yields lower percentages of disturbed evacuees. We also observed that higher confidence levels in the proposed distributionally robust data-driven models resulted in better performance of the resulting plan. Further experiments were conducted to compare the efficiency of $DRPBM_{Reduced}$ in reducing computation time. The numerical experiments indicate that using $DRPBM_{Reduced}$ results in a 63% decrease in computation time on average. More experiments projected the efficiency of $DRPBM_{Reduced}$ in solving evacuation problem for the large-scale network of the Houston metropolitan area.

Chapter 7

Conclusion and Future Research

In our research, we have addressed different problems pertaining to emergency evacuations under uncertainty in events. During the course of an evacuation, many unforeseen events may happen due to the unpredictable nature of hazardous events, influencing dynamics of the flow, road congestions and consequently prolonging completion time of the evacuation process. We contributed to the knowledge and research capacity in evacuation planning by introducing effective recovery and proactive strategies to mitigate the undesired effect of either probable occurrence of events or uncertainty regarding the data values associated with evacuation. We now illustrate the limitations of our proposed approaches and propose directions for future research.

Dynamic Network Flow Optimization for Real-time Evacuation Reroute Planning under Multiple Road Disruptions

In our rerouting framework we provided a recovery strategy to be used as a response to real-time road incidents. We used distinctive algorithms to calculate values for specific parameters related to road disruption. This enabled us to develop a MIP formulation for the problem. A heuristic algorithm was introduced to effectively calculate rerouting clearance time (the minimum amount of time required to mobilize disturbed evacuees to the safe shelters). Performance of the model was studied through various numerical experiments and the effect of three incident-related factors; (i) location of the disruption; (ii) time of disruption occurrence; and (iii) plan updating time, were investigated on the efficiency of rerouting plan. As future work, one can extend this work by considering a contra-flow strategy to further reduce rerouting clearance time. It is also possible to consider parameter uncertainty in the model, such as travel times, alternative road capacity, and evacuees' behavior. Extending the proposed approach which benefits from projecting variable traffic flow rates through the network framework as a basis for vulnerabilities analysis through developing a probabilistic mechanism that accounts for factors including simultaneous multiple occurrences can be another interesting topic for future work.

Two-Stage Stochastic Model for Evacuation Planning: Adjusting the Plan Robustness under Possible Road Disruption

In our proposed two-stage stochastic program we considered risk and impact of road disruptions in order to provide a proactive evacuation plan that is less affected under network disruptions. The mathematical model has two distinctive components: a structural component that is fixed and free of any variations in its input data, and a control component that is subjected to uncertainty in the input data. The upper level of the model consists of design variables that define our proactive evacuation plan. The lower level consists of both structural and control components and uses recourse variables to represent reroute planning for the disturbed flow (recovery strategy) after the realization of each disruption scenario. Two algorithms were introduced for their parameter calculations. With the help of these algorithms, specific parameters related to potential road incidents were calculated. The design and recourse variables were built in accordance with these parameters in such a way to develop a linear formulation structure and reduce computational complexity. Moreover, two robustness measures were introduced to assess the solution optimality, as well as solution feasibility under each disruption scenario and a controller was used to make a trade-off between these measures. The study can be extended in the future by taking into account real-time information on traffic flow speeds along with lane closures. Considering the evacuation plan on a zonal basis in order to better prioritize the evacuation can be another extension for this work. Providing a fast solution procedure to be adopted for large scale evacuations could be another interesting area to explore.

Data-Driven Robust Optimization Approach Using Support Vector Clustering (SVC)

In our data-driven robust optimization framework, we used an unsupervised machine learning approach which is often used in pattern recognition to efficiently capture the distributional geometry of massive demand data. Accordingly, we used intersection kernel support vector clustering (SVC) and a piecewise kernel method to build compact uncertainty sets that efficiently cover data associated with the evacuation demand (number of to be evacuees) at the evacuation source nodes. Based on KKT conditions and the dual problem of SVC, we incorporated the "SVC-based" uncertainty set into the proposed data-driven optimization framework. Next, we derived a more compact uncertainty set by intersecting the previous uncertainty set (SVC-based) and a conventional robust optimization uncertainty set (e.g., box uncertainty set) and derived its associated data-driven robust optimization framework. The study can be extended in the future by taking into account demand-loading approaches in evacuation planning, which addresses time-dependent evacuation demands. Another possible research direction is to adopt dimension reduction approaches such as PCA and ICA to be integrated with the data-driven optimization models to better handle data in feature spaces with high dimensions.

Distributionally Robust Chance-Constraint program for Evacuation Planning under Partial Information of Probability Distribution of Road Disruption Times

In our proposed distributionally robust chance-constraint program we considered that the probability distribution function of road disruption times is unknown and only partial information is available. Using moment information of the probability distributions, we developed a framework to provide an evacuation plan that is less affected by the probable road disruptions and lead to less disturbed evacuees stranded on the evacuation roads. To provide a tractable distributionally robust chance-constrained formulation, we decomposed the uncertainty related constraint into three different sets of constraints by using auxiliary variables. Moreover, to even further reduce the computational burden, we introduced a heuristic framework including: (i) a heuristic algorithm to calculate specific disruption related parameter; and (ii) a reduced model built upon the aforementioned parameter which results in less variables and constraints and, consequently, computational time. Extensions to this work could be simulating rerouting strategies after the realization of probable disruptions to more realistically reflect the undesired effect of road disruptions on the traffic flow. Another extension is to develop the distributionally robust program under other partial information assumptions, such as support or symmetry information, for the probability distribution function of the uncertain parameters.

References

Abdelgawad, H. & Abdulhai, B. (2009). 'Emergency evacuation planning as a network design problem: A critical review', *Transportation Letters* 1:1, 41-58.

Agustı, A., Alonso-Ayuso, A., Escudero, L. F., & Pizarro, C. (2012). 'On air traffic flow management with rerouting. Part II: Stochastic case'. *European Journal of Operational Research*, 219(1), 167-177.

Akgün, V., Parekh, A., Batta, R., & Rump, C. M. (2007). 'Routing of a hazmat truck in the presence of weather systems'. *Computers & operations research*, 34(5), 1351-1373.

Aronson, J. E. (1989). 'A survey of dynamic network flows' , *Annals of Operations Research,* 20(1), 1-66.

Bayram, V. (2016). 'Optimization models for large scale network evacuation planning and management: A literature review', *Surveys in Operations Research and Management Science*, 21(2), 63-84.

Ben-Tal, A., Bertsimas, D. & Brown, D. (2010). 'A soft robust model for optimization under ambiguity', *Operations Research*, 58(4), 1220–1234.

Ben-Tal, A., Chung, B., Mandala, S. & Yao, T. (2011). 'Robust optimization for emergency logistics planning: Risk mitigation in humanitarian relief supply chains', *Transportation Research Part B: Methodological*, 45(8), 1177–1189.

Beroggi, G. E., & Wallace, W. A. (1995). 'Operational control of the transportation of hazardous materials: An assessment of alternative decision models', *Management Science*, 41(12), 1962-1977.

Bertsimas, D., abd Sim, M. (2004). 'The price of robustness', *Operations research*, 52(1), 35-53.

Birge, J. R., & Ho, J. K. (1993). 'Optimal flows in stochastic dynamic networks with congestion', *Operations Research*, 41(1), 203-216.

Bish, D. R., & Sherali, H. D. (2013). 'Aggregate-level demand management in evacuation planning', *European Journal of Operational Research*, 224(1), 79-92.

Bish, D. R., Sherali, H. D., & Hobeika, A. G. (2014). 'Optimal evacuation planning using staging and routing', *Journal of the Operational Research Society*, 65(1), 124-140.

Bretschneider, S. & Kimms, A. (2011). 'A basic mathematical model for evacuation problems in urban areas', *Transportation research part A: policy and practice*, 45(6), 523–539.

Calafiore, G. & Campi, M. (2005). 'Uncertain convex programs: randomized solutions and confidence levels', *Mathematical Programming*, 102(1), 25–46.

Calafiore, G. & Ghaoui, L. (2006). 'On distributionally robust chance-constrained linear programs', *Journal of Optimization Theory and Applications*, 130(1), 1–22.

Carey, M. (1987). 'Optimal time-varying flows on congested networks'. *Operations research*, 35(1), 58-69.

Carpender, S. K., Campbell, P. H., Quiram, B. J., Frances, J., & Artzberger, J. J. (2006). 'Urban evacuations and rural America: lessons learned from Hurricane Rita', *Public Health Reports*, 121(6), 775-779.

Chalmet, L. G., Francis, R. L., & Saunders, P. B. (1982). 'Network models for building evacuation', *Management science*, 28(1), 86-105.

Chen, X., & Zhan, F. B. (2008). 'Agent-based modelling and simulation of urban evacuation: relative effectiveness of simultaneous and staged evacuation strategies', *Journal of the Operational Research Society*, 59(1), 25-33.

Chiu, Y. C., Zheng, H., Villalobos, J., & Gautam, B. (2007). 'Modeling no-notice mass evacuation using a dynamic traffic flow optimization model', *IIE Transactions*, 39(1), 83-94.

Chung, B., Yao, T. & Zhang, B. (2012). 'Dynamic traffic assignment under uncertainty: A distributional robust chance-constrained approach', *Networks and Spatial Economics*, 12(1), 167– 181.

Chung, B., Yao, T., Xie, C., & Thorsen, A. (2011). 'Robust optimization model for a dynamic network design problem under demand uncertainty', *Networks and Spatial Economics*, 11(2), 371– 389.

Church, R. L., & Cova, T. J. (2000). 'Mapping evacuation risk on transportation networks using a spatial optimization model', *Transportation Research Part C: Emerging Technologies*, 8(1), 321-336.

Church, R. L., & Sexton, R. M. (2002). 'Modeling small area evacuation: Can existing transportation infrastructure impede public safety?', Vehicle Intelligence and Transportation Analysis Laboratory. Final Report prepared for the California Department of Transportation Santa Barbara, CA.

Daganzo, C. F. (1994). 'The cell transmission model: A dynamic representation of highway traffic consistent with the hydrodynamic theory', *Transportation Research Part B:*

Methodological, 28(4), 269-287.

Daganzo, C. F. (1995). 'The cell transmission model, part II: network traffic', *Transportation Research Part B: Methodological*, 29(2), 79-93.

De Silva, F. N., & Eglese, R. W. (2000). 'Integrating simulation modelling and GIS: spatial decision support systems for evacuation planning'. *Journal of the Operational Research Society*, 51(4), 423-430.

Desai, S. S., & Lim, G. J. (2013). 'An information based routing model for hazardous material route selection problem'. *Industrial and Systems Engineering Review*, 1(1), 1-12.

Diao, X., & Chen, C. H. (2018). 'A sequence model for air traffic flow management rerouting problem', *Transportation Research Part E: Logistics and Transportation Review*, 110, 15-30.

Do Chung, B., Yao, T., Xie, C., & Thorsen, A. (2011). 'Robust optimization model for a dynamic network design problem under demand uncertainty', *Networks and Spatial Economics*, 11(2), 371-389.

DOT, U. (2006). 'Report to congress on catastrophic hurricane evacuation plan Evaluation', US Department of Transportation, Washington, DC.

Erdo˘gan, E. & Iyengar, G. (2006). 'Ambiguous chance constrained problems and robust optimization', *Mathematical Programming*, 107(1), 37–61.

FEMA (2008). 'Producing Emergency Plans: A Guide for All-Hazard Emergency Operations Planning', Federal Emergency Management Agency, Washington D.C.

FEMA (2010), ‘Developing and Maintaining Emergency Operations Plans’, Comprehensive Preparedness Guide (CPG) 101, Version 2.0.

FEMA, Robert T. (2014) ‘Stafford Disaster Relief and Emergency Assistance Act’

FEMA. (1984). ‘Application of the I-DYNEV system to compute estimates of evacuation travel times at nuclear power stations’, Federal Emergency Management Agency Report 8, Washington, DC.

Ford Jr, L. R., & Fulkerson, D. R. (1958). ‘Constructing maximal dynamic flows from static flows’, *Operations Research*, 6(3), 419-433.

Ford Jr, L. R., & Fulkerson, D. R. (2015). ‘Flows in networks’, Princeton university press.

Fu, H. & Wilmot, C. G. (2004), ‘Sequential logit dynamic travel demand model for hurricane evacuation’, *Transportation Research Record: Journal of the Transportation Research Board*, 1882(1), 19–26.

Geletu, A., Klöppel, M., Zhang, H., & Li, P. (2013). ‘Advances and applications of chance-constrained approaches to systems optimisation under uncertainty’, *International Journal of Systems Science*, 44(7), 1209-1232.

Gipps, P. G. (1981). ‘A behavioural car-following model for computer simulation’, *Transportation Research Part B: Methodological*, 15(2), 105-111.

Goerigk, M., Hamacher, H. W., & Kinscherff, A. (2018), ‘Ranking robustness and its application to evacuation planning’. *European Journal of Operational Research*, 264(3), 837-846.

Groen, J., & Polivka, A. (2008). ‘Hurricane Katrina evacuees: Who they are, where they are, and how they are faring', *Monthly Labor Review March*, 32–51.

Hamacher, H., & Tjandra, S. (2002). 'Mathematical modelling of evacuation problems–a state of the art', *Pedestrian and Evacuation Dynamics*, 2002, 227–266.

Han, A. F. (1990). 'TEVACS: Decision support system for evacuation planning in Taiwan', *Journal of Transportation Engineering*, 116(6), 821-830.

Hobeika, A. G., & Jamei, B. (1985). 'MASSVAC: A model for calculating evacuation times under natural disasters', *Emergency Planning*, 23-28.

Hobeika, A. G., & Jamei, B. (1985). 'MASSVAC: A model for calculating evacuation times under natural disasters', *Emergency Planning, Simulation Series*, 15, 23–28.

Hobeika, A. G., Kim, S., & Beckwith, R. E. (1994). 'A decision support system for developing evacuation plans around nuclear power stations', *Interfaces*, 24(5), 22-35.

Hoeffding, W. (1963). 'Probability inequalities for sums of bounded random variables', *Journal of the American Statistical Association*, 58(301), 13–30.

Hooke, W. H. (2000). 'US participation in international decade for natural disaster reduction'. *Natural Hazards Review*, 1(1), 2-9.

Janson, B. N. (1991). 'Dynamic traffic assignment for urban road networks', *Transportation Research Part B: Methodological*, 25(2-3), 143-161.

Janson, B. N. (1991a). 'Convergent algorithm for dynamic traffic assignment', *Transportation Research Record*, (1328).

Jones, J. A., Walton, F., Smith, J. D., & Wolshon, B. (2008). 'Assessment of Emergency Response Planning and Implementation in the Aftermath of Major Natural Disasters and Technological Accidents, Sandia National Laboratories, Report No. SAND2007-1776P, U.S. Nuclear Regulatory Commission Report No. NUREG/CR-6981, NRC Division of Preparedness and Response, Washington, D.C.

Kim, S., Shekhar, S., & Min, M. (2008). 'Contraflow transportation network reconfiguration for evacuation route planning, Knowledge and Data Engineering', *IEEE Transactions*, 20(8), 1115–1129.

Kok, A. L., Hans, E. W., & Schutten, J. M. (2012). 'Vehicle routing under time-dependent travel times: the impact of congestion avoidance', *Computers & Operations Research*, 39(5), 910-918.

Kwon, E., & Pitt, S. (2005). 'Evaluation of emergency evacuation strategies for downtown event traffic using a dynamic network model', *Transportation Research Record: Journal of the Transportation Research Board*, (1922), 149-155.

Lighthill, M. J., & Whitham, G. B. (1955). 'On kinematic waves II. A theory of traffic flow on long crowded roads. Proceedings of the Royal Society of London', *Series A. Mathematical and Physical Sciences*, 229(1178), 317-345.

Lim, G. J., Baharnemati, M. R., & Kim, S. J. (2016). 'An optimization approach for real time evacuation reroute planning', *Annals of Operations Research*, 238(1-2), 375-388.

Lim, G. J., Rungta, M., & Baharnemati, M. R. (2015). 'Reliability analysis of evacuation routes under capacity uncertainty of road links', *IIE Transactions*, 47(1), 50-63.

Lim, G. J., Zangeneh, S., Baharnemati, M. R., & Assavapokee, T. (2012). 'A capacitated network flow optimization approach for short notice evacuation planning', *European Journal of Operational Research*, 223(1), 234-245.

Lindell, M. (2008). ‘Emblem2: An empirically based large scale evacuation time estimate model’, *Transportation Research Part A: Policy and Practice*, 42(1), 140–154.

Lindell, M. K., & Prater, C. S. (2007). ‘Critical behavioral assumptions in evacuation time estimate analysis for private vehicles: Examples from hurricane research and planning’, *Journal of Urban Planning and Development*, 133(1), 18–29.

Lu, Q., George, B., & Shekhar, S. (2005). ‘Capacity constrained routing algorithms for evacuation planning: A summary of results, in Advances in spatial and temporal databases’, *Springer*, 291–307.

Luedtke, J., & Ahmed, S. (2008). ‘A sample approximation approach for optimization with probabilistic constraints’, *SIAM Journal on Optimization*, 19(2), 674–699.

Lv, Y., Huang, G. H., Guo, L., Li, Y. P., Dai, C., Wang, X. W., & Sun, W. (2013). ‘A scenario-based modeling approach for emergency evacuation management and risk analysis under multiple uncertainties’, *Journal of Hazardous Materials*, 246-247, 234-244.

Lv, Y., Yan, X. D., Sun, W., & Gao, Z. Y. (2015). ‘A risk-based method for planning of bus–subway corridor evacuation under hybrid uncertainties’, *Reliability Engineering & System Safety*, 139, 188-199.

Merchant, D. K., & Nemhauser, G. L. (1978a). ‘A model and an algorithm for the dynamic traffic assignment problems’, *Transportation Science*, 12(3), 183-199.

Merchant, D. K., & Nemhauser, G. L. (1978b). ‘Optimality conditions for a dynamic traffic assignment model’, *Transportation Science*, 12(3), 200-207.

Mukherjee, A., & Hansen, M. (2009). ‘A dynamic rerouting model for air traffic flow management', *Transportation Research Part B: Methodological*, 43(1), 159-171.

Mulvey, J. M., Vanderbei, R. J., & Zenios, S. A. (1995). 'Robust optimization of large-scale systems', *Operations Research*, 43(2), 264-281.

Murça, M. C. R. (2018). 'Collaborative air traffic flow management: Incorporating airline preferences in rerouting decisions', *Journal of Air Transport Management*, 71, 97-107.

Murray-Tuite, P., & Mahmassani, H. (2004). 'Transportation network evacuation planning with household activity interactions', *Transportation Research Record: Journal of the Transportation Research Board*, (1894), 150-159.

Murray-Tuite, P., & Wolshon, B. (2013). 'Evacuation transportation modeling: An overview of research, development, and practice', *Transportation Research Part C: Emerging Technologies*, 27, 25-45.

National Governors' Association. (1978). 'Emergency Preparedness Project: Final Report', Washington, DC:NGA, 1978.

Nemirovski, A., & Shapiro, A. (2007). 'Convex approximations of chance constrained programs', *SIAM Journal on Optimization*, 17(4), 969–996.

Newkirk, R. T. (2001). 'The increasing cost of disasters in developed countries: A challenge to local planning and government', *Journal of Contingencies and Crisis Management*, 9(3), 159-170.

Ng, K. K. H., Lee, C. K. M., Zhang, S. Z., Wu, K., & Ho, W. (2017). 'A multiple colonies artificial bee colony algorithm for a capacitated vehicle routing problem and re-routing strategies under time-dependent traffic congestion', *Computers & Industrial*

Engineering, 109, 151-168.

Ng, M., & Waller, S. (2010). 'Reliable evacuation planning via demand inflation and supply deflation', *Transportation Research Part E: Logistics and Transportation Review*, 46(6), 1086– 1094.

Ng, M., Szeto, W., & Travis Waller, S. (2011). 'Distribution-free travel time reliability assessment with probability inequalities', *Transportation Research Part B: Methodological*, 45(6), 852–866.

Peeta, S., & Ziliaskopoulos, A. K. (2001). 'Foundations of dynamic traffic assignment: The past, the present and the future', *Networks and Spatial Economics*, 1(3), 233-265.

Peeta, S., & Ziliaskopoulos, A. K. (2001). 'Foundations of dynamic traffic assignment: The past, the present and the future', *Networks and Spatial Economics*, 1(3-4), 233-265.

Pidd, M., De Silva, F. N., & Eglese, R. W. (1996). 'A simulation model for emergency evacuation', *European Journal of Operational Research*, 90(3), 413-419.

Pidd, M., Eglese, R., & de Silva, F. N. (1996). 'CEMPS: A prototype spatial decision support system to aid in planning emergency evacuations', *Transactions in GIS*, 1(4), 321-334.

Radwan, E., Mollaghasemi, M., Mitchell, S., & Yildirim, G. (April, 2005). 'Framework for modeling emergency evacuation', Florida Department of Transportation (RPWO#5).

Rathi, A. K., & Solanki, R. S. (1993, December). 'Simulation of traffic flow during emergency evacuations: a microcomputer based modeling system', *In Proceedings of the 25th Conference on Winter simulation*, 1250-1258.

Renne, J. L., Sanchez, T. W., & Litman, T. (2011). 'Carless and special needs evacuation planning: a literature review', *Journal of Planning Literature*, 26(4), 420-431.

Rungta, M., Lim, G. J., & Baharnemati, M. (2012). 'Optimal egress time calculation and path generation for large evacuation networks', *Annals of Operations Research*, 201(1), 403-421.

Seyyedhasani, H., & Dvorak, J. S. (2018). 'Dynamic rerouting of a fleet of vehicles in agricultural operations through a Dynamic Multiple Depot Vehicle Routing Problem representation', *Biosystems Engineering*, 171, 63-77.

Sheffi, Y., Mahmassani, H., & Powell, W. B. (1981). 'Evacuation studies for nuclear power plant sites: A new challenge for transportation engineers', *ITE Journal*, 51(6), 25-28.

Sheffi, Y., Mahmassani, H., & Powell, W. B. (1982). 'A transportation network evacuation model', *Transportation research part A: general*, 16(3), 209-218.

Sherali, H. D., Carter, T. B., & Hobeika, A. G. (1991). 'A location-allocation model and algorithm for evacuation planning under hurricane/flood conditions', *Transportation Research Part B: Methodological*, 25(6), 439-452.

Smith, K. (2003). 'Environmental hazards: assessing risk and reducing disaster', Routledge.

Southworth, F., & Chin, S. M. (1987). 'Network evacuation modelling for flooding as a result of dam failure', *Environment and Planning A*, 19(11), 1543-1558.

Tarhini, H., & Bish, D. R. (2016). 'Routing strategies under demand uncertainty', *Networks and Spatial Economics*, 16(2), 665-685.

The United States Congress (2006). 'A Failure of Initiative: Final Report of the Select

Bipartisan Committee to Investigate the Preparation for and Response to Hurricane Katrina'. Government Printing Office, Washington, D.C. Accessed at <http://www.gpoaccess.gov/katrinareport/ fullreport.pdf>, March 2008.

Theodoulou, G., & Wolshon, B. (2004). 'Alternative methods to increase the effectiveness of freeway contraflow evacuation', *Transportation Research Record: Journal of the Transportation Research Board*, (1865), 48-56.

Travis Waller, S., & Ziliaskopoulos, A. (2006). 'A chance-constrained based stochastic dynamic traffic assignment model: Analysis, formulation and solution algorithms', *Transportation Research Part C: Emerging Technologies*, 14(6), 418–427.

Treiber, M., Hennecke, A., & Helbing, D. (2000). 'Congested traffic states in empirical observations and microscopic simulations', *Physical Review* E, 62(2), 1805.

Tufekci, S. (1995). 'An integrated emergency management decision support system for hurricane emergencies', *Safety Science*, 20(1), 39-48.

Tweedie, S. W., Rowland, J. R., Walsh, S. J., Rhoten, R. P., & Hagle, P. I. (1986). 'A methodology for estimating emergency evacuation times', *The Social Science Journal*, 23(2), 189–204.

U.S. Department of Transportation, & the U.S. Department of Homeland Security. (2006). 'Congress on Catastrophic Hurricane Evacuation Plan Evaluation: A Report to Congress'. Retrieved from http://www.fhwa.dot.gov/reports/hurricanevacuation.

U.S. Nuclear Regulatory Commission (2005). 'Identification and Analysis of Factors Affecting Emergency Evacuations', *NUREG/CR- 6864*, Vol. 1.

Ukkusuri, S. V., & Waller, S. T. (2008). 'Linear programming models for the user and system optimal dynamic network design problem: formulations, comparisons and extensions', *Networks and Spatial Economics*, 8(4), 383-406.

Urbina, E. A. (2002). 'A state-of-the-practice review of hurricane evacuation plans and policies', Doctoral dissertation, Louisiana State University.

Wang, L., Yang, L., Gao, Z., Li, Sh. & Zhou, X. (2016). 'Evacuation planning for disaster responses: A stochastic programming framework', *Transportation Research Part C: Emerging Technologies*, 69, 150-172.

Wolshon, B., Urbina, E., Wilmot, C., & Levitan, M. (2005). 'Review of policies and practices for hurricane evacuation. I: Transportation planning, preparedness, and response', *Natural Hazards Review*, 6(3), 129-142.

Wolshon, P. B. (2009). 'Transportation's role in emergency evacuation and reentry', *Transportation Research Board*, 392.

Xie, C. (2008). 'Evacuation network optimization: models, solution methods and applications', Doctoral dissertation, Cornell University.

Xuan, B. B., Ferreira, A., & Jarry, A. (2003). 'Computing shortest, fastest, and foremost journeys in dynamic networks', *International Journal of Foundations of Computer Science*, 14(02), 267-285.

Yao, T., Mandala, S. R., & Do Chung, B. (2009). 'Evacuation transportation planning under uncertainty: a robust optimization approach', *Networks and Spatial Economics*, 9(2), 171.

Yazici, A., & Ozbay, K. (2010). 'Evacuation network modeling via dynamic traffic assignment with probabilistic demand and capacity constraints', *Transportation Research Record: Journal of the Transportation Research Board*, 2196(1), 11–20.

Yazici, M. A., & Ozbay, K. (2008). 'Evacuation modelling in the united states: does the demand model choice matter?', *Transport Reviews*, 28(6), 757–779.

Yazici, M. A., & Ozbay, K. (2007). 'Impact of probabilistic road capacity constraints on the spatial distribution of hurricane evacuation shelter capacities', *Transportation Research Record*, 2022(1), 55-62.

Yin, W., M.-T. P., & Gladwin, H. (2014). 'Statistical analysis of the number of household vehicles used for hurricane ivan evacuation', *Journal of Transportation Engineering*, 140(12), 04014060.

Yuan, F., Han, L., Chin, S. M., & Hwang, H. (2006). 'Proposed framework for simultaneous optimization of evacuation traffic destination and route assignment', *Transportation Research Record: Journal of the Transportation Research Board*, (1964), 50-58.

Yusoff, M., Ariffin, J., & Mohamed, A. (2008, August). 'Optimization approaches for macroscopic emergency evacuation planning: a survey', *In Information Technology, 2008. ITSim 2008. International Symposium*, 3, 1-7.

Zaghian, M., Lim, G. J., & Khabazian, A. (2018). 'A chance-constrained programming framework to handle uncertainties in radiation therapy treatment planning', *European Journal of Operational Research*, 266(2), 736-745.

Zheng, H., & Chiu, Y.-C. (2011). 'A network flow algorithm for the cell-based single-destination system optimal dynamic traffic assignment problem', *Transportation*

Science, 45(1), 121–137.

Ziliaskopoulos, A. K. (2000). 'A linear programming model for the single destination system optimum dynamic traffic assignment problem', *Transportation Science*, 34(1), 37-49.

Zymler, S., Kuhn, D., & Rustem, B. (2013). 'Distributionally robust joint chance constraints with second-order moment information', *Mathematical Programming*, 137(1-2), 167-198.

Pan, J., Popa, I. S., Zeitouni, K., & Borcea, C. (2013). 'Proactive vehicular traffic rerouting for lower travel time', *Transactions on Vehicular Technology*, 62(8), 3551–3568.

Ben-Tal, A., Mandala, S. R., & Yao, T. (2009). 'Evacuation under data uncertainty: robust linear programming model', *Transportation Research Board 88th Annual Meeting*, Washington DC, No. 09-2779.

Yao, T., Ben-Tal, A., Chung, B. D., & Mandala, S. R. (2010). 'Robust optimization for dynamic traffic assignment under demand uncertainty', *Transportation Research Board 89th Annual Meeting*, Washington DC, No. 10-3679.

Kulshrestha, A., Wu, D., Lou, Y., & Yin, Y. (2011). 'Robust shelter locations for evacuation planning with demand uncertainty', *Journal of Transportation Safety & Security*, 3(4), 272-288.

Bolia, N. B. (2020). 'Robust scheduling for large scale evacuation planning', *Socio-Economic Planning Sciences*, 71, 100756.

Wang, X. J., & Paul, J. A. (2020). 'Robust optimization for hurricane preparedness', *International Journal of Production Economics*, 221, 107464.

Goldfarb, D., & Iyengar, G. (2003). 'Robust portfolio selection problems', *Mathematics of Operations Research*, 28(1), 1-38.

Klabjan, D., Simchi-Levi, D., & Song, M. (2013). 'Robust stochastic lot-sizing by means of histograms', *Production and Operations Management*, 22(3), 691-710.

Ning, C., & You, F. (2017). 'Data-driven adaptive nested robust optimization: general modeling framework and efficient computational algorithm for decision making under uncertainty', *AIChE Journal*, 63(9), 3790-3817.

Shang, C., Huang, X., & You, F. (2017). 'Data-driven robust optimization based on kernel learning', *Computers & Chemical Engineering*, 106, 464-479.

Ning, C., & You, F. (2018). 'Adaptive robust optimization with minimax regret criterion: Multiobjective optimization framework and computational algorithm for planning and scheduling under uncertainty', *Computers & Chemical Engineering*, 108, 425-447.

Shang, C., & You, F. (2019). 'A data-driven robust optimization approach to scenario-based stochastic model predictive control', *Journal of Process Control*, 75, 24-39.

Lim, G. J., Rungta, M., & Davishan, A. (2019). 'A robust chance constraint programming approach for evacuation planning under uncertain demand distribution', *IISE Transactions*, 51(6), 589-604.